11-4-2012

International Conference on Recent Trends in Engineering & Technology

Prof.Srikanta Patnaik Mentor
IRNet India, patnaik_srikanta@yahoo.co.in

Proceedings of International Conference on

RECENT TRENDS IN ENGINEERING & TECHNOLOGY

(ICRTET-2012)
4th November, 2012
BANGALORE, India

Interscience Research Network (IRNet)
Bhubaneswar, India

International Conference on Recent Trends in Engineering and Technology

ICRTET-2012

Bangalore, 4th November , 2012

Home

Editorial

Editorial

The new economic millennium is surprisingly rushing with Innovation and Technology. There is a sharper focus on deriving value from the widespread global integration in almost all spheres of social, economic, political and technological subsystems. In the quest of making this earth a better place to live we have to make a strong hold upon sustainable energy source. Sustainable energy sources include all renewable energy sources, such as hydroelectricity, solar energy, wind energy, wave power, geothermal energy, bioenergy, and tidal power. It usually also includes technologies designed to improve energy efficiency. Energy efficiency and renewable energy are said to be the twin pillars of sustainable energy. Renewable energy technologies are essential contributors to sustainable energy as they generally contribute to world energy security, reducing dependence on fossil fuel resources, and providing opportunities for mitigating greenhouse gases. Although the discipline like electrical engineering has narrated academic maturity in the last decades, but the limitations of the non renewable energy sources, turbulence and disturbances in the energy propagation cascades various insightfulness and stimulation in post classical electrical era. Evidence shows that there are phenomenal supplements in power generation and control after the introduction of Energy Management System (EMS) supported by Supervisory Control and Data Acquisition (SCADA). As there is increasing focus on strengthening the capacity of the power houses with the existing resources or constraints some new dimensions like FACTS, Optimal System Generation, High Voltage DC transmission system, Power Generation Control, Soft Computing, Compensation of transmission line, Protection scheme of generator, Loss calculation, economics of generation, fault analysis in power systems are emerging. Since the world is suffering with water, food, and energy crisis, energy consumption has social relevancy.

Let me highlight some of the recent developments in Electronics discipline. The new integrated devices did not find a ready market. Users were concerned because the individual transistors, resistors, and other electronic circuit components could not be tested individually to ensure their reliability. Also, early integrated circuits were expensive, and they impinged on the turf that traditionally belonged to the circuit designers at the customer's company. Again, Bob Noyce made a seminal contribution. He offered to sell the complete circuits for less than the customer could purchase individual components to build them. (It was also significantly less than it was costing us to build them!) This step opened the market and helped develop the manufacturing volumes necessary to reduce manufacturing costs to competitive levels. To this day the cost reductions resulting from economies of scale and newer high-density technology are passed on to the user—often before they are actually realized by the circuit manufacturer. As a result, we all know that the high-performance electronic gadget of today will be replaced with one of higher performance and lower cost tomorrow.

The integrated circuit completely changed the economics of electronics. Initially we looked forward to the time when an individual transistor might sell for a dollar. Today that dollar can buy tens of millions of transistors as part of a complex circuit. This cost reduction has made the technology ubiquitous—nearly any application that processes information today can be done most economically electronically. No other technology that I can identify has undergone such a dramatic decrease in cost, let alone the improved performance that comes from making things smaller and smaller. The technology has advanced so fast that I am amazed we can design and manufacture the products in common use today. It is a classic case of lifting

ourselves up by our bootstraps—only with today's increasingly powerful computers can we design tomorrow's chips.

In the advent of modern research there is a significant growth in Mechanical Engineering as Computer Aided Design has become instrumental in many industrialized nations like USA, European Countries, Scotland and Germ Other CAE programs commonly used by mechanical engineers include product lifecycle management (PLM) tools and analysis tools used to perform complex simulations. Analysis tools may be used to predict product response to expected loads, including fatigue life and manufacturability. These tools include Finite Element Analysis (FEA), Computational Fluid Dynamics (CFD), and Computer-Aided Manufacturing (CAM). Using CAE programs, a mechanical design team can quickly and cheaply iterates the design process to develop a product that better meets cost, performance, and other constraints. No physical prototype need be created until the design nears completion, allowing hundreds or thousands of designs to be evaluated, instead of a relative few. In addition, CAE analysis programs can model complicated physical phenomena which cannot be solved by hand, such as viscoelasticity, complex contact between mating parts, or non-Newtonian flows.

As mechanical engineering begins to merge with other disciplines, as seen in mechatronics, multidisciplinary design optimization (MDO) is being used with other CAE programs to automate and improve the iterative design process. MDO tools wrap around existing CAE processes, allowing product evaluation to continue even after the analyst goes home for the day. They also utilize sophisticated optimization algorithms to more intelligently explore possible designs, often finding better, innovative solutions to difficult multidisciplinary design problems.

Apart from Industrial Development there is also an hourly need for creation of an influential professional body which can cater to the need of research and academic community. The current scenario says there exists a handfull of bodies like American Society of Mechanical Engineers (ASME). Hence we must strive towards formation of a harmonious professional research forum committed towards discipline of Mechanical Engineering.

In the current scenario of scientific development robotics takes a center stage in solving many social problems. As agriculture is the mainstay of many developing nations, efficiency building measures should be incorporated in the field to boost efficiency and productivity. In the context Robotics in agriculture has attracted much attention in the recent years. The idea of robotic agriculture (agricultural environments serviced by smart machines) is not a new one. Many engineers have developed driverless tractors in the past but they have not been successful as they did not have the ability to embrace the complexity of the real world. Most of them assumed an industrial style of farming where everything was known before hand and the machines could work entirely in predefined ways – much like a production line. The approach is now to develop smarter machines that are intelligent enough to work in an unmodified or semi natural environment. These machines do not have to be intelligent in the way we see people as intelligent but must exhibit sensible behavior in recognized contexts. In this way they should have enough intelligence embedded within them to behave sensibly for long periods of time, unattended, in a semi-natural environment, whilst carrying out a useful task. One way of understanding the complexity has been to identify what people do in certain situations and decompose the actions into machine control.

The use of MATLAB is actually increasing in a large number of fields, by combining with other toolboxes, e.g., optimization toolbox, identification toolbox, and others. The Math Works Inc. periodically updates MATLAB and Simulink, providing more and more advanced software. MATLAB handles numerical calculations and high-quality graphics, provides a

convenient interface to built-in state-of-the-art subroutine libraries, and incorporates a high-level programming language. Nowadays, the MATLAB/Simulink package is the world's leading mathematical computing software for engineers and scientists in industry and education.

Due to the large number of models and/or toolboxes, there is still some work or coordination to be done to ensure compatibility between the available tools. Inputs and outputs of different models are to-date defined by each modeler, a connection between models from two different toolboxes can thus take some time. This should be normalized in the future in order to allow a fast integration of new models from other toolboxes. The widespread use of these tools is reflected by ever-increasing number of books based on the Math Works Inc. products, with theory, real-world examples, and exercises.

The conference is designed to stimulate the young minds including Research Scholars, Academicians, and Practitioners to contribute their ideas, thoughts and nobility in these two integrated disciplines. Even a fraction of active participation deeply influences the magnanimity of this international event. I must acknowledge your response to this conference. I ought to convey that this conference is only a little step towards knowledge, network and relationship

I express best wishes to all the paper presenters. I extend my heart full thanks to the reviewers, editorial board members, programme committee members of the conference. If situations prevail in favor we will take the glory of organizing the second conference of this kind during this period next year.

Convenor

Bikash Chandra Rout
Technical Editor, IOAJ

MICRO UTILITIES : UTILITIES ON MOBILES

JAYALAKSHMI SRINIVASAN

Departmnet of Information Technology
V.E.S. College of Arts, Science & Commerce, Mumbai,India

Abstract- With the advent of 3G networks and subsequent increased speed in data transfer available, the possibilities for applications and services that will link people throughout the world who are connected to the network will be unprecedented. One may even anticipate a time when the applications available on wireless devices will replace the original versions implemented on ordinary desktop computers. Taking the current state of the technology available for accessing 3G networks into consideration although this situation is far from reality as mobile networks evolve into a more powerful medium for information sharing and the devices that are connected to them inevitably grow in their ability to process the data at increasingly faster rates. Chat applications are built-in with only some brand of mobile phones and they are compatible with them alone. They are costly and difficult for the naïve ones to procure. As per the recent statistics, out of 93 million mobile users only 7 million users are using internet on their handsets. So to serve the rest of 86 million users, designing mobile application with necessary utilities is mandatory. This research paper "Micro Utilities" is an attempt to bring the overall effectiveness of mobile applications with mail server and chatting via Bluetooth in a cost-effective manner to satisfy all types of mobile users. In this context, this paper is going to analyze the first section of the research, "Literature survey"- a detailed study on J2ME, the technology to design mobile applications.

Keywords- *J2ME, 3G Networks, Blue Tooth Transfer, Information sharing via mobile networks, mail transfer, mobile utilities.*

I. PROBLEM STATEMENT

Cell phones have becomes a part of our daily lives they have evolved to such a point now, that they have functions, than making call. a cell phone user can now take pictures, play games and most importantly send ,receive and store data.

The Problems identified in the following areas:

- ✓ No provision for Bluetooth chatting;
- ✓ Limited support in sending the characters via SMS;
- ✓ Limited device support in the sense that accessing of email needs web browser with proper authentication details, which is time-consuming;
- ✓ No Centralized control especially in intranet over e-mail services;
- ✓ Lack of enhancement in the character support.(Traditional char set such as EBCDIC,ASCII etc).;
- ✓ For sending the email one has to access the web browser & must have email account this process is time consuming.

SOLUTION: Micro 'U'

The **Micro 'U'** provide unique and innovative way to chat using Bluetooth technology, SMS sending module & Email sending facility .The system is ideal for professional corporatists ,hobbyist users, students or all other users of a mobile phone. Using MicroU puts you ahead of the crowd when it comes to communication; this is achieved very fast, saving transmission cost and valuable working time. Thus it is user friendly, cost effective, innovative and effective. The Email module can be use as Service provided by any corporate firm to give facility to its employees to send Email via company's SMTP server. Thus it acts as SaaS. It is platform Independent and does not require web browser and separate client portal for long in.

II J 2 M E

Sun Microsystems defines Java 2 Micro Edition (J2ME) as "A highly optimized Java runtime environment targeting a wide range of consumer products, including pagers, cellular phones, screen phones, digital set-top boxes and car navigational systems". Below is a diagram showing what devices and platforms each of the three editions of the Java technology are designed to provide solutions for. Java 2 Enterprise Edition (J2EE) provides solutions for the enterprise environment, Java 2 Standard Edition (J2SE) for desktop development and low-end business applications, and J2ME for consumer and embedded devices.

III. ARCHITECTURE OF THE JAVA TECHNOLOGY

Java and the Java VM together provide a set of services that Java programs can rely on, regardless of the underlying hardware and operating system. Announced in June 1999, J2ME brings the cross-platform functionality of the Java language to smaller devices, allowing mobile wireless devices to share applications. There is no J2ME specification due to the fact that it isn't a single standard. It is, instead, a group of related specifications that define what Java technology looks like on resource-constrained devices. Before I discuss and explain the various specifications that J2ME consists of, it's important to appreciate the broad variety of devices that could implement J2ME, ranging from mobile phones to

entertainment systems. From this appreciation it is easily recognizable that it would be impossible to define a single technology that would be optimal, or even close to optimal for all these devices. The differences between them as regards processor power, memory, persistent storage and user interface are simply too severe. To address this problem, Sun divided and then subdivided the definition of devices suitable for J2ME into sections. The first division separated devices based on processing power, memory, and storage capability. This resulted in the creation of two **J2ME configurations:**

Connected,Limited Device Configuration (CLDC) and

Connected Device Configuration (CDC).

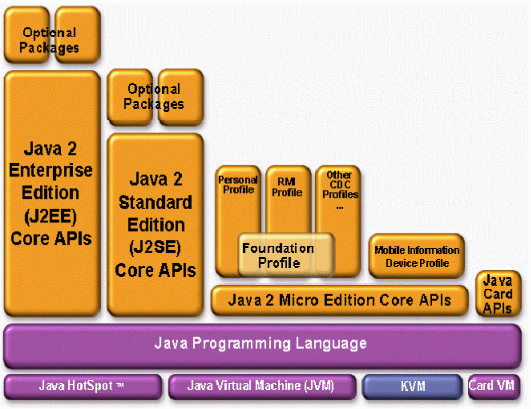

IV: J2ME CONFIGURATION

Fengetal(2001) has defined a configuration as: "A J2ME Configuration defines class libraries for a category or grouping of devices based on similar requirements for a total memory budget and processing power." Because there is such variability across user interface, function, and usage even within a configuration, these areas are not defined within a typical configuration. The definition of that functionality belongs, instead, to what is called a Profile.

V: J2ME PROFILE

Fengetal (2001) has stated that a profile is "Built on top of a specific configuration, a J2ME profile defines class libraries to address the specific demands of certain market segment." In other words a profile addresses a specific class of device, such as pagers and mobile phones. It supplements the already existing functionality in a configuration for these devices by sitting on top of the configuration. There are currently two profiles: the **Foundation Profile (FP)** which supplements the CLDC, and the **Mobile Information Device Profile (MIDP)** which supplements the **CLDC**.CLDC is the smaller of the two J2ME configurations, aimed at serving devices that have the following characteristics:

- ✓ 16-bit or 32-bit processor
- ✓ Limited memory – 512 KB or less
- ✓ A limited power supply (typically a battery)
- ✓ Limited or intermittent network connectivity
- ✓ A simple user interface, if any at all
- ✓ Limited screen size
- ✓ Limited input abilities

CLDC is concerned with applications destined for use on mobile phones, pagers, Personal Digital Assistants (PDAs), and similar devices. In order for the CLDC to fit onto these devices with such memory limitations much of the standard functionality present in the Java 2 Standard Edition (J2SE) is abandoned. For example, the java.util.package, which contains forty-seven classes and interfaces in the J2SE, was reduced to only ten classes in the CLDC. The result is that CLDC does not provide all of the functionality required to build useful applications (E.g. user interface classes). But this was Sun's intention, as CLDC was not intended to be a complete solution; it is a common base upon which profiles targeted at specific product types can add functionality too.

VI: MIDP

The Mobile Information Device Profile (MIDP) adds to the CLDC the functionality necessary to build useful applications for mobile phones, two-way pagers and similar devices. MIDP re-implements functionality to support user interfaces, timers, simple persistent storage, networking and messaging. Applications developed to the MIDP specification are called **Midlets.** An application developed for use on a MIDP device is referred to as a MIDlet. It does not have a main method; instead, a MIDlet extends the 'javax.microedition.midlet.MIDlet' class and implements its three abstract methods:

1. startApp(),
2. pauseApp(), and
3. destroyApp().

A MIDlet must also define a public noargument constructor which is the method instantiated by the **Application Management Software (AMS)** on the MIDP device when a MIDlet is launched. In order to develop an application to the MIDP/CLDC specifications, the MIDP and CLDC class packages must be downloaded [JavaSun J2ME, 2001] and their locations added to the classpath in the IDE where the MIDlet is being developed. All the class files belonging to a MIDlet are packaged into a single JAR file. This can then be downloaded and installed onto a wireless device via a serial cable connected to a PC or over-the-air (OTA) via a wireless network. This JAR file must also include a **manifest** file. A manifest file contains attributes describing the contents of a **JAR** such as name, version, and vendor of the MIDlet. One more file which the JAR must include is an **application descriptor** which is used in the deployment process of a MIDlet (especially OTA).

Before a JAR is downloaded to a device, the application descriptor is checked by the AMS to ensure the MIDlet is suited to the device. One other point to be made about packaging a MIDlet is that the code must be pre-verified in addition to compiling. Traditionally in J2SE, the verification process is performed at runtime by the Java Virtual machine (JVM). But due to the resource constraints on wireless devices, class verification is performed partially off-device and partially on-device to improve run-time performance. The off-device verification is referred to as **precertification**. The pre-verifier inserts a stack map attributes into the class file to help the in-device verifier quickly scan through the byte codes without costly operations. To aid with the packaging of MIDlets Sun provide the J2ME Wireless Toolkit (J2MEWTK) [JavaSun J2ME, 2001]. With this toolkit one can streamline several of the necessary tasks (creation of manifest file and application descriptor, compilation using MIDP compiler, and precertification) into one easy step. This facility is provided by a part of the toolkit called the Ktoolbar. Alternatively the J2MEWTK can be integrated with the 'Forte for Java' IDE. These features are subsequently accessible via 'Forte for Java' instead. The User Interface defined in MIDP is logically composed of two sets of APIs: -

1. **High-level UI API** which emphasizes portability across different devices –
2. **Low-level UI API** which emphasizes flexibility and control.

The portability in the **high-level API** is achieved by employing a high level of abstraction. The actual drawing and processing user interactions are performed by implementations. Applications that use the high-level API have little control over the visual appearance of components, and can only access high-level UI events. On the other hand, using the **low-level API**, an application has full control of appearance, and can directly access input devices and handle primitive events generated by user interaction. However the low-level API may be device-dependent, so applications developed using it will not be portable to other devices with a varying screen size.

VII: NETWORK PROGRAMMING IN J2ME MIDP

J2ME replaces the networking packages in J2SE with the Generic Connection Framework. To meet the small-footprint requirement necessary in mobile devices, the Generic Connection Framework generalizes the functionality of J2SE's network and file I/O classes: 'java.io' and 'java.net'. It is a precise functional subset of the J2SE classes, but much smaller in size. The J2ME classes and interfaces are all included in a single package javax.microedition.io', which supports the following forms of communication: HTTP, Sockets, Datagram, Serial Ports, and Files. CDC is the larger of the two J2ME configurations (the other being the CLDC already described above). It is best used for developing applications for television set top boxes, entertainment systems, automobile navigation systems (GPS), home appliances, point-of-sale terminals, and other devices of that scale.

These devices generally have the following features:

- ✓ Are powered by a 32-bit processor.
- ✓ Have 2MB or more of memory.
- ✓ Are connected to a network, often a wireless connection which is inconsistent and has limited bandwidth.
- ✓ Are designed with user interfaces that have varying degrees of sophistication, or maybe have no interface at all.
- ✓ They can support a complete implementation of the standard Java Virtual Machine (JVM) and Java language.

The CDC JVM named the CVM must be compatible with the standard JVM and Java programming language (J2SE). CDC provides the minimal set of APIs required to support the standard JVM. The CDC configuration adds APIs for file input and output, networking, security, object serialization, and a few more along with the ones already available in the CLDC. But CDC like CLDC does not include any type of user interface classes, as user interfaces vary considerably from device to device. Like MIDP is the profile that supplements the CLDC, similarly Foundation Profile (FP) is the profile defined for CDC. It extends considerably the APIs provided by CDC; however it does not provide the user interface APIs. FP must be augmented by one or more additional profiles that provide user interface support. Personal Profile is one such profile.

VIII:KVM – CVM

J2ME configurations also simplify the features of their underlying Java virtual machines compared with the standard JVM. CDC and CLDC each come with their own optimized virtual machine. The underlying virtual machine for CLDC is the K Virtual Machine (KVM). The KVM is a very small, yet very functional Java virtual machine specifically designed for resource-constrained devices. The K stands for Kilo as its memory is measured in kilobytes. The virtual machine for CDC is the C Virtual Machine (CVM). CVM is a fully featured, small footprint version of the standard JVM used with the J2SE specifically designed for high-end consumer devices. The figure below depicts the relationship between the different virtual machines, configurations and profiles. It also draws a parallel with the J2SE API and its Java virtual machine.KVM and CVM can be thought of as shrunken versions of the J2SE JVM.

IX: J2ME PROSPECTS

Cahners In-Stat Group has predicted that: "The number of MID subscribers will grow to more than 1.3 billion in 2004 with sales of more than 1.5 billion wireless handsets, PDAs and Internet appliances." A majority of companies are already choosing and supporting J2ME in order to provide a solution for their wireless applications. Companies that have worked on the MIDP include Ericsson, NEC, Nokia, NTT, DoCoMo, Palm Computing, Samsung, Sony, Alcatel, Psion, Siemens, Motorola and many more. Taking the lead in defining the MIDP is Motorola. The previous list of well-known mobile device manufacturers and mobile service providers shows that there is a significant vested interest in the J2ME technology. Considering this strong industry backing J2ME can really become the new platform to serve millions of mobile users with new, truly interactive, graphically appealing content. "Java's requirements exceed what today handset delivers" Hence, the wireless handsets available today need to evolve further before they will be capable of providing the services that become possible when using J2ME. But as I mentioned earlier, there is a large alliance of companies working to improve this situation, by producing more powerful handsets. Some of these companies are designing Java enabled phones for use with the current second-generation (2G) of networks and the 2.5G of networks, although the vast majority is focusing their interests on phones that are usable on 3G networks. According to Java Mobiles, 2001 there are about 34 Java enabled phones available at present, provided by various manufacturers. Below are some examples of some java enables phones, Motorola, Accompli 008, Nokia 7650 and Siemens SL45i: An example of such a company is Sprint PCS who says it'll use applications based on the Java language when it deploys its third-generation (3G) of wireless networks in mid-2002. Sprint is the forth-largest wireless carrier in the US. They are supporting J2ME because of its support for more graphical and personalized interactive services, as well as games. Sprint said "The Java platform will enable consumers to continually upgrade applications on a device and to interoperate with a variety of devices because it is an industry standard".

X: CONCLUSION

After successful analysis of the problem statement and the literature survey is being done, the research is entered into the next phase that is implementation in the methodology. The implementation details will be:

- ✓ Development of **chat controller** application and code to enable chat between users via Bluetooth
- ✓ Developing a **midlet that connects user to SMTP port** and sends the messages to the specified address
- ✓ Code to implement **deflation algorithm, which is the combination of Huffman coding and run-length pair**, for achieving compression of files in mobiles.

Surely the research "Micro Utilities" will provide the better feeling to the mobile users with the utilities being added onto their handsets. The micro utilities can be included with recycle bin in the near future.
The future enhancements regarding this project are -

- ✓ **Multiple chatting**
- ✓ **POP3 implementation**

REFERENCES

Books:

[1]. J2ME , The Complete Reference By JamesEdward Keogh

[2]. NetBeans : The Definitive Guide By Tim Boudreu

[3]. Beginning J2ME 3rd Edition Apress

Websites:

[4]. www.java.sun.com

[5]. www.Netbeans.com

[6]. www.forum.nokia.com

◈◈◈

HAND HELD TARGET DATA ACQUISITION DEVICE

BHAVANI.K & U.SUKRUTHI

ECE Department, Shri Vishnu Engineering College for Women, Bhimavaram– 534 202, A.P., India.

Abstract— In this paper, a design the hardware for interfacing the Charge Coupled Device(CCD), Thermal imager(TI),Global Positioning System (GPS), Laser Range Finder (LRF), Digital magnetic Compass (DMC), Organic Light-Emitting Diode (OLED) modules to FPGA processor(EP2S30F484). This paper involves the study of processor architecture, peripherals required for interfacing and code development tools.
Keywords—*Target Data Acquisition, CCD,TI,DMC,GPS, LRF,OLED.*

I. INTRODUCTION

Hand Held Target Acquisition device so desired by the infantry should be a light weight and ruggedized device to enable day and night view of the desired area include video, still photographs and able to display the captured data to the user.

Hand Held Target Acquisition Device is a compact multi function device for all weather and harsh battle field conditions. The TI is based on uncooled technology, Thermal imager for all ..Weather day and night observation and also consists of color CCD camera for day observation, eye safe LRF for range finding, digital magnetic compass for azimuth and elevation and GPS for latitude and longitude information. This is highly useful to army for effective engagement of targets. The target coordinates can be viewed in wgs84UTM format or in Indian grid.

II. BLOCK DIAGRAM

As shown Fig 1[1]. the FPGA EP2S30F484 is interfaced to GPS,DMC,LRF through RS232 protocol. CCD and TI is interfaced through multiplexer followed by analog to digital converter. The control lines of CCD is interfaced with switch box to FPGA. Each block need different power supply range 12V to 16.8V So adjustable power supply is used. FPGA need 3.3V.Target video along with co-ordinates and range can be viewed in OLED, this OLED preceded by DAC and interfaced to FPGA processor.

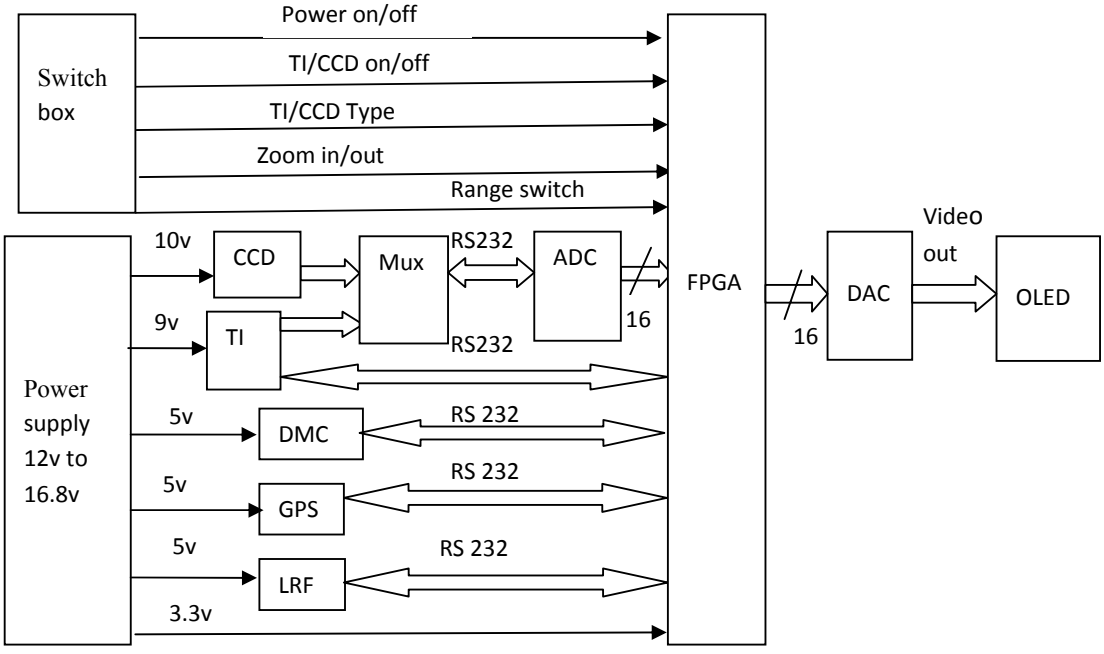

Fig 1. Block Diagram of Hand Held Target Data Acquisition Device

A . CCD

The KAF-0400C is a high performance silicon charge – coupled device(CCD) designed for a wide range of color image sensing application in the 0.4µm to 1.1µm wavelength band. Common applications include scientific , military , machine and industrial vision , copy stand , film digitizer and electronic still photography among others. The KAF-0400C consists of one vertical(parallel) CCD shift register , one horizontal (serial) CCD shift register and one output amplifier. Both registers incorporate two level polysilicon and true two-phase buried channel technology. The vertical register consist of 9µm x 9µm photo capacitor sensing elements (pixel) which also server as the transport mechanism. The pixels are arranged in a786(H) x 512(V) array in which an additional 16 columns and eight rows of non-imaging pixels are added as dark reference. As shown in Fig 2.

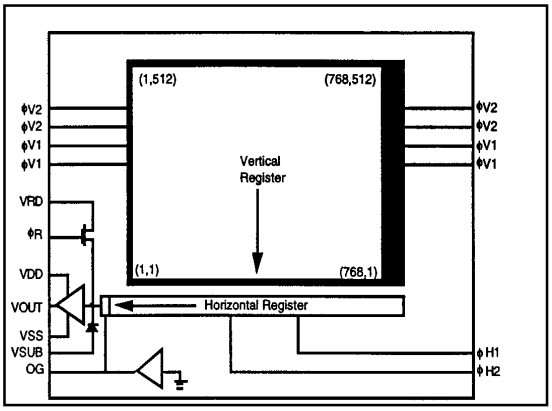

Fig 2 CCD camera functional block diagram

B. TI

Thermal Imaging devices work in absolute darkness. They do not require any ambient light to form an image. The principle of working is based on the fact that every object emits thermal radiations at temperatures, above absolute zero i.e., 0°K. These radiations fall in "Infrared band". The infrared radiations transmit through atmosphere in the wavelength bands of 3-5µm, and 8-12µm. An infrared detector in thermal imager detects these radiations and gives electrical signal which when processed form a visible image on a display. As glass is opaque to infrared radiation, optics based on Germanium, Silicon etc are used in the thermal imagers. These materials have good transmission characteristics over the specified wavelength bands, which get further enhanced by the application of thin film coatings. The ranges achieved by thermal imagers are much higher when compared to image intensifier based night vision devices.

Thermal imaging sensor image here in the Long Wave Infrared band 8-12µm.Since the infrared detector is the heart of any Thermal imaging camera. It is made out of Amorphous silicon, to coat the micro bolometer, a thin layer of 25µm vanadium oxide was used. This is based on the uncooled technology. Target detection 1.5km, recognition 0.5km and identification 0.3km.

It has electronically generated zoom that is 2x and 4x.The ability to see crystal clear picture through darkness, fog ,.haze and smoke all depends on the quality of the detector.

C.DMC

The Digital Magnetic Compass accurate and reliable Digital Magnetic Compass available today.It should be withstands under severe and extreme environmental conditions **.**Magneto resistive sensor circuit is a trio of sensors and application specific support circuits to measure magnetic fields. With power supply applied, the sensor converts any incident magnetic field in the sensitive axis directions to a differential voltage output. The magneto resistive sensors are made of a nickel-iron (Perm alloy) thin-film and patterned as a resistive strip element. In the presence of a magnetic field, a change in the bridge resistive elements causes a corresponding change in voltage across the bridge outputs. These resistive elements are aligned together to have a common sensitive axis (indicated by arrows on the pin outs) that will provide positive voltage change with magnetic fields increasing in the sensitive direction. Because the output only is in proportion to the one-dimensional axis (the principle of anisotropy) and its magnitude, additional sensor bridges placed at orthogonal directions permit accurate measurement of arbitrary field direction provide high performance for a wide range of consumer applications, including military applications .Azimuth and Elevation are angles used to define the apparent position of an object relative to a specific observation point..Azimuth angle is the angle between true north and target. Elevation angle denote the how much heading of object with respect to the observer. Its Azimuth accuracy≤1˚ and Elevation accuracy≤0.5 ˚. DMC Calibrated temperature range -32 …+55 °C. Communication interface is RS232, Serial interface

baud rate from 9600 to 38400. Device weight is 25grams.It needs 5v power supply.

D.GPS

Global Positioning System is for latitude and longitude information of the target. Latitude is measured from the equator, with positive values going north and negative values going south. Longitude is measured from Prime Meridian (which is the longitude that runs through Greenwich, England), with positive values going east and negative values going west. So, for example 65˚ west longitude, 45˚ north latitude is -65˚ longitude, +45˚latitude. Indian standard Longitude passes through Allahabad and Kakinada. Target co-ordinates can be viewed in WGS84UTM format, that is in metres.

E.LRF

Laser Range Finder is a device which uses a Laser beam to determine the distance to an object. It operates on the time of flight principle by sending a laser pulse in a narrow beam towards the object and measuring the time taken by the pulse to be reflected off the Target and returned to the sender.

$$D = Ct/2$$

C: speed of light in the atmosphere
t:Round trip between observer and Target

$$\text{since } t = \emptyset/\omega$$

$\emptyset$: phase delay
ω: Angular frequency of optical wave

$$\therefore D = C\emptyset/2\omega$$

Its wave length is 1.54µm and maximum range is 2km.

Fig 3 Laser Range Finder

Long operating range combined with compact design shape enabled by micro optics is characteristic for the DLEM series of laser rangefinder modules. The DLEM 2k measures distances from 10 meters to more than 2100 meters with an absolute accuracy of better than 1 meter. Based on a diode laser working at a wavelength of 1.5 µm, the rangefinder is eye safe according to laser protection class 1 and is not to detect with night vision devices based on image intensifier tubes.
The lightweight, compact optical and mechanical design allows for easy integration into various handheld, mobile or stationary measuring or fire control systems. Especially, its low power consumption recommends the
rangefinder as light infantry equipment The rangefinder is configured as a rangefinder module and can be controlled via a RS232 interface. It is suited for usage under harsh environmental conditions.
F.OLED

PT6808 is a 64-channel segment driver for dot matrix OLED graphic display systems. It utilizes CMOS Technology and provides display RAM, 64-bit data latch, 64 bit drivers and decoder logics. It features the internal display RAM used as storage for the display data which are transferred from an 8-bit microcontroller. It generates the dot matrix OLED driving signals corresponding to the given stored data. Paired with PT6807 (Common Driver IC), PT6808's pin assignments and application circuit are optimized for easier PCB Layout and cost saving advantages. It is shown in fig

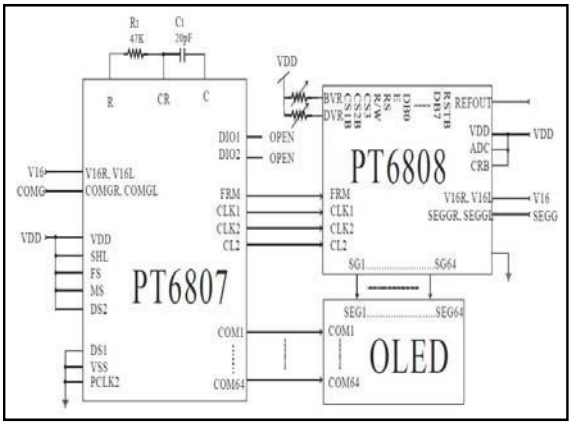

Fig 4. OLED interface with PT6807

III. SIMULATION RESULT

In this section the performance of the proposed recognition method is analyzed using simulated data. The result of Hand Held Target data Acquisition device. The Minimum period of this device is 5.733ns. the maximum operating frequency is 174.414MHz. The minimum input arrival time before clock: 5.507ns. The maximum output required

time after clock: 0.849ns. The maximum combinational path delay: 0.890ns. The entire system uses number of Slice Flip Flops 448 and number of 4 input Look Up Tables 467. Delay of signals between modules is 1.274 ns.

IV.CONCLUSION

In this paper we implemented the interfaced of the GPS,DMC,LRF,CCD,OLED to FPGA by which become most power full data acquisition like all weather condition ,Thermal imager for all weather day and night observation and also consists of colour CCD camera for day observation, eye safe LRF for range finding ,digital magnetic compass for azimuth and elevation and GPS for latitude and longitude information. This is highly useful to army for effective engagement of targets.

REFERENCES

[1] www.altera.com

[2] www.sony.com

[3] www.vectronix.com

[4] www.garmin.com

[5] www.jenoptik.com

[6] www.uwgb.edu

[7] www.bel.co.in

[8] www.cartome.org.htm

EMULATING THE ACTIONS OF HUMAN INTERFACE DEVICES USING BLUETOOTH TECHNOLOGY

AMIT BHANJA

B.E (Hons.) Computer-Science, BITS Pilani University

Abstract– Bluetooth Hid Emulation means emulating the behavior of any Human Interface Device on any host like Windows XP, Windows 7, etc. The Bluetooth hid emulation can be used to emulate various kinds of HIDs, which are available in the market, in reproducing the behaviors without having the real device available locally. There will be only the need of the configuration files of the human interface devices. The data pattern of the HIDs can be manually fed or can be generated from the traces collected remotely using the real device. In essence, the Bluetooth HID Emulation needs the Bluetooth protocols being implemented which would be used a Bluetooth device to set up a connection and then replicate the data which is to be emulated. This data could be collected by a real Bluetooth device or the data could be generated according to the protocol for a HID Data. Sometimes all the Human interface devices would not be available at all the time. Then the actions of the concerned human interface device could be emulated to get the desired behavior. The configuration file of the HID could be provided and the actions of the HID could be emulated. This method would be used for automation of the devices as per requirement.

Key words: *Emulation, Bluetooth, HID , Configuration file, data pattern*

I. INTRODUCTION

Bluetooth Hid Emulation means emulating the behavior of any Human Interface Device on any host like Windows XP, Windows 7, etc. The end use of this concept is to emulate various kinds of HIDs that are available in the market, in reproducing the behaviors in the lab without having the real device available locally. A Bluetooth Human Interface Device emulation script could be written which could be configurable to various Human Interface Device behaviors based on a configuration file which would be provided. The data pattern of the HIDs could be used to emulate the actions of a particular Human Interface Device. In essence, the script would act as a complete HID in the lab with respect to behavior and it does implement the Bluetooth protocols as needed by the HID.

II. DESCRIPTION

A. IMPORTANT TERMS

Bluetooth is a propriety open wireless technology standard for exchanging data over short distances (using short wavelength radio transmissions) from fixed and mobile devices, creating personal area networks (PANs) with high levels of security. Created by telecoms vendor Ericsson in 1994, it was originally conceived as a wireless alternative to RS-232 data cables. It can connect several devices, overcoming problems of synchronization. [1]

Bluetooth technology is a short-range communications technology that is simple, secure, and everywhere. The key features of Bluetooth technology are robustness, low power, and low cost. The Bluetooth Specification defines a uniform structure for a wide range of devices to connect and communicate with each other.[2] Bluetooth uses a radio technology called frequency-hopping spread spectrum, which chops up the data being sent and transmits chunks of it on up to 79 bands (1 MHz each; centered from 2402 to 2480 MHz) in the range 2,400–2,483.5 MHz (allowing for guard bands). Bluetooth is a packet-based protocol with a master-slave structure. A master bluetooth device can communicate with a maximum of seven devices. The devices can switch roles, by agreement, and the slave can become the master. At any given time, data can be transferred between the master and one other device (except for the little-used broadcast mode). The master chooses which slave device to address; typically, it switches rapidly from one device to another in a round-robin fashion.[1]

There are two types of connections possible: Synchronous Connection Orientated (SCO), or Asynchronous Connection Less (ACL).

The SCO (Synchronous Connection Oriented) channels are used for voice transfer by reserving slots, they are symmetric between the master and a slave. There is a maximum of three in a piconet, a slave being able to control two originating from different masters. One can use the voice packets or the mixed voice/data packets. [3]

An ACL (Asynchronous Connection Less) channel supplies an asynchronous access between master and slave (a single channel per couple), with the slot as base. The data packets only are used. In addition, a slave can only transmit after having received a packet from the master (the following slot). For this purpose, the master can send polling packets to the slaves (when there is nothing more asynchronous to transmit). [3]The specific characteristics of Bluetooth are low consumption management modes.

Active Mode: - In this mode, the Bluetooth module participates actively on the transmission channel. The master regularly sends a packet to the slaves (polling)

to enable the slaves to be able to send a packet to the master and re-synchronise themselves. [3]

Sniff Mode: - This is a low consumption mode. A Bluetooth module in the Sniff mode stays synchronised in the piconet. It listens to the piconet at regular intervals (Tsniff) for a short instant. This enables it to re-synchronise itself with the piconet and to be able to make use of this Sniff window to send or receive data. The consumption is as low as the Tsniff is large (compared to the Sniff window). If Tsniff is in the region of a second and the duration of Sniff (Twin) is in the region of several ms, the consumption will be about 1 to 5% of the maximum transmission consumption. (average consumption of 1mA to 5mA approximately).[3]

Hold Mode: - The module remains synchronised. This is lower consumption mode than the Sniff mode. Only the counter on the Bluetooth chip in hold mode is active. At the end of the Hold period, the Bluetooth module returns to the active mode.[3]

Park Mode: - A Bluetooth module in this mode is no longer an active member of the piconet. However, it remains synchronised with the master and can listen to a broadcast channel (Beacon Channel). [3]

A human interface device or HID is a type of computer peripheral device that interacts directly with, and most often takes input from, humans and may deliver output to humans. The term "HID" most commonly refers to the USB-HID specification. The term was coined by Mike Van Flandern of Microsoft when he proposed the USB committee create a Human Input Device class working group.[4]

Example of some HIDs include Keyboard, Mouse, Trackball, Touchpad, Pointing stick, Graphics tablet, Joystick, Gamepad, Analog stick, Headset, Webcam, Driving simulator devices and flight simulator devices have HIDs such as gear sticks, steering wheels and pedals., Wired glove (Nintendo Power Glove)

A Bluetooth HID is a wireless Human Interface Device which uses the Bluetooth technology to transmit data.

BD_ADDR:- BD_ADDR is the address used by a Bluetooth device . It is received from a remote device during the device discovery procedure.

B. BLUETOOTH PROTOCOL STACK

The HID stack in the picture above represents the actual HID. The emulation could use the same stack as the one used by the host and up to the HCI driver.

Layers in Bluetooth:

1. Radio Layer (RF): - The RF block is just like the physical layer in the OSI model. The RF block is responsible for transmitting and receiving packets of information on the physical channel. A control path between the baseband and the RF block allows the baseband block to control the timing and frequency carrier of the RF block. The RF block transforms a stream of data to and from the physical channel and the baseband into required formats. [5]

2. Baseband layer: - The baseband layer block consists of link controller, baseband resource manager, device manager.

2.1 Device Manager: - The device manager is the functional block in the baseband that controls the general behavior of the Bluetooth device. It is responsible for all operation of the Bluetooth system that is not directly related to data transport, such as inquiring for the presence of other nearby Bluetooth devices, connecting to other Bluetooth devices, or making the local Bluetooth device discoverable or connectable by other devices. The device manager requests access to the transport medium from the baseband resource controller in order to carry out its functions. The device manager also controls local device behavior implied by a number of the HCI commands, such as managing the device local name, any stored link keys, and other functionality. [5]

2.2 Link Controller: - The link controller is responsible for the encoding and decoding of Bluetooth packets from the data payload and parameters related to the physical channel, logical transport and logical link. [5]

2.3 Baseband Resource Manager: - The baseband resource manager is responsible for all access to the radio medium. It has two main functions. At its heart is a scheduler that grants time on the physical channels to all of the entities that have negotiated an access contract. The other main function is to negotiate access contracts with these entities. An access contract is effectively a commitment to deliver a certain QoS that is required in order to provide a user application with an expected performance. [5]

3. Link Manager Layer: - The link manager is responsible for the creation, modification and release of logical links (and, if required, their associated logical transports), as well as the update of parameters related to physical links between devices. The link manager achieves this by communicating with the link manager in remote Bluetooth devices using the Link Management Protocol (LMP.)The LM protocol allows the creation of new logical links and logical transports between devices when required, as well as the general control of link and transport attributes such as the enabling of encryption on the logical transport, the adapting of transmit power on the physical link, or the adjustment of QoS settings for a logical link. [5]

4. HCI: - HCI (host controller interface) is an interface between host layer containing the

application layer, L2CAP layer SDP layer and controller layer which consists of link manager layer, baseband layer and radio layer. [5]

5. L2CAP layer: - L2CAP layer (Logical Link Control and Adaptation Layer) is layered over the Baseband Protocol. L2CAP provides connection-oriented and connectionless data services to upper layer protocols with protocol multiplexing capability, segmentation and reassembly operation, and group abstractions. L2CAP permits higher level protocols and applications to transmit and receive L2CAP data packets. There are different types of L2CAP requests and responses like connection, configuration, disconnection, etc. [5]

6. SDP Layer: - The service discovery protocol (SDP) provides a means for applications to discover which services are available and to determine the characteristics of those available services. Like L2CAP, there are different types of SDP requests and responses like SDP service search, SDP attribute and SDP service search attribute. This helps to transfer the service records requested by the host. [5]

7. HID PROFILE: - Hid emulation script would be able to send and receive HCI commands and events. The implementation of the emulation could encapsulate the L2CAP/SDP and the HID behavior and would emulate the HID behavior based on the configurations and the data pattern fed to the script.

III. IMPLEMENTATION

The emulation of Bluetooth human interface device could be achieved through the implementation of L2CAP layer and encapsulation of Service Discovery protocol in the implementation. The emulation could use the existing HCI protocol for the emulation to be successful. The emulation script could act as the human interface device. The implementation could depend on the compiler present to convert the format of the data to the ones required for the transfer through Bluetooth technology.

The implementation would need the script to be treated as the device and any system on which the emulation is required be treated as a host.

- At first, the Human Interface device would be initiated. The initiation would mean that the script would check for the existence of any Bluetooth connection on the ports and assign the name to it. This connection will act as the Emulated HID.

- The configuration file of the actual Human interface device to be emulated could be read and stored. Then the needed parameters could be retrieved from the storage and sent as parameters of the HCI commands.

- There would be a HCI connection request sent and the script would wait for the event of connection complete to take place. After the connection being established, the required parameters could again be sent through HCI commands for the emulation of the concerned Human interface device on the host. Then pairing would be done by either pin code request or without any pin code request.

- After all the initiation, the script would wait for some events initiated by the host. If it is an ACL event, it would handle as a L2CAP request in the script. Then L2CAP layer on the remote device machine would interact with the L2CAP layer on the host side. It would respond to the requests or responses provided by the host by sending the corresponding requests or response packets. The packets could be sent according to the format set by the specifications provided.

- The SDP channel has to be set up as it would provide a means for applications to discover which services are available.

- After the SDP channel would be set up for transfer of requests, the host could start sending SDP requests or responses. Accordingly the device machine which is the one on which the script is run would send the corresponding requests or responses.

- After all the SDP transactions would be over, the host would send the request for HID control channel to be set up. Through this channel the control packets are sent and received. After this the HID interrupt channel could be created through which the actual data that has to be passed to the host side for emulation of HID.

- After both the channels are created, the data would be passed to the host. During this period, we could see the emulation of HID on the host side. And then SDP, HID control and HID interrupt channels could be disconnected respectively. After the disconnection complete event, the script would end execution.

The summary of the implementation of the script could be as follows:- The script sets the Bluetooth device as any HID, enables page scan and enquiry, accepts incoming connection from a host, handles SDP transactions, sets up HIDC and HIDI connection, sends HID data and disconnects.

Human Interface Device 1st Connection Sequence

1. Set up HCI parameters, Enable Scan - HID_Init

2. Accept Incoming Connection, Set encryption - HID_Init

3. Host initiates SDP connection and SDP Requests - event_resp

4. After successful completion of SDP Transaction, host initiates HID Control and Interrupt channels - event_resp.

5. Emulation script can start sending data once HID Interrupt and Control Channel are configured

IV. ENHANCEMENTS

A. Sniff Mode Implementation: - Now the Sniff mode could be implemented properly. Before sending the actual data to the host, the script could enter the sniff mode and it could utilize all the sniff parameters extracted from the configuration file it sends the data to the host. However it would help a bit to show the actual emulation of any HID.

B. Reconnection:-The script could store the BD_ADDR (Bluetooth Device Address) of the concerned Human Interface Device and then the HCI link would be set up. Then there is only the requirement for connection request. The SDP channel doesn't need to be set up. The HID control and Interrupt channels could be setup for the transfer of actual data for emulation.

Following is the sequence of events for the reconnection of the Human Interface Device

Human Interface Device Re-Connection Sequence

1. Set up HCI parameters, Enable Scan - HID_Init

2. Create connection to stored BD_Addr, Set encryption - HID_Init

3. Emulation script initiates HID Control and Interrupt channels - event_resp

4. Emulation script can start sending data once HID Interrupt and Control Channel are configured.

V. CONCLUSION

The emulation script could be used for emulating any Human Interface Device. The concept could be used for emulating the actions of any human interface device needed in the lab. It could be used for conducting automated work at particular periodic intervals without the presence of the real device.

VI. FURTHER IMPROVEMENTS

More detailed study could be made regarding the different low consumption management modes of operation mentioned. The Emulation script could enter and exit the sniff mode at various times. It could enter into other mentioned modes and transfer the data accordingly. This would result in showing more realistic behavior of the human interface devices.

VII. REFERENCES

[1]. http://en.wikipedia.org/wiki/Bluetooth

[2]. 2.http://www.bluetooth.com/English/Pages/default.aspx

[3]. http://www.baracoda.com/shared_docs/bluetooth_protocol.pdf

[4]. http://en.wikipedia.org/wiki/Human_interface_device

[5]. Core V2.1 + EDR.pdf (Specifications)

DESIGN AND DEVELOPMENT OF SYSTEM FOR PUBLIC SAFETY

**GURUDUTT DURGADAS SHETTI, SOORAJ JAYENDRAN,
SUDHANSHU DIXIT & B.PAVAN KUMAR**

Department of Instrumentation Technology
Dr Ambedkar Institute of Technology- B'lore-56

Abstract: The dictionary describes an accident as "an unexpected and undesirable event" and it describes safety as "free from harm or risk ". There are many ways to reduce accidents: regulations, proper infrastructure, and human behavior and as also many devices to assure safety at various areas. According to a news paper titled The Sunday Guardian, India's rank in global prosperity and well-being index slipped down by 10 spots since last year and one of the major reasons for such a slip is Safety. Safety does play a crucial role and do determine the state of development i.e. developing, developed , under developed, developed nations have very low chances of accidents due to high safety regulation and implementations at various levels . Most of citizens try to be unfettered from the safety rules and regulations; their assumption of being the veterans of safety also creates havoc situations.

key words : *PLC, IR sensors, sensors*

"PREVENTION IS BETTER THAN CURE"

The above proverb has inspired us to think over safety. Prevention is only possible at an area only when we follow safety measures or standards. Safety at all aspects is necessary - design, operations, regulations, planning, standards, testing, behavioral safety, and across different sectors, such as Fire, Transportation, Consumer, Industrial, Informal Sector, Buildings and Structures. Structures include our old monuments, houses, big apartments and commercial malls.

Introduction: In our daily life, we come across various situations in our surroundings where we feel strongly that a better safety parameter should be adopted. One of the most non-terminating news that we get to see in the newspaper is "Gas leakages" in every corner of the world; it could be industries, homes any where possible. The Bhopal Gas Plant tragedy that took some 2 decades ago is still influencing the lives of people over there with some unpredictable and incurable diseases. The main objective is to introduce safety at all corners of life i.e. homes, living place. For a safer nation, safety begins from within the day to day practices. So we are trying to propose a safety idea that would decrease the human interference to remarkable level.

Safety at homes : For this safety idea to be more user –beneficial, we have done a survey from the residents of 4-5 apartments and from the feedbacks from over 1.5k residents. We could infer the following were safety parameters which they require :

i. Gas leakage identification system
ii. Power Fluctuation system
iii. Water leakage system
iv. Failure of motor
v. Elevator malfunctioning
vi. Parking Space
vii. Fire Safety
viii. Perimeter Monitoring

Our idea was to monitor all the above eight parameters continuously and indicate it to the required authorities in case of any problem or malfunctions. In most of industries today they use a high speed automation device called PLC i.e. programmable logic controls, it's totally based on operation of logic gates. It works as preprogrammed by the user. We have preferred cause of fast response time of about 100 ms and it's very easy in terms of programming.

Gas leakage Identification system

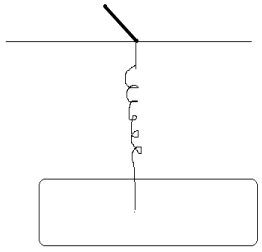

As we can see from the diagram, the rectangular shape would act as diaphragm the darker line will act as a switch, hence forth acting like a pressure switch. It is designed that it would be in equilibrium state at normal pressure any change in pressure would lead the misbalance and thereby operating the switch, which would send signal to PLC and further action, can be taken.

Power Overloading

Many of residents complained of existing method of tripping of MCB in case of overloading stating that tripping has really caused damage to other electrical goods also. So instead of tripping of MCB we can actually indicate the particular home or flat about overloading condition.

Water Leakage System:

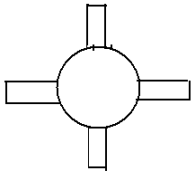

Many of residents have complained about irregular water flow coming and in order to chuck that problem we have thought introducing a water wheel as shown in diagram that rotate at a fixed speed and if only the speed is lower than the threshold the switch is operated actuating a signal to PLC.

Automatic motor ON/OFF

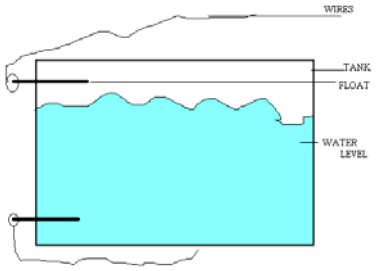

There will be two floats that are placed at low levels and maximum levels so that they actuate the switch according to the water levels. In case of two motor facilities the second motor would switch on if first motor is not operating in 20 seconds.

Elevator malfunction

The motor is provided with the shaft, the purpose of shaft is to indicate any cases of lift getting struck between two floors. Every lift comes with a microprocessor; we would program processor such a

way that it continuously sends an electric pulse to PLC stating its working condition, in case of failure of message to PLC within seconds the message appears on Engineering Console stating about the malfunction.

Parking Space

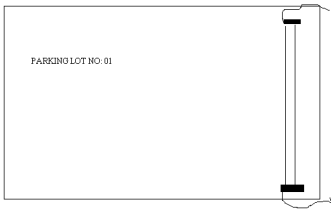

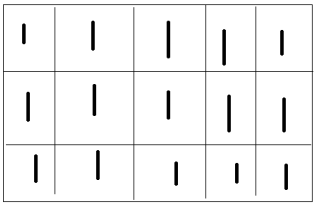

The above is setup for parking system, to left is plan at parking lot , the thick lines indicate IR sensors if the vehicle cuts the path of IR then Led will glow at the security end the right diagram shows the LED setup as soon as the all the lights glow a temporary parking gate opens up automatically indicating security person.

Fire safety

We use ionization smoke detectors that would detect fire and actuate signal to PLC which would inform the local near by fire brigade to take necessary action.

Perimeter Monitoring

We use same idea that's used for parking in case of signal interruption an alarm snoozes and a message is sent to nearest Police Station.

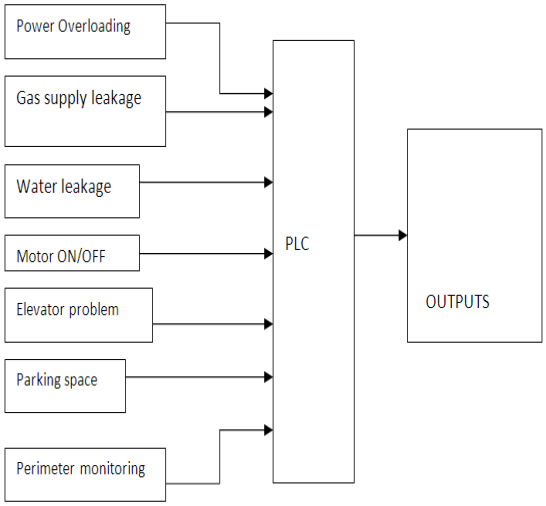

REFERENCE :

[1]. Introduction to Programmable Logic Controllers (3rd Edition) by Gary Dunning

[2]. PLC online material from NPCIL website

[3]. 3. Muhammad Ali Mazidi and Janice Gillespie Mazidi and Rollin D. McKinlay; "The 8051 Microcontroller and Embedded Systems – using assembly and C "- PHI, 2006 / Pearson, 2nd 2006

APPLICATION OF WIDE AREA MONITORING AND CONTROL

SHIKHA SWATI, KIRAN KUMARI, MAUSUMI SAHOO, A.NALINI

Dr. M.G.R. Educational and Research Institute, Chennai, Tamil Nadu-600037

Abstract : Presently India as well as other nation are facing a lot of problem in power sector. It is well known that power sector is a standard field which can raise the bar of India economy. The development and innovation can change the whole scenario and system to make the dark day into bright. In power sector, the protection of system is the major issue to provide a better onitoring and control. Wide Area Monitoring And Control system is one of the major part of it. It support and govern the data and area in short interval of time. In this system data ability and functioning need a proper step, to take work forward. Different types of faults like instability thermal overload are occurring in present system. This paper is basically to analyze and develop a new pattern of governing the power sector through wide area monitoring with the help of simulator. These simulators provides techniques for visualization of stability monitoring and control applications & data for phasor measurement unit.

Keywords: *Phasor measurement unit, PMU, wide area measurement and control WAMS, on-line stability assessment*

INTRODUCTION

Today power system is the essential need for the development of any of the country. Power sector is a field which we can increase the economy scenario of any of the country the increase demands on powersystem is increasing system problems such as instabilities and collapses. The recent series of blackout in different countries has emphasized the need for operator to have better information regarding the actual state of the power system they are operating. One of the promising way to provide a system wide protection and control is wide area measurements system based on phasor measurement units (PMUs). This has become a proven technology and are seen by many utilities as one of the ways of providing phasor information. WAMS provide measure at update rates of 10-20 HZ which enables monitoring of voltage &load evolution dynamics as well as faster phenomena such as oscillatory. Transient and frequency dynamics WAMC system in PMUs offers the measurement of phasors of voltage &current together with a satellite triggered time stamp in time interval down to 20ms. An important role of WAMs to serve as the infrastructure necessary to implement ide area stability control or system protection schemes. This paper present algorithms for power system applications such as frequency stability assessment oscillation detection and voltage stability assessment for few key location. WAMs project equipped with PMUs have more advanced applications such as state and topology calculation and provide snap shots of the powers system 10-20. Time per second load ability calculation using optimization techniques & facts set point optimization.This paper also describe on simulation platform used visualize to the output of the basic & advanced application. This tool can simulate any combination of events or load changes and observe the effect on computed stability margin.

WAMC APPLICATIONS

There will be two different types of applications. Firstly there are applications that can be implemented based on phasor measurements from a few key locations. Secondly, a range of more advanced applications based on a detailed network model can be used, once a sufficient number of PMUs has been placed so that the network state ca be completely observed.

APPLICATION IN KEY LOCATION

A. Transmission corridor voltage

stability Practical application of methods for detection of voltage instability are generally based solely on local measurements. The first methods were based on a local voltage measurement; if voltage becomes abnormally low (below a preset threshold value). Other approaches are based on the estimation of a Thevenin equivalent of the network at a single bus. The current through a single line feeding that bus is used to estimate an equivalent Thevenin equivalent of a potentially complex network and the generation at the remote end.

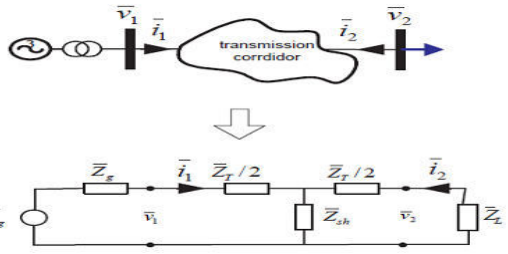

Figure1: T- and Thevenin equivalents of the transmission corridor

This method uses measurements from both ends of the transmission corridor, enabling the splitting of the estimation part into two stages. Firstly, the arameters of a T equivalent of the transmission corridor can be

determined through direct calculation. Secondly a Thevenin equivalent of the feeding generators is computed. Once the parameters of the T- and Thevenin equivalents are known, stability analysis can be carried out analytically and various stability indicators. The main advantage over the present state of the art is that parameters of the equivalent network can be computed from a single set of phasor measurements, and thus this method does not have the time delay. Applying Ohm's and Kirchhoff's laws, with the known complex quantities (measured phasors) v1, i1and v2, i2 , we can calculate the complex impedances ZT, Zsh and Zl as follows.

$$Z_2=2\{(v_1-v_2)/(i_1-i_2)\}$$

$$Z_{SH}=\{(v_1i_2-v_2i_1)/(i_2^2-i_1^2)\}$$

$$Z_L=v_2/-i_2$$

If the genV2erators have voltage controllers and can be assumed to stay within their capability limits, Eg can assumed to be constant and Zg could then be calculated using:

$$Zg=(Eg-Vi)/i_1$$

It is therefore preferential to calculate the equivalent complex voltage of the generators as follows:

$$Eg = v_1 + Zgi_1$$

Once we have calculated the parameters of the T- and Thevenin equivalents, a second Thevenin equivalent for the combined generation and transmission corridor can be calculated as follows:

$$Zth=(Zt/2)+1/\{(1/Zsh)+1/(Zt/2-Zg)\}$$

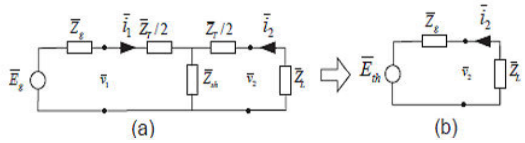

Figure2:- Illustration of T- and Thevenin equivalents of transmission corridor and generation (a), and the reduction to a second Thevenin equivalent modeling the combined generation and transmission corridor (b).

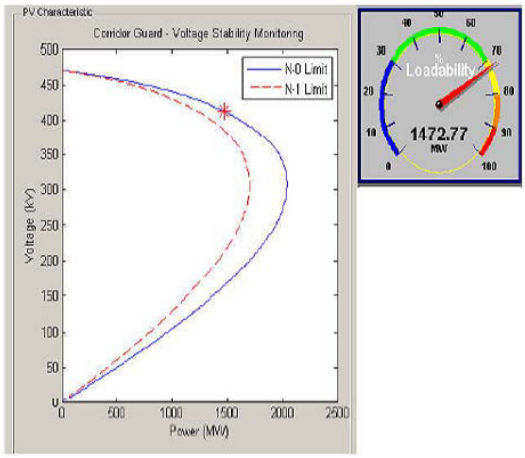

Figure3:- Closeup of the output of the Corridor Voltage Stability Monitoring Algorithm.

B. Oscillatory Stability Monitoring

The oscillatory stability monitoring algorithm uses the collected measured data from one or more locations to estimate the frequency and damping of the dominant electro-mechanical oscillatory modes during normal operation of the power system. Electromechanical oscillations occur in power systems due to lack of damping torque at the generator rotors. Oscillations of the generators rotors cause oscillations of other power system variables, e.g., bus voltage and frequency, and reactive and active powers on transmission lines. Depending on the number of involved generators and the size of the power network, power system oscillations have been reported in the range of 0.05–2 Hz. In general, power system oscillations are ever-present, poorly damped, and not dangerous as long as they do not become unstable. The objective has been to develop an algorithm for a real-time monitoring of oscillations from online measured signals; in other words, to estimate the parameters characterizing the electromechanical oscillations such as frequency and damping and to present this information to the operator in a user-friendly environment of the operator station. An adaptive Kalman filter is used to evaluate the parameters of a reduced-order linear equivalent dynamic model of the power system based on selection of the measurement inputs.

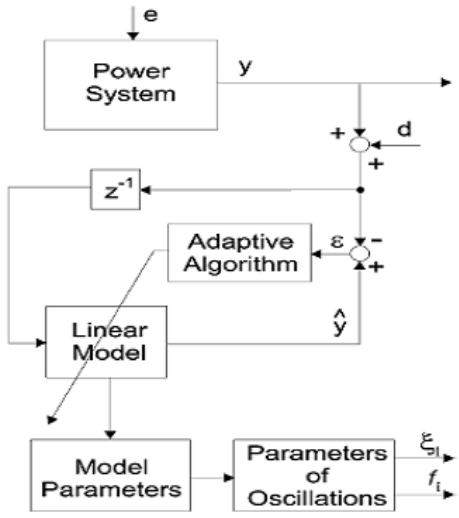

Figure4:-The graphical output of the monitoring algorithm.

In the time series to the left, the top curve shows the signal on which the damping and frequency estimation is based, and the middle and lower ones show the estimated damping and frequency, respectively. In this case, the system is initially well damped. At around 40 seconds the parameters of the generator power system stabilizers are changes such that the oscillation becomes poorly damped, and between 80 and 90 seconds the system is made unstable.

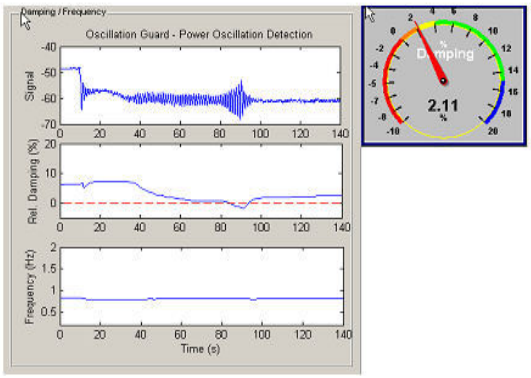

Figure5:- Graphical output of the Oscillatory Stability Monitoring Algorithm

APPLICATION BASED ON WIDE LOCATION

When enough measurements are available, it is possible to completely detect the status of each network element and to calculate each voltage and current of the network. This opens up for more advanced applications as described in the following sections.

A. Line Temperature Monitoring

Loading of the lines is in many cases constrained more by thermal limits than by voltage instability concerns. The thermal limit of a line is usually set according to conservative and stable criteria, i.e. high ambient temperature and no wind. This results an assumption of very limited cooling possibilities and thus low loading. However, often the ambient conditions are much better in terms of possible cooling. This is possible if an on-line working tool for line temperature assessment is available. One of the algorithms serves precisely this purpose.

B. Power Oscillation Assessment Power Oscillation

Assessment is the algorithm used for the detection of power swings in a power system. The algorithm is fed with the selected voltage and current phasors. The algorithm processes the input phasors and detects the various swing (power oscillation) modes. The algorithm quickly identifies the frequency and the damping of the least damped swing modes, that can e.g. lead to angular instabilitycausing major power system disturbances (blackout) The algorithm employs adaptive Kalman filtering techniques.

C. Frequency Stability Assessment

Frequency Stability Assessment receives the data from Basic Monitoring. It early detects the disproportion between the consumed and generated power. The Frequency Stability Assessment algorithm estimates the impact of such a power unbalance on the frequency by modeling of the loads' responses and the generators' inertias. If the estimated frequency is not acceptable, the proposed actions to reach the desired frequency are computed and proposed.

D. Topology detection and state calculation

Topology detection and state calculation are used to provide snapshots of the power system 10-20 times per second. The present topology of the network isinferred from the raw PMU measurements, and therefore the WAMS need not rely on other sources, such a SCADA system for topology information. Following topology detection, an islanding identification is made to detect if the system has separated in to smaller areas. State-calculation is executed once for each island, and serves the purpose of computing the voltages and currents at each bus in the island, also those where no PMUs have been installed. Figure shows the buses

F. Measures against frequency/angular instability

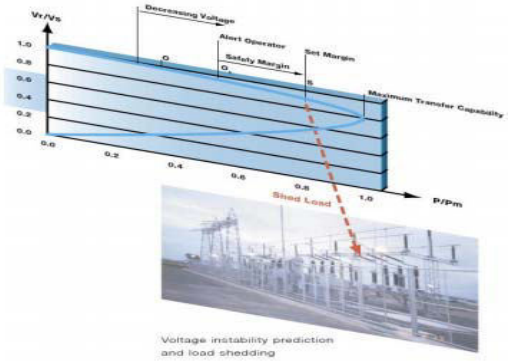

Figure 6:- Voltage instability prediction and load Shedding.

Frequency/angular instability occurs after the tripping of generators or heavily loaded trans- mission lines. In the event of imbalance of generation and load, the optimal actions have to be determined to restore equilibrium taking the actual network topology into account. To prevent the spreading of frequency instability, which leads to large area disturbances, it is necessary to have information available on the power system conditions at several locations in terms of voltage and current phasors. In addition to this, a defence plan has to be established to determine which circuit breakers are to be blocked or to be tripped for under-frequency initiated load-shedding or, as last defence measure, islanding of subsystems. It mightalso be necessary to adapt the setting of the protection relays concerned.

PROPOSED PLATFORM FOR WAMC

The core idea of the WAMC systems is the centralized processing of the data collected from various locations of a power system, aiming at the evaluation of the actual power system operation conditions with respect to its stability limits. In this section, we discuss this fundamental structure of the proposed WAMC system both from the hardware and software point of view.

HARDWARE PLATFORM

The hardware can be explained based on the three stages of the data handling in WAMC.

- Data acquisition
- Data delivery
- Data processing

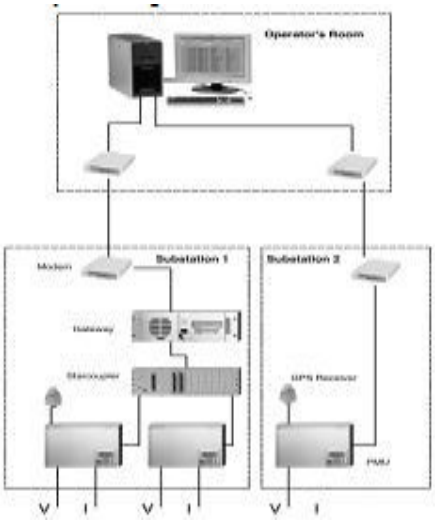

Figure 7:- Hardware model of WAMS.

SOFTWARE PLATFORM

The software structure is modular, as shown in Fig 8.

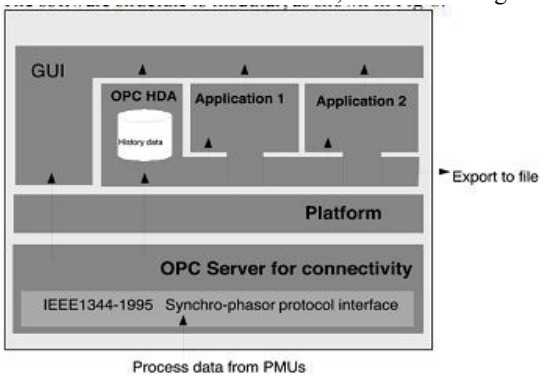

The software packages can be divided into two groups.

- Instability assessment and control applications,
- Auxiliary programs common to all installations of WAMC:

1) Object linking and embedding (OLE) for a process control (OPC) server connecting the PMUs to the platform.
2) The platform itself—storing the data and linking the software packages together.
3) A GUI interpreting the result of the measurement and instability assessment to the user (dispatcher/ operator); history data package.
4) OPC history data access (OPC HDA) provides a set of standard interfaces that allow clients to access historical archives of measurements to retrieve and store the data in a uniform manner.

SIMULATION PLATFORM

We use SIMULINK as a computational engine and MATLAB for the various application and user interface codes. The simulator is comprised of main parts.

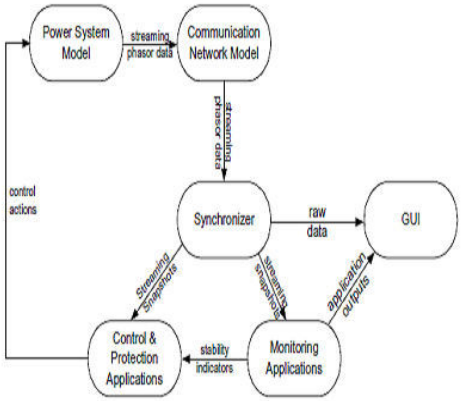

Figure 9:-Simulation engine structure.

POWER SYSTEM MODEL

The power supply module contains a built-in, self regulated DC/DC converter that provides full insulation between the terminal and the external battery system. The PSM, converts a DC input voltage range either from 24 to 60 V or from 110 to 250 V, including a ±20% tolerance on the EL voltage. The output voltages are +3.3, +5, +12 and -12 Volt and the module can provide 50W. The core of the simulation is the dynamic model of the power system that contains the network, the connected loads and generators as well as connected PMUs. The simulator uses a test network based on an actual customer network shown above. The network used here has a longitudinal structure with a clearly defined generation area in the northern end above Cut
1. Generation here is about 2400 MW and the local load is about 600 MW and contains also shunt reactors rated at a total of 275 MVAr. In the southern end is a load area with about 2200 MW of load and 700 MW local generation. In between the cuts is a transmission corridor with five parallel transmissions lines but also about 300 MW of load.

SYNCHRONIZER

The synchronizer collects the data from PMU measurements that are received through the communication network. Each measurement are time-stamped and based on those time stamps, snapshots of synchronized phasors are assembled according to the individual requirements by eachapplication. Data

is collected and accordingly compared with the original data.

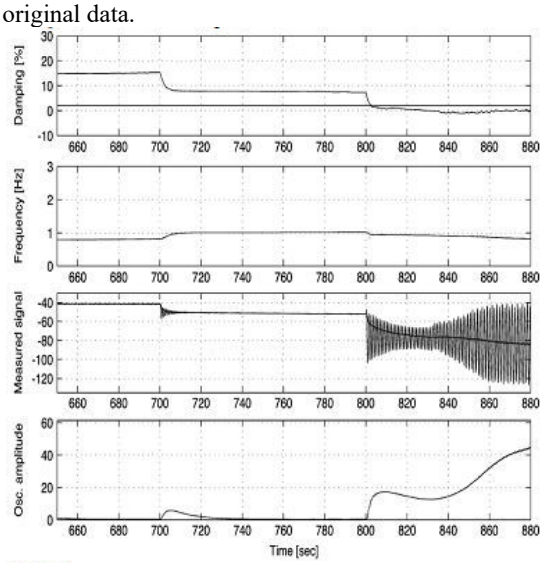

graph 1

MONITORING AND CONTROL APPLICATIONS

Monitoring includes collecting, recording and reporting information which is received from the synchronizer each application executes independently at a predefined interval. Monitoring applications mainly process measurement snapshots into stability indicators that are displayed by the graphical user interface. Controlling process uses data from monitor activity to bring actual performance to planned performance. Control applications determine preventive or corrective controls based on these stability indicators and/or the measurement snapshots received from the synchronizer.

GRAPHICAL USER INTERFACE

In computing, a graphical user interface is a type of user interface that allows users to interact with electronic devices using images rather than text commands. GUIs can be used in computers, hand-held devices such as MP3 players, portable media players or gaming devices, household appliances and office equipment. A GUI represents the information and actions available to a user through graphical icons and visual indicators such as secondary notation, as opposed to text-based interfaces, typed command labels or text navigation. The results of the various applications and in some cases the raw data are visualized by the graphical userinterface. The user interface has been built using Matlab. There are several special features which include: contour mapping, 2-D and 3-D dynamics visualizations, line load flow visualizations, line power oscillation visualizations, voltage stability indicator, contingency assessment, oscillatory stability indicator, oscillation guard, islanding identification, and gauges.

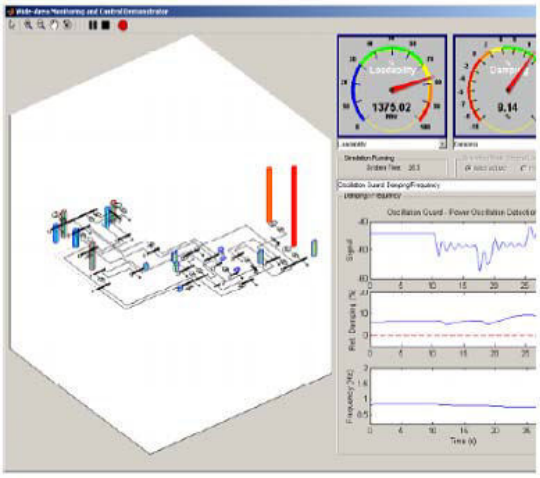

Figure 10:- Visualization of frequency dynamics in 3D and results of oscillatory stability monitoring.

CONCLUSION

The aim of this paper is to describe the simulation platform that will demonstrate and implement the application of wide area monitoring and control. Some of the application is operating in room environment can be operated and control with the help of simulation. The described online monitoring applications will in the future to significantly reduce investment cost for utilities while guaranteeing high levels of dynamic grid loading and availability. Wide Area Monitoring extends the capability of existing local monitoring and protection equipment to further levels of asset utilization.

REFERENCE

[1]. G. Phadke, J. S. Thorpe and M. G. Adamiak, A New Measurement Technique of Tracking Voltage Phasors, Local System Frequency and Rate of Change of Frequency, IEEE Transactions on Power Apparatus and Systems, Vol. PAS-102, No. 5, May 1983.

[2]. CIGRE, “System protection schemes in power networks,”CIGRE Task Force 38.02.19, Tech. Rep., 2000.

[3]. Korba, P., Larsson, M., Rehtanz, C., Detection of Oscillations in Power Systems Detection of Oscillations in Power Systems using Kalman Filtering Techniques, IEEE Conference on Control Applications, Istanbul, Turkey, 2003.

[4]. Larsson, M., Rehtanz, C., and Bertsch, J., Real-time Voltage Stability Assessment for Transmission Corridors, Proceedings of IFAC Power Plants and Power Systems Control Conference, Seoul, Korea, 2003.

[5]. Improved Power System Performance through Wide Area Monitoring, Protection and Control computed by psguard.

[6]. M. Larsson, R. Gardner, and C. Rehtanz, “Interactive simulation and visualization of wide-area monitoring and control applications,” in Proc. Power Systems Computation Conf., Liège, Belgium, 2005, submitted for publication.

AUTOMATIC REPORTING OF WATER QUALITY, LEAKAGE ETECTION AND AUTOMATION OF MOTOR USING WIRELESS TECHNOLOGY

MD QUAISER SAQUIB, MAITRAEE SAMADDER, PRAWEEN KR. BISI, SHUDHANSHU SHRIVASTAVA WEDS KABYA SHREE PRUSHTI, SHUSHANT PALUG

Dept of Electrical and Electronics Department, Dr. M.G.R. University, India

Abstract— In this paper we introduce the notion of leak detection, water environment monitoring and management within the context of properties of the water. More specifically, we investigate the microcontroller based water level sensing and controlling in a wired and wireless environment. Water Level management approach would help in reducing the home power consumption and as well as water overflow. Furthermore, it can indicate the amount of water in the tank that can support Global Water types including cellular dataloggers, satellite data transmission systems for remote water monitoring system. Moreover, cellular phones with relative high computation power and high quality graphical user interface became available recently. From the users perspective it is required to reuse such valuable resource in a mobile application. Finally, we proposed a web and cellular based monitoring service protocol would determine and senses water level globally.

I. INTRODUCTION

The water environment, consisting of the surface water environment and underground water environment, can be differentiated to water bodies like rivers, lakes, reservoirs, oceans, swamps, glaciers, springs, and shallow or deep underground waters. The water environment, as well as other environmental elements like soil, organism and atmosphere, etc, constitute an organic complex. Once a change or damage to the water environment is observed in this complex, changes to other environmental elements inevitably occurs. Detecting and repairing leaks is one of the main components of water conservation. Old or poorly constructed pipelines, inadequate corrosion protection, poorly maintained valves and mechanical damage are some of the factors contributing to leakage. Leak detection has historically assumed that all, if not most, leaks rise to the surface and are visible. In fact, many leaks continue below the surface for long periods of time and remain undetected. With an aggressive leak detection program, water systems can search for and reduce previously undetected leaks. Water lost after treatment and

Pressurization, but before delivered for the intended use, is water, money and energy wasted. Accurate location and repair of leaking water pipes in a supply system greatly reduces these losses. Once a leak is detected, the water utility must take corrective action to minimize water losses in the water distribution system It is obvious that in a country like India, which has such an enormous water area, so diverse water bodies, so scattered spots on a water monitoring network, it will be insufficient to rely on the present numbers of monitoring stations and traditional monitoring technologies to satisfy the current monitoring needs, which emphasizes the fact that water environment monitoring must be continuous, dynamic, macro-scale, and swift; the water quality forecast must be prompt and accurate. Compared with the present water detecting methods, constructing a monitoring system based on the WSNs (wireless sensor networks) would present us with several advantages such as low cost, convenient monitoring arrangements, collection of a variety of parameters, high detection accuracy and high accountability of the monitoring network, etc. A WSN (wireless sensor network) is an *ad-hoc* network system composed of a great number of tiny low cost and low power consumption sensing nodes which are capable of sensing, calculating and communicating data . It is also an intelligent system, which automatically accomplishes all types of monitoring tasks in accordance with the changing environment. The existing automated method of level detection is described and that can be used to make a device on/off. Moreover, the common method of level control for home appliance is simply to start the feed pump at a low level and allow it to run until a higher water level is reached in the water tank. This is not properly supported for adequate controlling system. Besides this, liquid level control systems are widely used for monitoring of liquid levels, reservoirs, silos, and dams etc. Usually, this kind of systems provides visual multi level as well as continuous level indication. Audio visual alarms at desired levels and automatic control of pumps based on user's requirements can be included in this management system. Proper monitoring is needed to ensure water sustainability is actually being reached, with disbursement linked to sensing and automation. Such programmatic approach entails microcontroller based automated water level sensing and controlling.

1. LITERATURE SURVEY

1.1. REVIEW ON LEAK DETECTION AND LEAK LOCATION IN UNDERGROUND WATER PIPE LINESs

1.1.1. LEAK DETECTION AND REPAIR STRATEGIES

There are various methods for detecting water distribution system leaks. These methods usually involve using sonic leak-detection equipment, which identifies the sound of water escaping a pipe. These devices can include pinpoint listening devices that make contact with valves and hydrants, and geophones that listen directly on the ground. In addition, co-relator devices can listen at two points simultaneously to pinpoint the exact location of a leak. Large leaks do not necessarily constitute the greatest volume of lost water, particularly if water reaches the surface where they are usually found quickly, isolated, and repaired. However, undetected leaks, even small ones, can lead to large quantities of lost water since these leaks might exist for a long time. Ironically, many small leaks are easier to detect because they are noisier and easier to hear using hydrophones. The most difficult leaks to detect and repair are usually those under stream crossings. Leak detection efforts should focus on that portion of the distribution system. Active leak detection is crucial in identifying unreported water leakage and losses in the distribution system. Finding and repairing water losses through an active leak detection program will reduce water loss and, in many cases, save substantial money. Without a leak detection program, leaks may only be found when they become visible at the surface, or when major infrastructure collapses. Active leak control will reduce expensive emergency overtime repairs and the associated liability costs. The impact on customers is also greater in emergency repair situations as is the possible impact on other infrastructure (roads, sewers, utilities) and on the environment due to possible discharges of chlorinated water. Detecting leaks is only the first step in eliminating leakage. Leak repair is the more costly step in the process. On average, the savings in water no longer lost to leakage outweigh the cost of leak detection and repair.

1.1.2. LEAK DETECTION METHODS

A few leak detection techniques are known. Their performances regarding to detecting sesitivity are presented in . Because of their advantages we shall concentrate attention on the helium mass spectrometer tecniques but at first a short description of others is presented,

- **Volume change method**
- **Pressure change method**
- **Acoustical leak detection**

1.1.3. BENEFITS OF LEAK DETECTION AND REPAIR

Minimizing leakage in water systems has many benefits for water customers (and their suppliers). These
benefits include:
• Improved operational efficiency.
• Lowered water system operational costs.
• Reduced potential for contamination.
• Extended life of facilities.
• Reduced potential property damage and water system liability.
• Reduced water outage events.
• Improved public relations.
Some added benefits of leak detection and repair that are difficult to quantify include
• inspecting hydrants and valves in a distribution system;
• updating distribution system maps;
• using remote sensor and telemetry technologies for ongoing monitoring and analysis of source, transmission, and distribution facilities. Remote sensors and monitoring software can alert operators to leaks, fluctuations in pressure, problems with equipment integrity, and other concerns.
• inspecting pipes, cleaning, lining, and other maintenance efforts to improve the distribution system and prevent leaks and ruptures from occurring. Utilities might also consider methods for minimizing water used in routine water system maintenance.

1.1.4. ACOUSTIC LEAK DETECTION

Signal detection is the most important part of passive acoustic leak detection. The leak generates a quasi-steady state signal, which is super imposed on background noise (caused by pumps, flow through the pipe, vehicle etc.). To locate the leaks in this environment it is necessary to find a signal characteristics that belong only to the leaks itself and that cannot be a part of the background. This was accomplished in the experiment by bracketing a suspected leak site with two sensors and then searching for similarities in the signals produced by both sensors. When such similarities were found, the time difference of their arrival at each sensor was determined. Using the time difference and sensor placing, it was possible to determine the location of the leaks. The detection frequency of the sensor that is used to detect the sound from underground pressurized pipeline leaks is another major consideration. Environmental noise, such as tht from pumps vehicles and so forth tends to have most of its energy at low frequencies that is below 30 khz.

Attenuation of the sound, however, increases wit ythe frequency of the sound. Thus, although the leaks might stand out more from environmental noise at higher frequencies (have a better signal to noise ratio), the sensor spacing needed to reliably detect the leak that could be so small as to be impractical. To obtain information on this effect, sensor resonant at 15 khz, 30khz,150khz were used. 15 khz produce the most reliable leak location across the variety of leak sources. However for specific leak sources even 150 khz sensors produced useful results. Another interesting result was how variations in the pressure, as well as the introduction of nitrogen gas into the fluid in the pipe line, helped to enhance leak location.
In order to precisely locate a leak in a pipeline it is necessary to determine a time difference,
using the following five steps:
1. Position two sensors so that they bracket (surround) the possible leak. If the sensors do not surround the leak, location cannot be done, no matter what signal processing method is used!
(Only leak detection can be accomplished if the sensors do not surround the leak.)
2. Acoustically couple the sensors to the pipe so that both sensors receive distinct leak signals.
Leak location cannot be performed without signal arrivals at both sensors. This step implies that quick, reproducible methods exist to acoustically couple sensors to pipes in the field.
3. Measure the distance between the sensors along the pipe, D, and determine the velocity of sound in the media contained in the pipe, V.
4. Use signal processing (coincidence detection, cross-correlation, etc.) to determine a time difference, Δt, for the arrival of a specific signal feature at both sensors.
5. Using the time difference (Δt) obtained in Step 4, calculate the location of the leak using the following equation:
Location from first sensor detecting signal(L) = (D - (V *Δt)) / 2

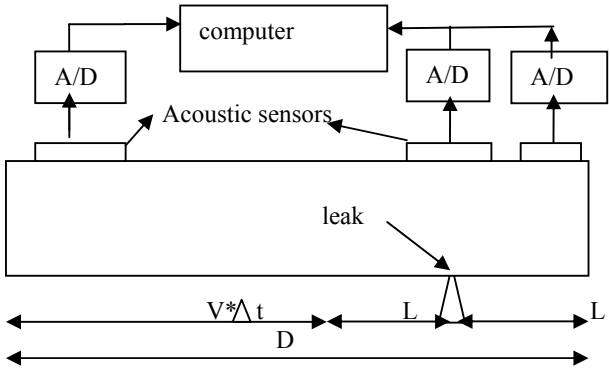

Fig:- leak location by acoustic correlation

2. REVIEW ON TINY LEAK SYSTEM FOR OIL TRANSSMISSION PIPELINES.

- leak detection plays an important role in ensuring public safety, protecting environment.
- Pipeline leak detection methods commonly used can be divided into direct and indirect detection method.
- Direct detection method is to detect the leakage material outside the pipeline, such as cable leak detection method, optical fiber leak detection method.
- indirect detection method is to locate the leak through detection of pipeline's operating parameters, such as negative pressure wave method, mass balance method, pressure gradient method.

2.1. THE PRINCIPLES OF DETECTION

- a sphere detector is used to records pipe wall corrosion, wall defects and conditions etc. The wall defects can be used to determine whether there is a leakage.
- spherical detector adjusts its internal mass distribution and rolls around an axis of the sphere at the bottom of the pipe.
- The leak will be located after the data is processed by wavelet transform methods.
- The location of leak can be identified through the acceleration data from the rolling process and magnetic induction intensity data.

2.2 MACHANISM OF ACOUSTIC WAVE GENERATED BY LEAKS

- When there is a leak the product gushing through the leak produces eddy current due to different pressure inside and outside.
- The vortex generated oscillatory changes with pressure or sound waves The sound waves can spread and reflect leakage point.

ACOUSTIC SENSOR

2.3. THE PRINCIPLE OF LEAK LOCATION

- As the spherical detector rolls forward around an axis along the bottom of the pipe the acceleration of gravity shows variation in at least one component in the three axis components.
- The basic function of the detector is to simultaneously collect kinds of sensor data in the process of detection using different communication protocols.
- Accelerometer, magnetometer and sound modules use SPI, IIC, IIS communication protocols.

LEAK

- The power management is crucial to ensure the smooth progress of detecting
- The obvious advantage of this design is to achieve a balanced distribution of the quality so as to ensure the spherical detector rolls forward around an axis.
- Power management module converts the battery voltage of each module to a suitable operating voltage, and uses the analog switch to operate these voltages according to control signal of microprocessor.

2.2 SUMMARY

- In this paper, a spherical detector is designed based on varieties of pipeline leak detection methods. The device has low risk in pipe blockage and its diameter is smaller than the measured pipe's damage.
- The detector rolls close to the leak in the pipeline internal.
- The results show that the detector has low cost, but sufficient safety and reliability benefits in the pipeline tiny leak detection.

3. REVIEW ON A NOVEL DESIGN OF WATER ENVIRONMENT MONITORING SYSTEM BASED ON WSN

3.1. WATER MONITORING

This paper explains the method of monitoring the water environment by a system based on wireless sensor network. The quality of water which includes PH value, DO, Conductivity etc. The system possesses typical WSN structure with a novel design of sensor nodes, which is easy configured as an arbitrary parameter or multi-parameter monitoring networks. Comparing with the traditional water monitoring system, it has the following merits: the sensor nodes are low cost and low power; the monitoring parameters are flexible; the sensor network on the monitored area is self-organization; the capacity of network is big and the node distribution can be much denser. With the local/remote data monitoring center, a complete monitoring interface can be implemented to carry out historical data queries, real-time data and network state display, data analysis and alarming for non-normal status, etc.

3.2. SYSTEM STRUCTURE

The WSN-based water environment monitoring system is shown. It consists of wireless sensor nodes, sink nodes and a data monitoring center. The sensor nodes are deployed in the water field, it is responsible for the collection and storage of site- pecific parameters, such as water temperature, PH value, DO, conductivity etc. To facilitate network management, the WSN is divided into several sensing clusters according the distance and rangeIt onsists of wireless sensor nodes, sink nodes and a ata monitoring center. The sensor nodes are deployed in the water field. The system mainly includes sensor node and sink node.

1.The sensor node :- the sensor node mainly consists of three parts: water environmrnt sensor, control and wireless communication module, and power supply module.

I) Water environment sensor.
2) Control and communication module.
3) Power supply.

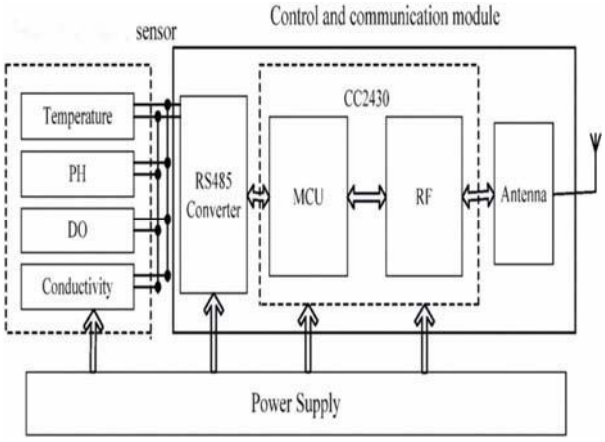

Fig:- structure of sensor node.

2. The sink node:- It also uses CC2430 as main processor to transmit monitoring data based on the ZigBee protocol between the sink node and the data monitoring sub-network. Since the sink node works outdoors, a large capacity battery and reliable DC-DC converting circuit are required for the power supply.

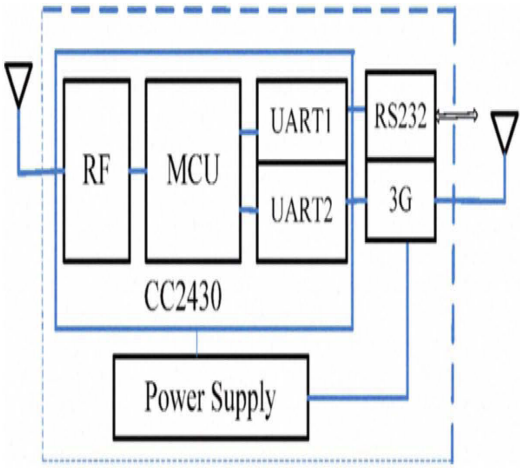

Fig:- structure of sink node

4. REVIEW ON MICROCONTROLLER BASED AUTOMATED WATER LEVEL SENSING AND CONTROLLING: DESIGN AND IMPLEMENTATION ISSUE

4.1. AUTOMATION ON MOTOR

In this paper we introduce the notion of water level monitoring and management within the context of electrical conductivity of the water.
The water level sensing and controlling system are consist of some basic part :

- Water level indicator
- Water level sensor
- Water pump controlling system
- Microcontroller

4.1.1. PIC MICRCONTROLLER:

- PIC is the integrated circuit which is developed to control peripherals devices. We are using a low cost 8-bit PIC microcontroller.

4.1.2. DESIGN AND IMPLEMENTATION:

- **System architecture**:

Microcontroller is to control overall system which reduces the design and control complexity. It takes input from the sensor unit which senses the water level.

- **Sensor unit:**

Water level sensor unit consists two parts, one sensor is used in reserved tank and other four sensors placed inside water tanks.

- **Control unit:**

It performs two operations:

- **Off-operation**: when microcontroller sends 0 volts to the base of the transmitter it becomes OFF and its emitter and collector becomes open. Then no ground signal is collected.
- So the negative side in cable of motor pumps getting positive signal at one side and due to this motor pump will turn OFF and 220v ac at other side.
- **On- operation:** when the microcontroller sends positive signal and its emitter and collector becomes short the transistor becomes ON. Then the circuit and motor pump will get ground signal at negative side.
- Due to this it become ON and 220v ac to the other side.

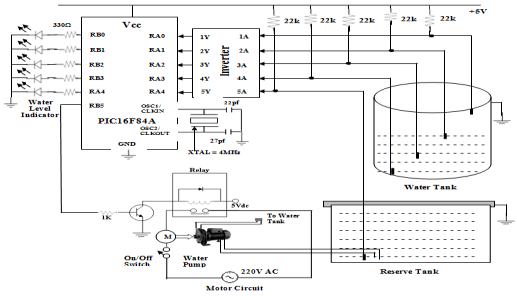

4.2. PROPOSED WATER LEVEL MONITORING NETWORK

- Water is the most important basic needs for all living beings. But a huge amount of water is being wasted during daily life due to lack of control.
- We tried to overcome these problems and implemented an efficient automated water level monitoring and controlling system.
- We established a flexible, economical and easy configurable system which can solve our water losing problem.
- We used a low cost PIC microcontroller in this system which reduced the cost.

4.2.1. DATA COMMUNICATION

- The WLS could be connected to a computer via wireless or USB cable. Controlling server should get serialized data in a fixed time duration via external port.
- Each of these bits represents different sensors activities. Microcontroller should deliver data in data communication.

4.2.2. DATA ACQUISITION AND REPRESENTATION

- Received data should store in buffer and process stored data. Data should be transformed into XML format.
- Data sending method should maintain interface serializability.

4.2.3. REMOTE COMMUNICATION

- Data should be in the graphical interface for integration of the wireless water level monitoring.
- Display the the whole network structure for maintenance user.

6. CONCLUSION

- A new leak location method, based on passive acoustic techniques, is being investigated under an applied research program sponsored by SERDP.
- This method offers significant speed and cost advantage over established techniques that are based on volumetric changes and on pressure loss.
- Choose low-power and the sleeping function devices to design coordination of wireless sensor networks and sensor node.
- The sensor node was designed to suit with arbitrary parameter or multi-parameter sensor modules such as PH, DO, conductivity and temperature.
- Appling the advanced WSN technology and wide coverage of GPRS technology for data collection and transmission, it can solve numerous difficulties.
- The automation of motor helps in reducing the water loss as whenever the leak is detected the

motor is switched on and as the leak is repaired motor is switched on.

• Beside this the sediment is prevented from entering in the motor by sensing the sediment level and indicating if it reaches the pre-defined level and hence the motor is protected from damage and continuous supply of water to the needed areas.

• It finds application in both industrial and domestic use.

7. REFERENCES

[1]. Microcontroller Based Automated Water Level Sensing and Controlling: Design and plementation Issue S. M. Khaled Reza, Shah Ahsanuzzaman Md. Tariq, S.M. Mohsin Reza. - 0958, 2010

[2]. Cao Jian, Qian Suxiang, Hu Hongsheng, et al. ireless Monitoringand Assessment System of Water uality Based on GPRS, ICEMI'07. 8th International Conference on Electronic Measurement and Instruments, Xi'an,China, Aug. 16 2007, vol 2, pp: 124 - 127.

[3]. Microcontroller chip Technology, 2001, PIC16F84A Datasheet www.microchip.com

[4]. "Acoustic Leak Survey of the Underground Potable Water System".Sean Morefield Engineer Research and Development Center, Construction Engineering Research Laboratory, 2902 Newmark Drive, Champaign, IL 61822-1076, USA and John Carlyle

[5]. Carlyle Consulting, 1009 Buckingham Way, Yardley, PA 19067, USA,sean.morefield @erdc. usace.army.mil, jcarlyle@carlyleconsulting.com

[6]. Milenkovic, A., Milenkovic, M., Jovanov, E., Hite, D., and Raskovic, D.: An environment for runtime power monitoring of wireless sensor network platforms, Proc. of SSST' 05, 406–410, 2005.

ASSESSMENT OF MAXIMUM POWER POINT TRACKING (MPPT) TECHNIQUES FOR SOLAR PV SYSTEMS

DEEPAK VERMA, SAVITA NEMA & ARUN M. SHANDILYA

Department of Electrical Engineering Maulana Azad National Institute of Technology, Bhopal

Abstract- Presently so many methods are available for maximum power point tracking (MPPT) of solar photovoltaic (PV). There are some constraints like accuracy, ease of implementation, cost and tracking time, which decides the advantages and disadvantages of the particular methodology. In this paper an assessment among the common methods with comparison is given. This helps in further research, in the direction of maximum power point tracking of solar PV.

Keywords- *MPPT Techniques, Solar PV, Renewable energy.*

I. INTRODUCTION

Now a day's mankind is facing a massive challenge. The overall socio economic growth results the energy demand more and more, as we know to fulfill this energy needs the conventional sources of energy is not sufficient. Many factors are there but the most important is that the sky-rocketing growth of fossil fuels prices shows that we are approaching the ceiling of oil supply. Another factor is that the carbon emission by the conventional energy sources cause increase in the global warming. Renewable energies like solar and wind energy are the best option to achieve all above requirements[11].

Solar energy is a large source of energy which is free of cost, and available to all at fairly equal manner. Two methods are there to extract the solar energy 1) Solar thermal plants 2) Solar cells i.e. photovoltaic cells. Among wide variety of renewable energy projects in progress the photovoltaic cell (Solar PV) is the most promising future energy technology option. The direct conversion of solar radiation to electricity by PV cells has a number of significant advantages as an electricity generator. but some significant challenges to be overcome to make use of Solar energy like Energy cost, Energy fluctuation, Location dependence, Huge investment requirements. The efficiency enhancement is a big issue in reducing cost of PV system since maintenance requirement is very low in PV systems the only real cost savings to be made is in reducing capital cost of installation.[28] Figure 1 shows the IV characteristic and power versus voltage curve of a solar PV system; from the figure it is clear the only one point is there at which solar PV gives maximum power. For extracting the maximum power from the cell the operating voltage or current should be corresponding to the maximum power point (P_{max}) i.e. V_m and I_m respectively under a given temperature and solar radiation.[6][7]

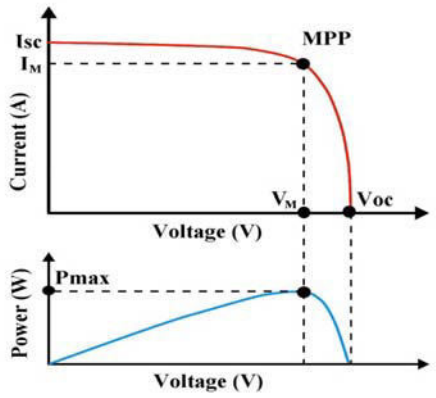

Figure1. Solar PV characteristic. [10],[11]

Since the solar radiation falling on the solar PV module varies with time the operating point or maximum power point (MPP) also changes. The phenomenon of tracking the maximum power point is same as impedance matching by tape changing transformer in case of AC. Here we can use the DC to DC converter and match the resistance by changing duty ratio.

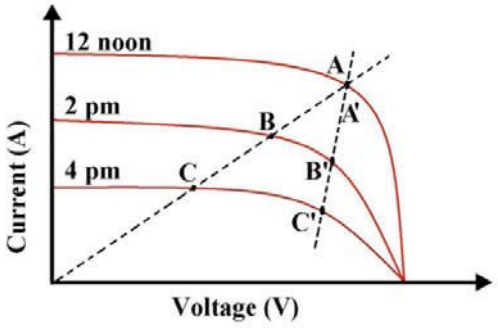

Figure2. Maximum power point for different time [10],[11]

In figure 2 three operating time consider, as an example i.e. 12 noon, 2 pm and 4 pm. With change in time solar radiation also changes. Solar PV in this example with a load resistive type gives the three characteristic with different time also the maximum

power points would be change. Maximum power point tracking is all about the solar PV module to run at the maximum power point A', B' and C' instead of operating point A, B and C. Also the electronic circuitry used to track the maximum power point is known as maximum power point tracker. So many methods are there to track the maximum power point. In this paper we discuss some usual methods.[10]-[27],[29]-[34]

2. EXISTING MPPT TECHNIQUES

Many techniques of finding are MPP reported in literature. Few among them are listed here.

2.1 Constant voltage [5][11]

Constant voltage method is based on the observation that is the maximum power point is occurs between 72-78% of the open circuit voltage Voc for the standard atmospheric condition. The solar PV module is always operates at this constant voltage. The duty ratio of the DC to DC convertor ensures that the PV voltage is equal to:

$$V_M = K \times V_{oc}$$

…….1

Where K = 0.72 to 0.78

2.1.1 Advantages and disadvantages of the method

A) Simple method
B) Easy to implement
C) Not highly accurate
D) V_{oc} needs to be measured at regular interval
E) Fast method
F) Only used where temperature varies very little.

2.2 Constant current

Constant current method based on the same phenomenon of the constant voltage method. The maximum power point arrives between 78-92% of the short circuit current I_{sc}. [3]

$$I_M = K \times I_{sc}$$

…….2

Where K = 0.78 to 0.92

2.2.1 Advantages and disadvantages of the method

A) Simple method
B) Easy to implement
C) Less accurate
D) I_{sc} needs to be measured at regular interval
E) Fast method

2.3 Perturb and observe (P&O) or Hill climbing

Perturb and observe (P&O) method is basically iterative approach in this method the operating point of solar PV oscillates around the maximum power point. In figure 1 the power versus voltage curve of solar PV shows that, change in power with respect to voltage (dP/dV) is positive, negative and zero for region before maximum power point, after maximum power point and at maximum power point respectively.

This method is applied by perturbing the duty cycle at regular interval. And oscillate around the point dP/dV=0 i.e. MPP [3]

TABLE I
METHODOLOGY OF P&O METHOD [3]

Perturbation	Change in power	Next perturbation
Positive	Positive	Positive (increment in duty cycle 'd')
Positive	Negative	Negative (decrease in duty cycle 'd')
Negative	Positive	Negative (decrease in duty cycle 'd')
Negative	Negative	Positive (increment in duty cycle 'd')

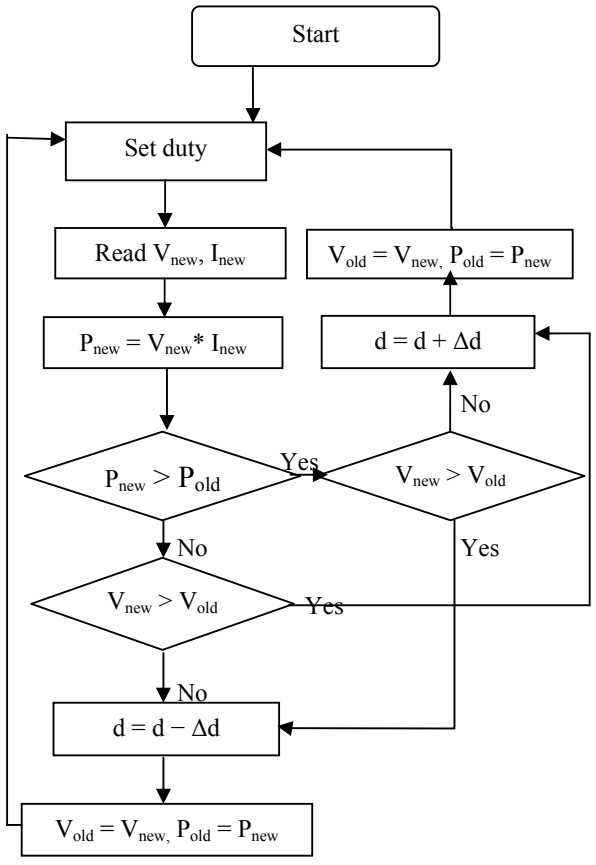

Figure 3. Flowchart of P&O method [11]

2.3.1 Advantages and disadvantages of the method

A) Easy to implement

B) Less accurate operating point oscillate around MPP
C) Iterative approach
D) Slow method, not suitable for fast changing condition
E) Solar characteristic not required to be known earlier
F) Oscillation can be minimized by reducing perturbation step size which slow down the MPPT
G) Voltage and current both to be measured.
H) Some modification in P&O methods also there:
a) Variable perturbation step size
b) Two stage P&O tracking: in which fast tracking is obtained in first stage and finer tracking in second stage. [4]

2.4 Incremental conductance (IC)

Power

$$P = V \times I$$

$$\frac{dP}{dV} = I + V\frac{dI}{dV}$$

At true MPPT

$$\frac{dP}{dV} = 0$$

$$I + V\frac{dI}{dV} = 0$$

$$\frac{dI}{dV} = -\frac{I}{V}$$

Where dI/dV : Incremental conductance
I/V : Instantaneous conductance

Before MPP

$$\frac{dP}{dV} > 0 \quad or \quad \frac{dI}{dV} + \frac{I}{V} > 0$$

After MPP

$$\frac{dP}{dV} < 0 \quad or \quad \frac{dI}{dV} + \frac{I}{V} < 0$$

At MPP

$$\frac{dP}{dV} = 0 \quad or \quad \frac{dI}{dV} + \frac{I}{V} = 0$$

In this method MPP can be found by comparing Instantaneous conductance to the Incremental conductance by changing the duty ratio (d) [8][9]

2.4.1 Advantages and disadvantages of the method

A) MPP is not exactly obtained, oscillation around the MPP.
B) As compared to P&O more time required for computation
C) Voltage and current both to be measured.
D) Required extra circuitry, Complexity increased.
E) Modification can be done same as in case of P&O.

2.5 System oscillation

This method is based on the principle of maximum power transfer and based on comparing the ac component (due to the variation of the duty cycle) and the average value of the input voltage of the Power Conversion Stage to determine the duty cycle. At MPP the ratio of oscillation amplitude and average voltage is constant [1][2]

2.5.1 Advantages and disadvantages of the method

A) Easy to implement
B) Only voltage needs to be measure

2.6 Ripple correlation control (RCC)

This method takes advantage of the signal ripple, which is automatically present in power converters. The ripple is interpreted as a perturbation from which a gradient ascent optimization can be realized. Oscillation in power provided through all pass filter. [1][2]

2.6.1 Advantages and disadvantages of the method

A) Voltage and current both required to be measured
B) Easy to implement, simple circuitry

2.7 Temperature method

In this method temperature of solar PV measured. Variation in MPP with respect to the temperature is obtained in similar way of constant voltage method. [1][2]

2.7.1 Advantages and disadvantages of the method

A) Easy to implement, simple circuitry.
B) Voltage and Temperature both required to be measured

2.8 Beta method

In this method a constant called beta (β) is given, the value of β is given by the formula

$$\beta = ln\frac{Ipv}{Vpv} - \left(\frac{q}{k \times T \times \eta}\right) \times Vpv$$

Where 'k' is Boltzmann's constant, 'η' is diode quality factor, 'T' is ambient temperature in Kelvin and 'q' is electric charge.
It is clear from above equation β is independent from the solar radiation but depends on the temperature. In this method the solar PV operates near to this value β.[1][2]

2.8.1 Advantages and disadvantages of the method

A) Applicable for changing solar radiation but temperature should be constant.
B) There is inverse relationship between the value of β and temperature.
C) Tracking speed is high.

2.9 Some methods are also available which uses the optimization techniques such as *fuzzy logic control, Neural Network, Particle Swarm Optimization (PSO*) which gives excellent results.[35][36][37]

III. CONCLUSION

There are so many methods to obtain Maximum Power Point in solar PV. Some of them are discussed in this paper. There are some constraints which are associated with MPPT techniques like cost, ease of implement, tracking time, accuracy etc., for different application of solar PV out of above constraints, one or two of them are more imperative. Selection of the particular MPPT technique for a specific application is decided by those imperative constraints. For example P&O and IC are widely used where low cost is imperative factor. This assessment of MPPT techniques helps in further research in the area of MPPT also for choosing MPPT technique for specific application.

REFERENCES

[1] M.A.G. De Brito, L.G. Junior, L.P. Sampaio, G.A. e Melo, and C.A. Canesin, "Main Maximum Power Point Tracking Strategies Intended For Photovoltaics", in IEEE Power Electronics Conference (COBEP), 2011, pp. 524 - 530.

[2] M.A.G. De Brito, L.P. Sampaio, L.G. Junior, and C.A. Canesin, "Evaluation Of Mppt Techniques For Photovoltaic Application", in IEEE Conference, 2011, pp. 1039 – 1044.

[3] T. Esram, and P. L. Chapman, "Comparison Of Photovoltaic Array Maximum Power Point Tracking Techniques", in IEEE transaction on Energy Conversion, Vol. 22 No 2 2007, pp. 439 - 449 .

[4] K. Kobayashi, I. Takano, and Y. Sawada, "A Study On A Two Stage Maximum Power Point Tracking Control Of A Photovoltaic System Under Partially Shaded Insolation Conditions", in IEEE Power Eng. Soc. Gen. Meet., 2003, pp. 2612-2617.

[5] Hardik P. Desai and H. K. Patel, "Maximum Power Point Algorithm in PV Generation: An Overview" IEEE International Conference on Power Electronics and Drives Systems PEDS 07, 2007, pp. 624-630.

[6] D. Diallo, F. Belkacem, Eric Berthelot, "Design and Control of a Low Power DC-DC Converter fed by a Photovoltaic array", IEEE International Conference on Electrical Machines and Drives IEMDC 07, Vol. 2, 2007, pp 1288-1293.

[7] Atiqah Hamizah Mohd Nordin, Ahmad Maliki Omar, "Modeling and Simulation of Photovoltaic (PV) Array and Maximum Power Point Tracker (MPPT) for Grid-Connected PV System", International Symposium & Exhibition in Sustainable Energy & Environment, June 2011, pp. 114-119.

[8] Geoff Walker, "Evaluating MPPT Converter Topologies Using A MATLAB PV Model", Journal of Electrical & Electronics Engineering, Australia, Vol. 21, No. 1, 2001, pp. 49-55. 97

[9] Md. Rabiul Islam, Youguang Guo, Jian Guo Zhu and M. G. Rabbani, "Simulation of PV Array Characteristics and Fabrication of Microcontroller Based MPPT", IEEE International Conference on Electrical and Computer Engineering ICECE, December 2010, pp. 155-158.

[10] B. H. Khan "Non Conventional Energy Resources",Fourth edition Book published by Tata McGraw-Hill Publishing company limited, New Delhi

[11] Chetan Singh Solanki "Solar Photovoltaics: Fundamental, Technology and application" Second Edition-2011, Book Published by: PHI Learning Private Ltd., New Delhi

[12] O. Wasynezuk, "Dynamic Behaviour of A Class of Photovoltaic Power Systems", IEEE Transactions on Power Apparatus and Systems, Vol. 102, No. 9, September 1983, pp. 3031-3037.

[13] G. Vachtsevanos and K. Kalaitzakis, "A Hybrid Photovoltaic Simulator for Utility Interactive Studies", IEEE Transactions on Energy Conversion, Vol. 2, No. 2, June 1987, pp. 227-231.

[14] S. Rahmam, M. A. Khallat, and B. H. Chowdhury, "A discussion on the Diversity in the Applications of Photo-Voltaic System," IEEE Transaction on Energy Conversion, Vol. 3, Dec. 1988, pp. 738–746.

[15] F. Mocci and M. Tosi, "Comparison of Power Converter Technologies in Photovoltaic Applications", IEEE International Conference on Industry and Education in Energy and Communication Engineering MELECON 89, 1989, pp. 11-15.

[16] Hebertt Sira-Ramirez, " Non Linear PI Controller Design for Switch mode dc-to-dc Power Converter", IEEE Transaction on Circuits and Systems, Vol. 38, No. 4, April 1991, pp. 410-417.

[17] K. H. Hussein, I. Muta, T. Hoshino and M. Osakada, "Maximum photovoltaic power tracking: an algorithm for rapidly changing atmospheric conditions", IEE Proceedings-Generation, Transmission and Distribution, Vol. 142, No. 1, January 1995, pp. 59-64.

[18] Jesus Leyva and Jorge Alberto Morales, "A Design Criteria for the Current Gain in Current-Programmed Regulators", IEEE Transactions on Industrial Electronics, Vol. 45, No. 4, August 1998, pp. 568-573.

[19] J. A. Gow and C. D. Manning, "Development of a photovoltaic array model for use in power-electronics simulation studies", lEE Proceedings - Electrical Power Applications, Vol. 146, No.2, March 1999, pp. 193-200.

[20] G. R. Walker and P. C. Sernia, "Cascaded DC-DC Converter Connection of Photovoltaic Modules", IEEE Conference on Power Electronics Specialists PSEC 02, Vol. 1, 2002, pp. 24-29.

[21] Soeren Baekhoej Kjaer, John K. Pedersen and Frede Blaabjerg, "Power Inverter Topologies for Photovoltaic Modules – A Review", Research & Development (PSO-F&U) program under Grant No. 91.063 (FU1303), 2002, pp. 782-788.

[21] Weidong Xiao, William G. Dunford and Antoine Capel, "A Novel Modeling Method for Photovoltaic Cells" IEEE Conference on Power Electronic Specialist (PESC, 04), Vol. 3, 2004, pp. 1950-1956.

[22] Pablo Sanchis, Jesús López, Alfredo Ursúa, and Luis Marroyo, "Electronic Controlled Device for the Analysis and Design of Photovoltaic Systems", IEEE Power Electronics Letters, Vol. 3, No. 2, June 2005, pp. 57-62.

[23] Frede Blaabjerg, Florin lov, Remus Teodorescu and Zhe Chen, "Power Electronics in Renewable Energy Systems", IEEE Conference on Power Electronics and Motion Control, 2006, pp. 1-17.

[24] I. H. Atlas, A. M. Sharaf, "A photovoltaic Array Simulation Model for Matlab- Simulink GUI Environment", IEEE International Conference on Clean Electrical Power ICCEP 07, 2007, pp. 341-345.

[25] Vineeta Agarwal and Alok Vishwakarma, "A Comparative Study of PWM Schemes for Grid Connected PV Cell", IEEE International Conference on Power Electronics and Drives Systems PEDS 07, 2007, pp. 1769-1774.

[26] Hiren Patel and Vivek Agarwal, "MATLAB-Based Modeling to Study the Effects of Partial Shading on PV Array

Characteristics", IEEE Transactions on Energy Conversion, Vol. 23, No. 1, March 2008, pp. 302-310.

[27] Jan T. Bialasiewicz, "Renewable Energy Systems with Photovoltaic Power Generators: Operation and Modelling", IEEE Transactions on Industrial Electronics, Vol. 55, No. 7, July 2008, pp. 2752-2758.

[28] R. K. Nema, Savita Nema, and Gayatri Agnihotri, "Computer Simulation Based Study of Photovoltaic Cells/Modules and their Experimental Verification", International Journal of Recent Trends in Engineering, Vol. 1, No. 3, May 2009, pp. 151-156.

[29] Youjie Ma, Deshu Cheng, Xuesong Zhou, "Hybrid Modelling and Simulation for the Boost Converter in Photovoltaic System", IEEE International Conference on Information and Computing Science, Vol. 4, 2009, pp 85-87.

[30] Athimulam Kalirasu and Subharensu Sekar Dash, "Simulation of Closed Loop Controlled Boost Converter for Solar Installation" Serbian Journal of Electrical Engineering, Vol. 7, No. 1, May 2010, pp. 121-130.

[31] M. Elshaer , A. Mohamed, and O. Mohammed, "Smart Optimal Control of DC-DC Boost Converter in PV Systems", IEEE/PES Conference Publication- Transmission and Distribution Conference and Exposition, Nov 2010, pp. 403-410.

[32] X.Felix Joseph, Dr. S. Pushpakumar, D. Arun Dominic and D. M. Mary Synthia Regis Prabha, "Design and Simulation of a soft switching scheme for a DC-DC Boost Converter with PI controller" International Journal of Engineering (IJE), Vol. 4, No. 4, Nov 2011, pp. 285-385.

[33] Mitulkumar R. Dave and K. C. Dave, "Analysis of Boost Converter Using PI Control Algorithms", International Journal of Engineering Trends and Technology, Vol.3, No. 2, 2012, pp. 71-73.

[34] S. P. Sukhatme, "Meeting India□s future needs of electricity through renewable energy sources", General Article- Current Science, Vol. 101, No. 5, September 2011, pp. 624-630.

[35] D. Menniti, A. Pinnarelli, G Brusco, "Implementation of a novel fuzzy-logic based MPPTfor grid-connected photovoltaic generation system" IEEE Conference Publications 2011 , pp 1 - 7

[36] Hong Hee Lee, Le Minh Phuong, Phan Quoc Dzung, Nguyen Truong Dan Vu, Le Dinh Khoa, "The new maximum power point tracking algorithm using ANN-based solar PV systems" IEEE Conference Publications, 2010 , pp 2179 – 2184.

[37] M Miyatake, M Veerachary, F Toriumi, N Fujii, H Ko, "Maximum Power Point Tracking of Multiple Photovoltaic Arrays: A PSO Approach" IEEE JOURNALS & MAGAZINES, 2011 , pp 367 – 380

HOME AUTOMATION THROUGH WIRELESS USING VOICE RECOGNITION AND WEB STATUS INDICATION SYSTEM

S.K.S.SINDHU.ANANTHPALLI
M.TECH(VLSI&ES), Student,
Sasi Institute of Technology & Engineering,
Tadepalligudem-534101,
Andhra Pradesh, India.

T.VENKATESWARA REDDY
M.TECH, Asst Prof.,
Sasi Institute of Technology & Engineering,
Tadepalligudem-534101,
Andhra Pradesh, India.

N.G.V.PRASAD
M.TECH, HOD of ECE Dept.,
Sasi Institute of Technology & Engineering,
Tadepalligudem-534101,
Andhra Pradesh, India.

Abstract-In this paper we are designing a system which is capable of switching ON/OFF the electrical devices based on the speech (command) and monitor through web, which indicates the status of the device. Home automation systems must comply with the household standards and convenience of usage. This system creates a new era in the automation system. This system integrates human-machine interface. Here Zigbee based remote control system that transmits the wireless signals according to the input being selected based on speech commands given by the user through PC using microphone. Zigbee is a wireless technology developed as an open global standard to address the unique needs of low-cost, low-power; wireless sensor networks and is the set of specs built around the IEEE 802.15.4 wireless protocol. Speech is the primary and most convenient means of communication among human beings. Speech recognition is the process of recognizing the spoken word to take necessary actions accordingly. The controlling device of the whole system is done using ARM-7 Microcontroller. The ARM-7 Microcontroller performs appropriate task related to the data received like devices ON/OFF control, intensity control and is programmed using Embedded C language. The system can also control the intensity of the light using Dimmer Interfacing Circuit, though speech commands from the user up to two levels. The ARM-7 microcontroller is also interfaced with GPRS module which is used to display the devices monitoring status directly to the predefined webpage. The microcontroller also takes the responsibility to announce the feedback of the operated devices using APR 9600 voice circuit. The tests involved a mix of male and female subjects with different English accents. Different voice commands were sent by each person of these commands was recognized correctly.

Key Words:- *Home Automation, Zigbee Transreceiver, GPRS, Voice Recognition*

I. INTRODUCTION

Today, the energy consumption in private households is great potential to make the consumers aware of their own consumption patterns so that they will actively help to change their energy use and habits. There is already a lot of electronic equipment in private homes with features which can help to manage and reduce energy consumption and improve comfort in the home. Unfortunately, only a few people can find ways to apply it in everyday life. This means that there is a large untapped potential for energy savings and amendment of energy-using behavior and habits in the home without compromising the comfort of the users. In some applications, human beings have been replaced by unmanned devices that will acquire data and relay the data back to the base[1]. Caring for and supporting this growing population is a concern for Governments and Nations around the Globe [2].

Home automation is one of the major growing industries that can change the way people live. Some of these home automation systems target those seeking luxury and sophisticated home automation platforms; others target those with special needs like the elderly and the disabled. The aim of the reported Wireless Home Automation System (WHAS) is to provide those with special needs with a system that can respond to voice commands and control the on/off status of electrical devices, such as lamps, fans, television etc., in the home. Home automation security system is a specialized field dealing with specified requirements of homes in the usage of easy-to-use technologies for security and comforts of the residents. There have been several commercial and research projects on smart homes and voice recognition systems. Figure 1 shows an integrated platform for home security, monitoring and automation (SMA) from uControl [3]. The system is a 7-inch touch screen that can wirelessly be connected to security alarms and other home appliances. The home automation through this system requires holding and interacting with a large panel which constraints the physical movements of the user [4].

Fig. 1 uControl Home Security, Monitoring and Automation system.

Some applications adding remote accessibility are detailed in [5] and [6], which are built to collect and send data through a modem to a server. Although these are well-built systems that serve the purpose for a specific task, the user cannot interact with the system. Another unidirectional data transfer

is presented in [7], which uses the Global System for Mobile Communications (GSM): a popular wireless choice for connectivity between the data-acquisition units and clients. There are also several systems that allow data to be remotely accessed. As a solution to wireless data collection through the Internet, General Packet Radio Service (GPRS) is a popular choice in several applications. A surveillance system based on GPRS is presented in [8]. A recent work [9] has presented a GPRS solution to the data-acquisition problem for remote areas. A distributed system capable of road vehicle locating, monitoring, and telemetering with GPRS is presented in [10]. A long-distance data-collection system for the Earth tide gravimeter, collecting information on temperature, humidity, atmospheric pressure, etc., is designed with GPRS using a hardcoded static Internet Protocol (IP) address. These systems use GPRS without concerns about minimizing the cost of data transfer.

Similar types of Internet-based systems, such as those in[11]–[13], are designed to gather a bulk of data before serving them upon request. In these applications, data are compiled in a central server and are then served to the clients via the Internet. The client framework is in a central server and has all the applications. A person that needs to access any data must first access the server. An indirect access to the data-acquisition unit makes the system unattractive for real-time control applications, where direct interaction with the system may be required. The need to maintain an additional server will also increase the setup costs and the costs to maintain the acquisition systems, such as regular maintenance costs, system updates, etc.

In Section II, we will introduce the details of the designed system overview. In Section III, we will provide the hardware design in detail that will introduce some of the capabilities of the system using a collection of modules. The software design is detailed in Section IV. The experimental results are discussed in Section V. Section VI presents the conclusion.

II. SYSTEM OVERVIEW

The Wireless Home Automation System (WHAS) is an integrated system to facilitate elderly and disabled people with an easy-to-use home automation system that can be fully operated based on speech commands. The system is constructed in a way that is easy to install, configure, run, and maintain. The functional blocks of the overall system are shown in Figure 2.

GSM and GPRS are developed for cellular mobile communication. A GPRS connection with unlimited duration of connectivity is charged only for the data package transfers and adopted in several mobile remote control/access systems. GPRS becomes a cost-effective solution only if the data transfers can be optimized. Once a GPRS connection has been established, queried data can be relayed to the client via a central server. Using a central server to relay the acquired data has some disadvantages. First, a central server needs a client interface framework. An additional data transfer corresponds to time delays before the data are made available to the client. In addition, since the server acts as a relay, no direct bidirectional communication between the client and the embedded system can be established.

Direct communication, on the other hand, enables access to only relevant information in the embedded system by preprocessing the data. The embedded system should also handle the web services. This eliminates the need for a central server and reduces the amount of data sent from the remote unit since only the queried data will be transferred. This system is configured to be virtually online at all times in a GSM network. An admin script is executed after the boot of the operating system, initiating the GPRS connection software module. A PPP connection is established by a GPRS modem that works at 900/1800/ 1900 MHz operating frequencies.

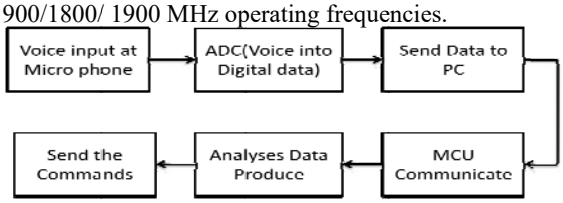

Fig 2 Sequence of activities in the Wireless Home Automation System

- Handheld Microphone Module which incorporates a microphone with RF module (ZigBee protocol).
- Central Controller Module (PC based).
- Zigbee RF Communication
- Appliance Control Modules.

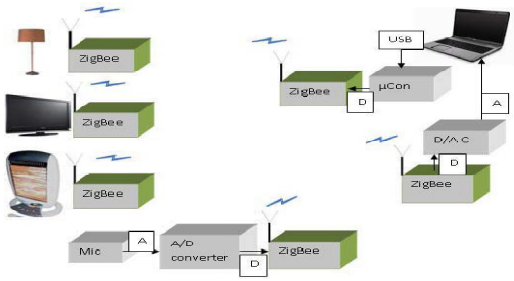

Fig. 3 Functional block diagram of the Wireless Home Automation System (WHAS). Legends- A: Analogue, D: Digital.

Figure 3 illustrates the sequence of activities in the WHAS. The voice is captured using a microphone, sampled, filtered and converted to digital data using an analogue-to-digital converter. The data is then compressed and sent serially as packets of binary data. At the receiving end (Central Controller Module), binary data are converted to analogue, filtered and passed to the computer through the sound card. A Visual Basic application program, running on the PC, uses Microsoft Speech API library for the voice

recognition. Upon recognition of the commands, control characters are sent wirelessly to the specified appliance address. Consequently, appliances can be turned ON or OFF depending on the control characters received those are based on voice intensity as well as Integrating variable control functions to improve the system versatility such as providing control commands other than ON/OFF commands.

III. HARDWARE DESIGN

A. Handheld Microphone Module(MM)

The components of the microphone module are shown inFigure 4. The system captures human voice using a sampling rate (f_s) of 8 kHz. It is known that the highest frequency component of the human voice is 20 kHz, however the most significant parts of the information is encoded in frequencies between 6 Hz and 3.5 kHz. To meet Nyquist sampling criteria, an anti-aliasing filter is used to block all the frequencies above the Nyquist frequency (F_n).

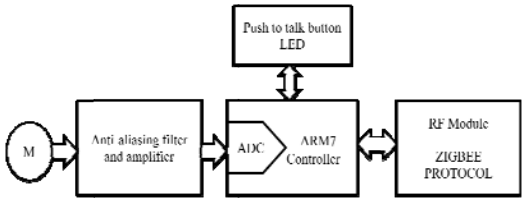

Fig 4 Block diagram of the handheld Microphone Module

The incoming speech wave goes through a low pass filter (Figure 5). A 3-pole Butterworth low pass filter is used as an anti-aliasing filter. The signal is then amplified in order to utilize the full range of the ADC. A voltage divider and a DC blocking capacitor provide a voltage translation from the filters to the ADC. In the microcontroller, data is first converted to digital format using the in-built ADC, the data is compressed from 12 bits to 6 bits. Data are sent serially from the microcontroller to the ZigBee RF module at the baud rate of 115200 bits/s. This is the maximum configurable baud rate provided by ZigBee.

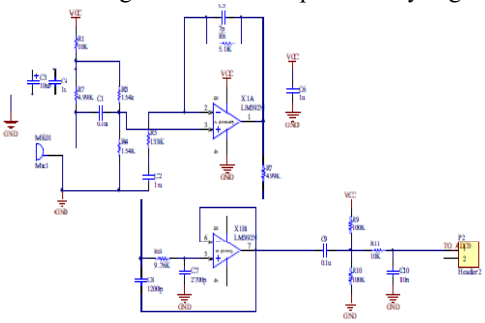

Fig. 5 Portable Microphone Circuit.

B. Central Controller Module

The functional blocks of the central controller module are shown in Figure 6. At the central controller module (coordinator), when data are received, is assigned to the digital-to-analogue converter (DAC). The analogue output of the DAC is filtered and fed to the computer.

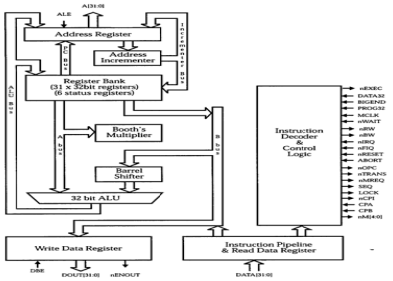

Fig. 6 Central Controller Module.

C. ZigBee RF communication

Zigbee protocol is the communication protocol that's used in this system. Zigbee offers 250 kbps as maximum baud rate, however, 115200 bps was used for sending and receiving as this was the highest speed that the UART of the microcontroller could be programmed to operate at. For each byte transmitted, there is a start and stop bit and the Zigbee RF communication module specification are shown in the below table 1.

Table 1 Zigbee RF communication module specification.

Zigbee RF Communication Specs	
Itron OpenWay Centron Meter v1.0 rev7	
Radio transmit output power	+15 dBm
Receive Sensitivity	-98 dBm
Antenna Type	half-wave slot
Antenna Gain	+3 dBi
Total effective transmit output power	+18 dBm (~64mW)
White Rodgers PCT	
Radio transmit output power	+18 dBm
Receive Sensitivity	-102 dBm
Antenna Type	RPSMA
Antenna Gain	+2 dBi
Total effective transmit output power	+20 dBm (~100mW)

D. Appliance Control Module

Once the speech commands are recognised, control charterers are sent to the specified appliance address through ZigBee communication protocol. Each appliance that has to be controlled has a relay controlling circuit shown in Figure 8.

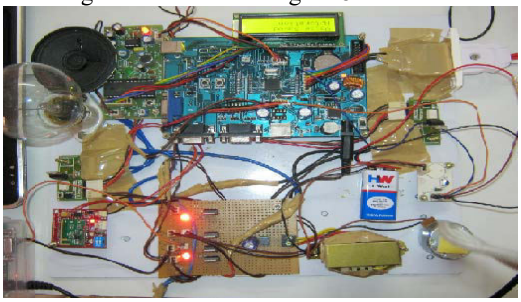

Fig. 8 Receiver section of the appliances control.

IV. SOFTWARE DESIGN

A. Voice Recognition Application

The voice recognition application implements Microsoft speech API. The application compares incoming speech with an obtainable predefined dictionary. The Microsoft speech API run time environment relies on two main engines: Automatic Speech Recognition (ASR engine) and Text To Speech (TTS engine) as shown in Figure 8. ASR implements the Fast Fourier Transform (FFT) to compute the spectrum of the fingerprint data [4]. Comparing the fingerprint with an existing database returns a string of the text being spoken. This string is represented by a control character that gets sent to the corresponding appliance's address and it is shown in figure 9.

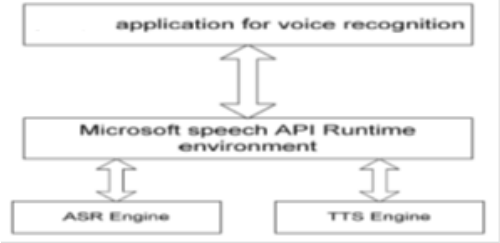

Fig. 9 Voice Recognition application Hierarchy.

The designed graphical user interface (GUI) offers the user the choice of selecting the desired serial communication port as well as it provides a record of all the commands that have been recognised and executed. The application implements the hierarchy described earlier in Figure 8 and the flow chart shown in Figure 9. The Application window is shown in the Figure 12. When designing the programme GUI, making it a user friendly application was a huge priority since the target clients need to avoid any possible complications in the system. A screen shot of the GUI is shown in Figure 11. Control characters corresponding to the recognized commands are then sent serially from the central controller module to the appliance control modules that are connected to the home appliances.

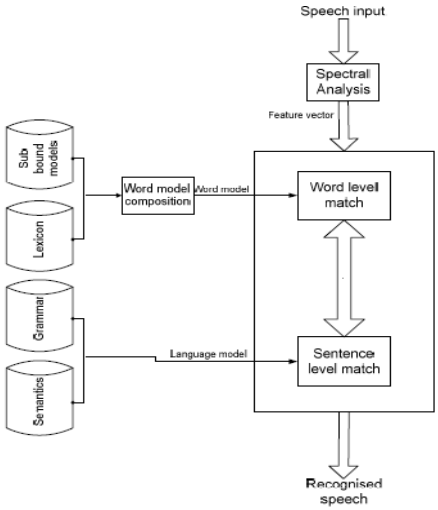

Fig. 10 Flow chart of the Voice Recognition application

Fig. 11 Voice Recognition GUI

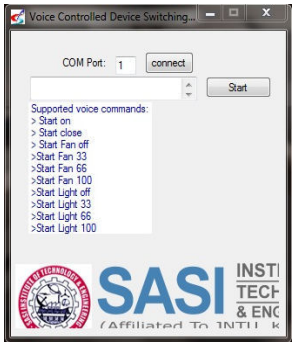

Fig. 12 Application Window

V. EXPERIMENTAL RESULTS

The prototype of the system has been fabricated and tested. Figure 13 shows the complete transmitter model and Figure 14 shows the appliances control module. The tests involved many subjects; the trails were conducted with people with different English accents. The test subjects were a mix of male and female and different voice commands were sent by each person. When a command is not recognized correctly, the software ignores the command and does not transmit any signals to the device control modules. The accuracy of the recognition can be affected by background noise, speed of the speaker, and the clarity of the spoken accent. Finally the status of the device

may displayed in the web pages, which can be interfaced with GPRS.

Fig. 13 Voice Command Transmitting Section.

Fig. 14 Appliances Control Module.

VI. CONCLUSION

The system implements Automatic Speech Recognition engines through Microsoft speech APIs. The system implements the wireless network using ZigBee RF modules for their efficiency and low power consumption. The project "Home Automation Through Wireless Using Voice Recognition and Web Status Indication System" was designed to switch ON/OFF the electrical devices based on the speech (command) according to the input being selected based on speech commands given by the user through PC using microphone. The system uses wireless Zigbee technology and the feedback is announced using Voice module with monitoring status on predefined webpage using GPRS module. The preliminary test results are promising.

REFERENCES

[1] C. E. Lin, C.-W. Hsu, Y.-S.Lee, and C. C. Li, "Verification of unmanned air vehicle flight control and surveillance using mobile communication, "*J. Aerosp.Comput. Inf. Commun.*, vol. 1, no. 4, pp. 189–197, Apr. 2004.

[2] Population Division, DESA, United Nations. (2009). World Population Ageing: Annual report 2009. [29/07/2010].Available:http://www.un.org/esa/population/publications/WPA2009/WPA2009_Workingpaper.pdf.

[3] (2010) uControl Home security system website. [Cited 2010 14th Oct]. Available: http://www.itechnews.net/2008/05/20/ucontrol-homesecurity- system/

[4] R. Gadalla, "Voice Recognition System for Massey University Smart house," M. Eng thesis, Massey University, Auckland, New Zealand, 2006.

[5] W. Kattanek, A. Schreiber, and M. Götze, "A flexible and cost-effective open system platform for smart wireless communication devices," in *Proc. ISCE*, 2002.

[6] J. E. Marca, C. R. Rindt, and M. G. Mcnally, "The tracer data collection system: Implementation and operational experience," Inst. Transp. Studies, Univ. California, Irvine, CA, Uci-Its-As-Wp-02-2, 2002.

[7] E. Bekiroglu and N. Daldal, "Remote control of an ultrasonic motor by using a GSM mobile phone," *Sens. Actuators A, Phys.*, vol. 120, no. 2,pp. 536–542, May 17, 2005.

[8] C. Xiaorong, S. Zhan, and G. Zhenhua, "Research on remote data acquisition system based on GPRS," in *Proc. 8th ICEMI*, 2007, pp. 2-20–2-23.

[9] M. A. Al-Taee, O. B. Khader, and N. A. Al-Saber, "Remote monitoring of vehicle diagnostics and location using a smart box with Global Positioning System and General Packet Radio Service," in *Proc. IEEE/ACS AICCSA*, May 13–16, 2007, pp. 385–388.

[10] C. Zhang, J. Ge, H. Yu, and X. Zhang, "ET gravimeter data collecting system based on GPRS," in *Proc. 8th ICEMI*, Jul. 18–Aug. 16, 2007, pp. 2-86–2-92.

[11] G. Zhenyu and J. C. Moulder, "An Internet based telemedicine system," in *Proc. IEEE EMBS Int. Conf. Inf. Technol. Appl. Biomed.*, 2000, pp. 99–103.

[12] J. Dong and H. H. Zhu, "Mobile ECG detector through GPRS/Internet," in *Proc. 17th IEEE Symp. CBMS*, Jun. 24–25, 2004, pp. 485–489.

[13] P.Wang, J.-G.Wang, X.-B. Shi, andW. He, "The research of telemedicine system based on embedded computer," in *Proc. 27th IEEE Annu. Conf. Eng. Med. Biol.*, Shanghai, China, Sep. 1–4, 2005, pp. 114–117.

DYNAMIC VOLTAGE RESTORER BASED ON FLYING CAPACITOR MULTILEVEL CONVERTERS OPERATED BY REPETITIVE CONTROL

LAVANYAREDDY.B & D.CHINNAKULLAY REDDY

Abstract—This paper presents the control system based on the so-called repetitive control for a five-level flying-capacitor dynamic voltage restorer (DVR). This DVR multilevel topology is suitable for medium-voltage applications and operated by the control scheme developed in this paper. It is able to mitigate power-quality disturbances, such as voltage sags, harmonic voltages, and voltage imbalances simultaneously within a bandwidth. The control structure has been divided into three subsystems; the first one improves the transient response of the filter used to eliminate the modulation high-frequency harmonics, the second one deals with the load voltage; and the third is charged with maintaining balanced voltages in the flying capacitors. The well-developed graphical facilities available in PSCAD/EMTDC are used to carry out all modelling aspects of the repetitive controller and test system. Simulation results show that the control approach performs very effectively and yields excellent voltage regulation.

Index Terms—*Dynamic voltage restorer (DVR), flying capacitor multilevel converter, harmonic distortion, power quality (PQ), repetitive control, voltage sag.*

I. INTRODUCTION

Power quality (PQ) has become an important issue over the past two decades due to the relentless integration of sensitive loads in electrical power systems, the disturbances introduced by nonlinear loads, and the rapid growth of renewable energy sources. Arguably, the most common PQ disturbance in a power system is voltage sags [1], but other disturbances, such as harmonic voltages and voltage imbalances, may also affect end user and utility equipment leading to production downtime and, in some cases, equipment terminal damage.

The dynamic voltage restorer (DVR) is one of the most efficient and economic devices to compensate voltage sags [2]. The DVR is basically a voltage-source converter in series with the ac grid via an interfacing transformer, conceived to mitigate voltage sags and swells [3]. For low-voltage applications, DVRs based on two-level converters are normally used [4] and, therefore, much of the published literature on DVRs deals with this kind of converter. Nevertheless, for higher power applications, power-electronic devices are usually connected to the medium-voltage (MV) grid and the use of two-level voltage converters becomes difficult to justify owing to the high voltages that the switches must block.

One solution is to use multilevel voltage-source converters which allow high power-handling capability with lower haronic distortion and lower switching power losses than the two-level converter [5].

Among the different topologies of multilevel converters, the most popular are: neutral-point clamped converters (NPC),flying-capacitor converters (FC), and cascaded-multimodular or H-bridge converters [6]. NPC converters require clamping diodes and are prone to voltage imbalances in their dc capacitors. The H-bridge converter limitations are the large number of individual inverters and the number of isolated dc voltage sources required. The main drawback of FC converters is that the number of capacitors increases with the number of levels in the output voltage. However, they offer more flexibility in the choice of switching combinations, allowing more control of the voltage balance in the dc capacitors. Furthermore, the extension of a converter to a higher level one, beyond three levels, is easier in FC converters than in NPC converters [7], which makes the FC topology more attractive. A more comprehensive list of the merits and drawbacks of each topology can be found in [8], while a detailed description of multilevel-converter topologies as well as control strategies and applications can be found in [9]-[11].

In the past few years, research work has been reported on the use of FC-converter topology for flexible ac transmission system (FACTS) applications. In [5], a unified power-flow controller (UPFC) based on a five-level FC multilevel converter is proposed for power-flow control. The shunt and series converters are operated by phase-shifted sinusoidal pulse-width modulation (see [10]) where the control system uses several proportional-integral (PI) controllers implemented in the d-q synchronous reference frame. The same authors developed an HVDC transmission system by using a three-level FC converter with interesting hybrid pulse-width modulation [12]: in normal conditions, a selective harmonic elimination-pulsewidth modulation (PWM) (SHE-PWM) is used, which allows eliminating certain low-order harmonics by choosing the switching instants and provides a low switching power loss due to the low equivalent switching frequency. This kind of modulation produces triple harmonics in the converter output voltage which are eliminated by means of the delta or floating star-connected transformer secondary windings. Nonetheless, for asymmetrical faults, the converter is required to generate unbalanced three-phase voltages

and large triple harmonics would appear on the grid side as they could not be completely cancelled out by the transformer. For those situations, the solution proposed is to

change from the SHE-PWM to the phase-shifted PWM, which does not produces low-order harmonic voltages, although it exhibits a higher power loss than the SHE-PWM due to the higher switching frequency of the converter. Reference [13] studies the design of a five-level FC converter-based STATCOM and SSSC connected to a single-machine infinite bus (SMIB). The

work analyses the stability of the SMIB when the STATCOM and the static synchronous series compensator (SSSC) are used to compensate it. Since in FC converters a specific voltage level can be obtained by several switching combinations, the control of the voltage capacitors is achieved by carefully choosing such combinations for either charging or discharging the capacitors and, hence, to balance the voltage capacitors. In this area of work, the following control techniques have been employed: PI regulators are used to control the voltage in the dc link, the root mean square (rms) value of the voltage at the point of connection (in the case of the STATCOM), and the injected voltage into the SMIB (in the case of the SSSC). In [14], a distribution STATCOM was made up with a five-level FC converter. In this paper, hysteresis current control was designed to regulate the current injected into the distribution system by the STATCOM, while a PI regulator was used to control the dc-bus voltage of the converter. The flying capacitor voltage balance is achieved by comparing the capacitor voltages with the reference values by means of hysteresis comparators. These comparators govern the charge/discharge actions of the flying capacitors as a function of the voltage error. This balancing technique provides good dynamic performance compared with other methods.

Research work has been reported on several DVR multilevel topologies [15]-[18], but so far, no work seems to have been published on DVRs by using FC multilevel converters.

This paper focuses on the design of a closed-loop control system for a DVR by using a five-level flying-capacitor converter, based on the so-called repetitive control. Repetitive control was originally applied to eliminate speed fluctuations in electric motors [19], [20], but it has also been successfully used in power-electronics applications, such as power-factor control in three-phase rectifiers and active-filter control [21]-[23].

The control system presented in this paper has a wide range of applicability. It is used in a DVR system to eliminate voltage sags, harmonic voltages, and voltage imbalances within a bandwidth. Unlike other control schemes with a comparable range of applicability, only one controller is needed to cancel out all three disturbances simultaneously, while exhibiting good dynamic performance. On the one hand, a closed-loop

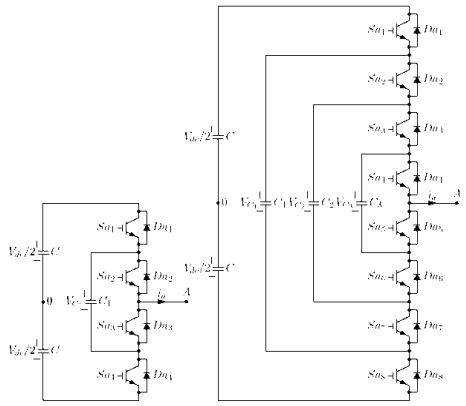

Fig. 1. Phase leg of two different flying-capacitor multilevel converter topologies. (a) Three level. (b) Five level.

controller, which consists of a feedback of the load voltage and the repetitive controller, guarantees zero tracking error in steady state. On the other hand, the applied control strategy for the voltage balancing of the flying capacitors, along with a feedforward term of the grid voltage and a controller for the output voltage of the DVR filter, provides excellent transient response.

This paper is organized as follows. The model of a five-level flying-capacitor DVR is presented in Section II. The complete control-scheme structure is studied in Section III, including the three different control subsystems, namely, the filter output voltage controller, the repetitive control structure for the load voltage, and the flying-capacitor voltage regulator scheme, as well as the modulation method used to operate the multilevel converter. Simulation results obtained by implementing the control system and the five-level flying-capacitor DVR in PSCAD/EMTDC are presented in Section IV. Finally, the main

conclusions are given in Section V

II. CONFIGURATION OF THE DVR

A. Five-LevelFC

Fig. 1 shows two different topologies of the flying-capacitor multilevel converter. The converter in Fig. 1(a) provides a three-level output voltage and the flying capacitor C \ is charged to Vdc/2, whereas Fig. 1(b) depicts a phase leg of a five-level flying-capacitor converter. In both cases, each phase leg has the same structure in three-phase converters, and the flying capacitors of one phase are independent from those of the other phases. One advantage of the flying capacitor multilevel converter topology is that the extension to converters with more than three levels is easier than in the neutral-point-clamped option (see

[7] and [10]). Nevertheless, the number of capacitors becomes excessive as the number of levels increases.

Regarding the five-level topology shown in Fig. 1(b), the flying capacitors Ci, C_2, and C_3 are charged to $3Va_c/4$, $Vdc/2$ and $Vd_c/4$, respectively. Therefore, each switch must block only a voltage value equal to $Va_c/4$, allowing the use of switches with lower-rated voltage compared with those used in a conventional two-level converter. There are several switching combinations for the same given output voltage, which is known as switching redundancy [7]. These switching combinations result in different charging or discharging states of the flying capacitors, which provide a degree of freedom for balancing the flying capacitor voltages. Comprehensive explanations of the switching combinations and their results can be found in [7] and [13].

B. DVR Connection System

The location of the DVR placed between the grid and the sensitive equipment is shown in Fig. 2. Different kinds of

DYNAMIC VOLTAGE RESTORER

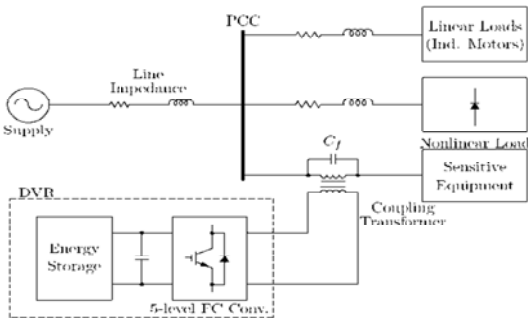

Fig. 2.Basic scheme of the system configuration with the DVR.

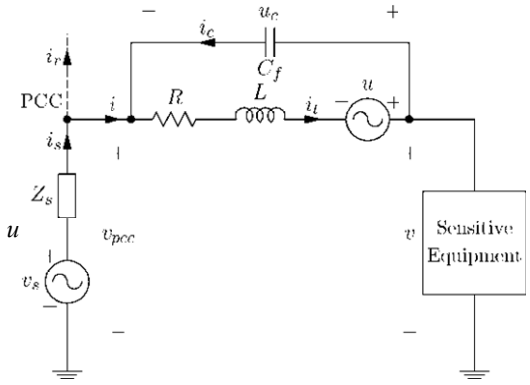

Fig. 3.Equivalent circuit for the DVR-connection system.

loads are assumed to be connected to the point of common coupling (PCC), such as linear loads (e.g., induction motors), nonlinear loads, and sensitive equipment. The DVR consists of a five-level flying-capacitor voltage-source converter and energy storage which provides the necessary voltage to the dc link. The series connection of the DVR is achieved by means of a coupling transformer. A passive LC filter has been used to filter out the high harmonics generated by the PWM process (see, for example, [16]).

The equivalent circuit for the one-line system in Fig. 2 is depicted in Fig. 3, where v_s is the supply voltage, Z_s models the line impedance, i_s is the current injected by the supply, which splits at the PCC into the current flowing through the sensitive equipment i (this current is divided into the current through the coupling transformer i_t and the current through the filter capacitor i_c), and the current injected into the loads i_r. The voltage v_{pcc} is the measured voltage at the PCC, u stands for the DVR voltage which has been modelled as an ideal voltage source, the parameters R and L are the resistance and the leakage inductance, respectively, of the coupling transformer whereas Cf is the capacitor used together with the coupling-transformer leakage inductance to filter out the high-frequency harmonics. Finally, u_c and v are the voltages across the filter capacitor and the measured voltage across the sensitive equipment, respectively.

$$\frac{d}{dt}\begin{bmatrix} i_t(t) \\ u_c(t) \end{bmatrix} = \begin{bmatrix} -\frac{R}{L} & -\frac{1}{L} \\ \frac{1}{C_f} & 0 \end{bmatrix}\begin{bmatrix} i_t(t) \\ u_c(t) \end{bmatrix} + \begin{bmatrix} \frac{1}{L} & 0 \\ 0 & -\frac{1}{C_f} \end{bmatrix}$$

where the state variables are $i_t(t)$ and $u_c(t)$, the control input is $u(t)$ and $i(t)$ is a disturbance input.

III. CONTROL SYSTEM AND MODULATION STRATEGY

A. Control System for the Output Voltage of the LC Filter

System (2) is a second-order filter with natural frequency $uj_n = 1/yjLCf$ and damping coefficient £ $= R/2 \bullet yJCfjL$. This filter exhibits a large resonance since the resistance R usually has a very small value and, therefore, the damping coefficient is also very small. To overcome this problem, closed-loop control of the filter output voltage is required.

(3)

A proportional state-feedback controller plus a feedforward term are proposed for (2), with the following structure:

where **K** is the feedback-gain matrix, $u^*_c(t)$ is the reference value, and the feedforward term $h(i(i))$ is a function of $i\{t)$ which will be calculated to cancel out the effect of the disturbance $i(t)$ on the voltage $u_c(t)$.

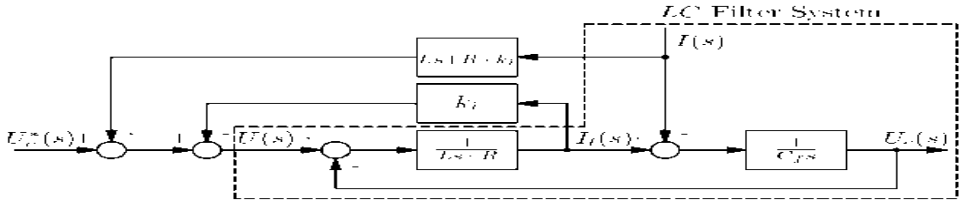

Fig. 4.Filter-output-voltage control scheme.

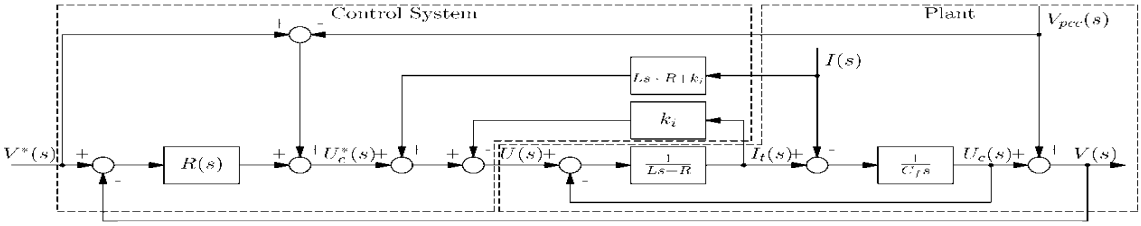

Fig. 5. Load-voltage closed-loop control scheme including the regulator for the filter output voltage.

B. Load-Voltage Control Scheme

The control system developed in the previous section requires further development since it may be not able to guarantee a perfect compensation of the load voltage for every situation. In order to counteract possible disturbances which can affect the load voltage, an outer closed-loop control system is required. The control scheme proposed in this paper uses a feedforward term of the voltage at the PCC to improve the transient response and a feedback term of the load voltage to guarantee zero error in steady state against disturbances.

Fig. 5 shows the complete continuous-time control system for the load voltage. Assuming that there are no modelling errors and neglecting any delay in the control system, the DVR can be seen as an ideal linear amplifier (see [24]). The coupling transformer, together with the capacitor Cf, has been included in the figure as well as the detailed control system for the filter output voltage. The input $V^*(s)$ is the setpoint for the load voltage $V(s)$, $U(s)$ is the DVR voltage, and $V_{pcc}(s)$ is the supply voltage.

Recalling that

$$U_c(s) = \frac{LC_f s^2 + C_f(R + ki)s + 1}{} = G_u(s)U^*_c(s). \quad (5)$$

Then, the load voltage can be calculated as By analyzing the frequency response, it can be seen that $F(jujh) = 1$ and $F_w(jujh) = 0$ for frequencies $uh = huj\backslash$ with . Hence, if the closed-loop system is stable, this frequency response shows that the error in steady-state is zero for sinusoidal reference inputs or sinusoidal disturbance inputs of frequency uuh.

Unfortunately, the implementation of the controller is not ideal due to factors, such as modelling errors, inverter time delay [24], or dead-time effects in the converter switches [25], which may substantially affect the dynamic performance or even end up in unstable systems. To solve this problem, the following transfer function for the controller is proposed:

$$1 - Q(s)e^{-T\circ}$$

where $Q(s)$ is the transfer function of a low-pass filter [20] with $T = 2\,TT/UJI - [3$, and $(3$ is a design parameter which is smaller than the period of the supply voltage $(/3 < 2n/uji)$. Transfer functions (7)-(8) become

$$F(s) = \frac{\sim 2 - Q(s)e^{-Ts}]\ G_u\{s)\ 1 - Q(s)e^{-Ts} + G_u(s)\ [1 - G_u(s)\}\ [1 - Q(s)e^{-T\circ}]}{Q(s)e^{-T}\gg + G_u(s)} \quad (13)$$

$$F_w(s) \quad (14)$$

with $V(s) = F(s)V^*(s)$

$$F(s) + F_w(s)V_{pcc}(s) \quad (6)$$

$$) \quad (7)$$

$$\frac{[1 + R(s)\}\ G_u(s)}{1 + R\{s)G_u(s)} \quad (8)$$

$$\underline{1 - G_u(s)\ l + R(s)G_u(s)}$$

In order to illustrate the main features of the repetitive control, a basic transfer function of the controller $R(s)$ is proposed as

$$R(s) = \frac{1}{} \quad (9)$$

where $u)\backslash$ is the fundamental frequency of the supply voltage. The substitution of (9) into (7) and (8) yields

$$F(s) = \frac{1 - e^{-27r/\wedge s} + G_u(s)\ [1 - G_u(s)]\ [1 - e^{-2}\text{-}/\wedge]\,1}{- e^{-27r}/\wedge i^* + G_u(s)} \quad (10)$$

$$= \quad (11)$$

$$R(s)$$

The characteristic equation of the resulting closed-loop system is

$$1 + G_u(s) \cdot Q(s) e^{G(s)}$$

In order to guarantee stability, the term $G(s)$ in (15) must comply with the Nyquist criterion: if the number of unstable poles of the open-loop system $G(s)$ is equal to zero (P = 0), then the number of counterclokwise encirclements of the point $(-1,0)$ of the term $G(JUJ)$must be zero $(N = 0)$ with — oo<.

The low-pass filter $Q(s)$ has been chosen so that its poles are stable and, as the poles of the transfer function $G_u(s)$ are also stable (see (5)), the number of unstable poles of the open-loop $G(s)$ is $P = 0$. In this paper, a continuous-time second-order Bessel filter has been used since it can be approximated by a constant time delay $(Q(jou) \approx e^{-J/3g})$ within its pass-band, with $(3Q$ being the time delay of the filter [26]. In order to obtain $F(jujh) = 1$ and $F_w(jujh) = 0$, the time delay of the term $Q(s)e^{\sim(27T\wedge 1\sim'3'>8}$must be $2-\kappa/UJL$Since this delay is equal to $ftq + 2-\kappa/UJI-ft$within the Alter passband, the parameter ft is chosen to cancel out the Alter time delay $(ft = ftq)$ and, under such conditions, the closed-loop-system frequency response will satisfy $F(juj_h) = 1$ and $F_w(juj_h) = 0$ while the approximation of a constant time delay is valid.

Obviously, the bandwidth of the controller will be limited because the magnitude characteristic of the filter will decrease as frequency increases.

C. Phase-Shifted Pulsewidth Modulation

Several modulation methods have been used in multilevel converters according to the switching frequency [10]. In this paper, the well-known phase-shifted PWM method has been used since its implementation is simple and provides a certain degree of flying-capacitor voltage balance [7].

In a scheme with an n-level converter, n — 1 triangular carriers with frequency f_c have to be compared with a common sinusoidal modulating signal with frequency /m[27]. It is assumed that the carrier frequency is high enough to consider the modulating signal as a constant value in a period of the carrier. The switching instants are determined by the intersection between the modulating signal and the different carriers. A shifting phase of $2-\kappa/(TI-1)$ is introduced in each carrier, which ensures an effective switching frequency of (n - l)/c and improves the total harmonic distortion of the output voltage, while the frequency modulation ratio yields $rrif = (n - l)f_c/f_m$- For the three-phase case, three modulating signals with a shifting phase of 120° are used.

D. Flying-Capacitor Voltage Control

In theory, the phase-shifted PWM method is able to balance the flying-capacitor voltages. Nevertheless, in practical implementations, there may be $-T\theta$. factors, such as asymmetrical conditions, different characteristics of power switches, etc, that produce voltage imbalances in the flying capacitors. For that reason, a control scheme, which guarantees the balance of the FC voltage, is required.

Although there are several research papers which report on FC voltage control, (see, for example, [7], [12]-[14]), in this paper, the method proposed in [28] has been used because of its simplicity and ease of implementation.

Voltage control is based on a closed-loop control scheme which corrects, for each switch, the modulating signal by adding a square-wave in order to increase or decrease the capacitor voltages. In this paper, only a brief description of the method is provided since the algorithm is fully explained in [28].

Let n and m be the number of FC-converter levels and the index of the switches be connected to the positive terminals of the different flying capacitors, respectively, with . Then, the general law of the square waveform for each switch can be written as where "sign" is the sign function, i is the phase current, D is the amplitude of the square wave, and D_{sm}stands for the change of the duty cycle: a value of D_{sm}= -1 means a duty cycle decrease, D_{sm}= 1 corresponds to a duty cycle increase, and the duty cycle remains no change when $D_{sm} = 0$.

The different FC voltages are compared with their references by means of hysteresis comparators, and the outputs of these comparators are used as inputs of a logic function in order to calculate the values of $D_{sm}$and, hence, to modify the (15) switch duty cycle.

The calculated waveform d_m is added to the sinusoidal modulating signal, and the resulting waveform is compared with the corresponding carrier for each switch in order to obtain the switching instants.

IV. STUDY CASE

In order to verify the proposed control algorithm in a five-level flying-capacitor DVR, the test system depicted in Fig. 2 has been implemented in PSCAD/EMTDC. The test system is comprised of a three-phase voltage source of 11 kV at 50 Hz which feeds a linear load, a nonlinear load, and a sensitive load: the linear load is a three-phase squirrel-cage induction motor of 1350 kW, the nonlinear load consists of an uncontrolled three-phase rectifier with a capacitive filter in the dc side of the rectifier in parallel with an inductive-resistive load. The sensitive load is made up of a 120-kW three-phase squirrel-cage induction motor and an inductive-resistive load of 300 kVA and power factor PF = 0.92. The five-

level flying-capacitor converter is connected to the PCC by means of three single-phase coupling transformers of 160 kVA, with unity turns ratio and a star-connected secondary winding. The dc voltage of the multilevel converter is 8 kV. The output filter cutoff frequency was set at $f_c = 2$ kHz with a capacitor $C_f = 1.05$ //F. Finally, the value of each flying capacitor is $C\backslash = C_2 = C_3 = 250\,fjF$ [see Fig. 1(b)], while the switching frequency was set at $f_{sw} =$ 1650 Hz for each switch. For the five-level converter studied here ($n = 5$), the effective switching frequency is $f_{SWT} = 6600$ Hz. The main parameters of the test system are summarized in Table I.

A. Controller Parameters

The parameters of the control systems for the LC output filter and the load voltage have been calculated from the values of the copper loss resistance, the leakage inductance, and the capacitor Cf using MATLAB. The cutoff frequency of the LC filter is 2 kHz. Hence, the computed matrix gain that is necessary to obtain this cutoff frequency is $\mathbf{K} = [A;,;k_u] = [150.30\ 0]$ and, with reference to (3), it is shown that this design implies that there is no need to measure the LC-filter output voltage.

In order to design the regulator based on the repetitive control, the parameter ω_1 was chosen to be $\omega_1 = 2\text{-}nfi =$, while the cutoff frequency of the second-order Bessel filter $Q(s)$ was set at 4 kHz. The filter has a linear phase lag on its passband that is equivalent to a constant time delay of 68.92 /is. The Bode diagram of the transfer function $G(s)$ is shown in Fig. 6: the system has zero gain at frequencies and guarantees the closed-loop system stability since it exhibits a phase margin that is equal to $PM = 34.8°$ at a gain-crossover frequency $\omega_0 = 17.8 \cdot 10^3$ rad/s, and a gain margin $GM = 2.91$ dB at a phase-crossover frequency $\omega_u = 23.3 \blacksquare 1()^3$rad/s. The Bode diagram of $G_u(s)$ is also provided, showing

TABLE I
PARAMETERS OF THE TEST SYSTEM

Electrical grid

RMS line-to-line voltage 11 kV Frequency fi = 50 Hz

Line parameters

Resistance R_4 = 60 mQ Inductance L_4 3 mH

Linear load (Induction motor 1)

Connection inductance $L\backslash$ = 0.5 /iH

Mechanical power P_{MN} = 350 kW Rated voltage V = 11 kV

Nonlinear load (Rectifier, DC load)

Connection inductance $L2$ = 0.5 /iH

Capacitor Cd_c = 50 $/JF$

Resistance $R^{\wedge}C$ = 120 f2

Sensitive Equipment (Resistive-Inductive load + Induction motor 2)

Resistive-inductive load (S = 300 kVA)

Resistance R_{S1} 370 n Inductance L_4 = 0.5 H

]

Induction motor 2

Mechanical power P_{RN} = 120 kW Rated voltage V = 11 kV

Coupling transformer (single phase)

Rated complex power S = 160 kVA

Rated voltage windings U_{N1}/U_{N2} = 8 kV/8 kV

Copper loss resistance R = 0.5 £2 \ Leakage inductance L = 6 mH

No-load losses have not been taken into account

Output filter

Capacitor C_f = 1.05 fiF Cutoff frequency f_c = 2 kHz

Flying capacitor converter

Flying capacitors 250 /kF Single switching freq. 1650 Hz

Fig. 6. Bode diagram of the transfer functions $G(s)$(-) and $G_u(s)$(-).

that the control system eliminates the resonance peak that the LC filter exhibits.

Figs. 7 and 8 plot the Bode diagrams of the closed-loop transfer functions $F(s)$ and $F_w(s)$, respectively. As Fig. 7 shows, perfect tracking of the reference input with zero phase is achieved within a bandwidth. Furthermore, Fig. 8 shows that the transfer function $F_w(s)$ has zero gain at the fundamental frequency and its harmonics within a bandwidth.

Finally, the amplitude of the added square-wave signal D, used in the general law (16) to control the flying-capacitor voltages, was set at 80 V for each converter leg.

B. Simulation Results

The test system shown in Fig. 2 is used to carry out a comprehensive simulation scenario where the multilevel DVR and its control system show their worth. The following sequence of events is assumed to take place: 1) the nonlinear load is connected at time $t = 0$ s and the charging of the flying capacitors also starts at this point in time, a process that is fully completed at time $t = 0.6$ s; 2) At this point, the whole control system is activated a
nd the DVR is connected to the grid together with

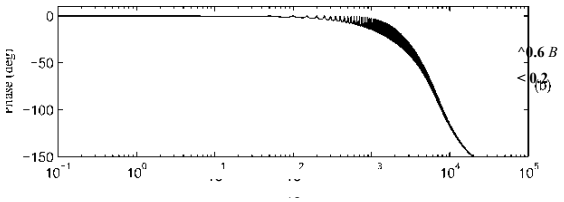

Fig. 7. Bode diagram of the transfer function .

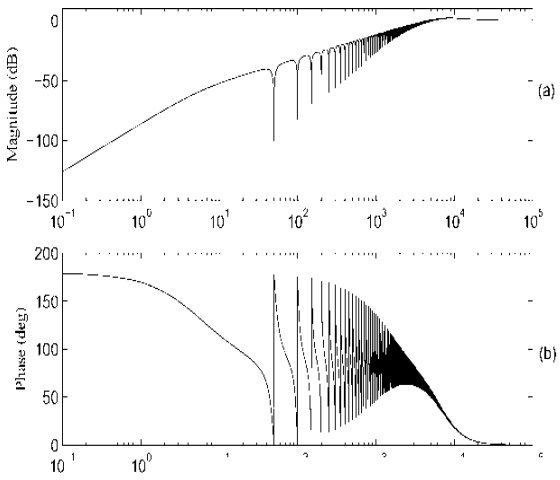

Fig. 8. Bode diagram of the transfer functions $F_w(s)$.

the inductive-resistive load (sensitive load); 3) in the time period 0.7-1.1 s, induction motor 1 is assumed to be connected with a constant rotor speed of 0.98 p.u.; 4) from t=0.8stot=1.1s,a two-phase-to-ground short-circuit fault is applied at the PCC via a 1.8-^2 resistor; 5) a second induction motor comes into operation right through the fault period, at t = 0.9 s until the end of the simulation time; 6) the nonlinear load is disconnected at t = 1.3 s and, at this point in time, a second short-circuit fault applied at the PCC takes place; this time, there is a three-phase-to-ground fault, with a duration of 200 ms. The total simulation time is 1.6 s.

Fig. 9(a) and (b) shows the rms voltages at the point where the sensitive load is connected and at the PCC, respectively. The two-phase-to-ground short-circuit fault produces a 30% voltage sag in the two affected phases in the time period 0.8-1.1 s. Also notice the minor voltage dip caused by induction motor 1 in the period 0.7-0.8 s. It is clear that in the period 0.8-1.1 s, the induction motor contributes to some minor extent to the voltage sag but, by and large, the major contributor to the sag is the short-circuit fault. It should be noticed that the 30% is not shown quite accurately in Fig. 9(b) since this is an unbalanced fault measured with the three-phase root mean square (rms) voltmeter block available in PSCAD/EMTDC. At the time of fault clearing, t = 1.1 s, and before the second short-circuit fault takes place t = 1.3 s, no voltage sags are present at the PCC, and the only anomalous phenomenon is the harmonic voltages due to the nonlinear load. The three-phase-to-ground fault at t = 1.3 s produces a 30% voltage sag and this is correctly measured by the rms voltmeter block since this is a symmetrical fault. As shown in Fig. 9(a), the control system and DVR are able to maintain the rms voltage supply to the sensitive equipment close to 11 kV, notwithstanding the voltage fluctuations at the PCC caused by the various disturbances previously discussed.

Fig. 10(a) and (b) shows the results obtained when the linear load (induction motor 1) and the nonlinear load are connected. Fig. 10(a) plots the line-to-line voltage at the PCC (v_{pcCgih}): it can be seen that the waveform is distorted, owing to the harmonic currents that the rectifier produces. Also, the total current provided to the linear load, the rectifier, and the sensitive equipment causes a voltage drop at the PCC. The voltage at PCC has an rms value of 10.52 kV (95.6% of 11 kV) for the fundamental-frequency component, while the voltage total harmonic distortion is THD^ = 8.48%. However, Fig. 10(b) shows that the line-to-line voltage across the sensitive equipment is relatively sinusoidal: the fundamental-frequency component has an rms value of 11 kV, with a voltage total harmonic distortion THD_V = 1.70%. The control system and the multilevel DVR are not only able to compensate the voltage drop at the PCC, but also cancel out the harmonic voltages caused by the rectifier. Fig. 11(a) and (b) gives the harmonic spectrums of the line-to-line voltages at the PCC and across the sensitive equipment, respectively. It can be appreciated that in the frequency interval 0 Hz < / < 2000 Hz, practically all harmonics have been removed from the voltage across the sensitive equipment (recall that the control system of the filter output voltage achieves a closed-loop system with a cutoff frequency of 2 kHz).

At t= 0.8 s, the asymmetrical fault involving phases A - C and ground is applied at the PCC; hence, the three line-to-line voltages have been plotted to assess the DVR performance more fully. Fig. 12 shows the unbalanced line-to-line voltages at the PCC: the three voltage waveforms have different amplitudes and they also contain harmonic voltages caused by the rectifier

The rms values of the fundamental-frequency components are

(i)

(i) $V_{R\ pcCab}$ = 8.05 kV, $V\$_{HC}$ = 9.87 kV, and Vp^$_{ca}$ = 7.52 kV, where the superscript (1) stands for the fundamental frequency. The voltage total harmonic distortions are THD_V = 6.25%, $THD_{,,}$ = 5.13%, and $THD^{\wedge}_{P^{cbc}}$ = 2.03%. $^{\wedge pcc_{ca}}$

The voltage across the sensitive equipment is plotted in Fig. 13. The DVR, operated by the control system, compensates the unbalanced voltages with a fast transient response owing to the feedforward term of the sensitive-equipment voltage, while the repetitive

control ensures zero-tracking error in steady state. Furthermore, the large current drawn by the induction motor 2 at its connection time t = 0.9 s (see Fig. 14) has no influence in the transient response of the voltage across the sensitive

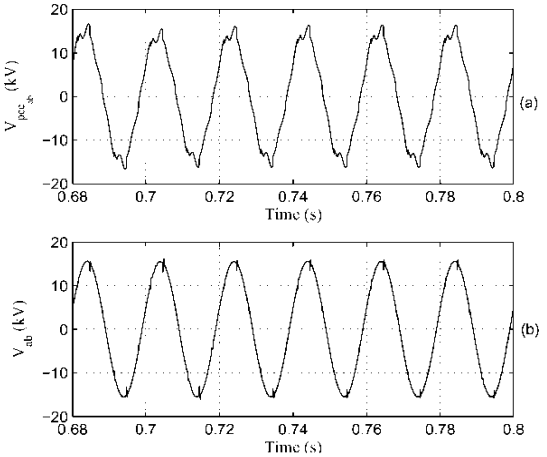

Fig. 10.Line-to-line voltage (0.68 s <t < 0.8 s) (a) at the PCC and (b) across the sensitive equipment.

equipment due to the feedforward of the load current (note that only phase A current has been plotted in Fig. 14 since the sensitive equipment is a three-phase, three-wire system and, hence, currents are balanced). The rms values of the fundamental-frequency components are equal to 11 kV for the three line-to-line

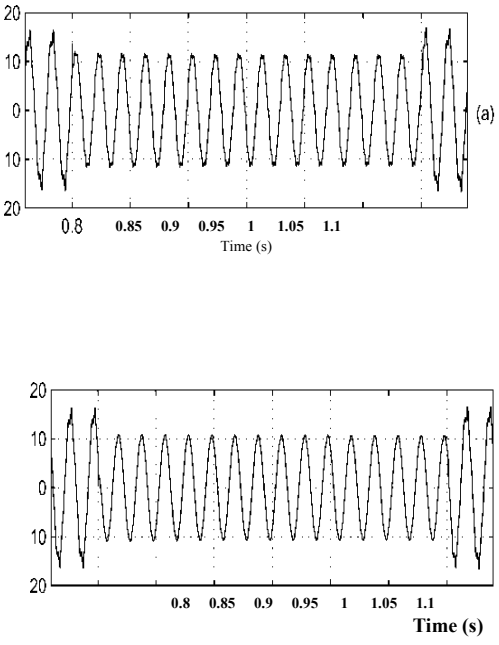

Fig. 12. Line-to-line voltages at the PCC in kilovolts (0.76 s <t < 1.14 s): (a) ^PCCab, (b) ^PCCbc, and (c) v_{pcCca}.

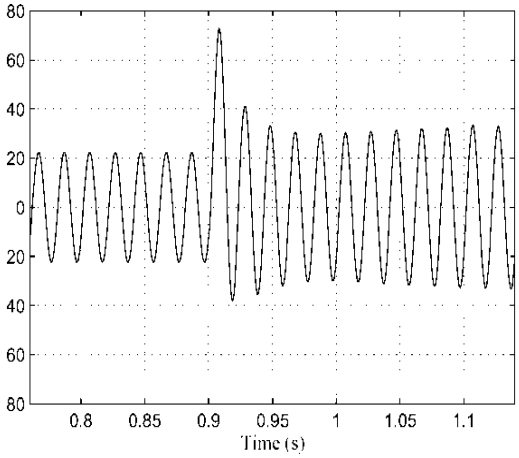

Fig. 14. Line-sensitive-equipment current i_a in amps (0.76 s <t < 1.14 s).

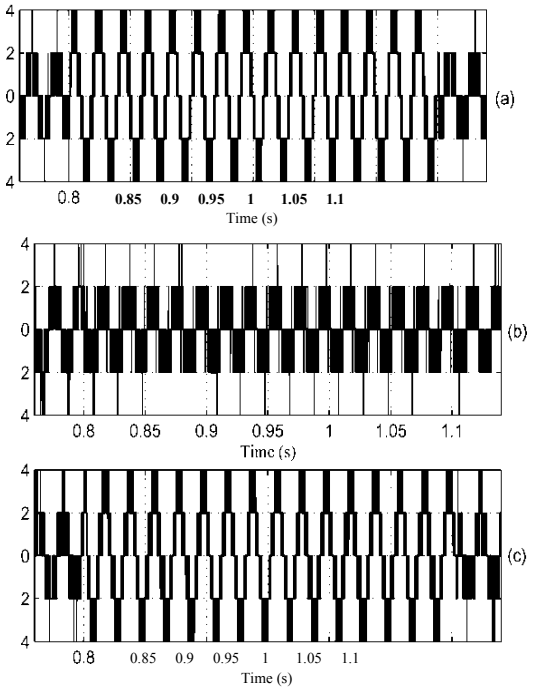

Multilevel-converter output voltages in kilovolts (1.14o, (b) u_{b0}, and (c) u_{c0}.

voltages across the sensitive load, while the voltage total harmonic distortions are TKD_{Vab} = 0.90%, TED_{Vbc} = 1.02%, and THD_{Vca} = 0.91%.

Fig. 15 shows the three output voltages of the five-level converter with reference to the point 0 (see Fig. 1). Since phase B is not involved in the fault, the DVR injects a lower voltage value in this phase than in the other two phases. Therefore, the voltage has several unused levels (see [29] for more details), unlike the voltages $u_{a}o$ and u_{c0}, which all use five levels.

The scenario in the time interval 1.1 s < t < 1.3 s is similar to the one depicted in Figs. 10 and 11, but

with only the rectifier and sensitive equipment connected to the PCC. The main information for this time interval is summarized in Table II.

At t = 1.3 s, the nonlinear load is disconnected from the PCC. Simultaneously, the three-phase-to-ground fault is applied via a resistance of $1.8\,ft$. Fig. 16(a) and (b) shows the line-to-line voltage at the PCC and across the sensitive load. Since the fault is symmetrical, only one of the line-to-line voltages has been plotted for each case. The rms value of the line-to-line voltage at the PCC is 7.7 kV (70% of its rated value) with no voltage distortion. The transient response of the sensitive-load voltage can be seen in Fig. 16(b): the DVR cancels out the voltage sag

TABLE II

FUNDAMENTAL HARMONIC RMS VALUE AND VOLTAGE TOTAL HARMONIC DISTORTION OF THE LINE-TO-LINE VOLTAGE AT THE PCC AND ACROSS THE SENSITIVE EQUIPMENT FOR DIFFERENT INSTANTS

	$V^{\wedge}_{s}$ (kV)	$THDy$ (%)
Time interval (s): 0 <t < 0.6 (charge of the flying capacitors)		
Time interval (s): 0.6 <t < 0.8 (balanced conditions)		
PCC (aft)	10.52	8.48
Sensitive equipment (ab)	11	1.70
Time interval (s): 0.8 <t < 1.1 (unbalanced conditions)		
PCC (ab)	8.05	6.25
PCC (6c)	9.87	5.13
PCC (ca)	7.52	2.03
Sensitive equipment (ab)	11	0.90
Sensitive equipment (6c)	11	1.02
Sensitive equipment (ca)	11	0.91
Time interval (s): 1.1 <t < 1.3 (balanced conditions)		
PCC (ab)	10.84	8.33
Sensitive equipment (ab)	11	1.70
Time interval (s): 1.3 <t < 1.5 (balanced conditions)		
PCC (ab)	7.7	
Sensitive equipment (ab)	11	0.91

caused by the fault with fast performance. The Fourier analysis shows that the fundamental-frequency component of the line-to-line voltage is 11 kV and that the waveform has a voltage total harmonic distortion $THD_{,,}$ = 0.91%.

Finally, Fig. 17(a)-(c) shows the three flying-capacitor voltages for the converter legs A, B, and C, respectively. Each figure plots the three capacitor voltages of one leg: vc_3 is drawn in solid lines, while vc_2 and vc_x use dashed lines and dashed-dotted lines, respectively [see Fig. 1(b) for more details]. Capacitors are charged to $V_{dc}/4$ = 2 kV, $V_{dc}/2$ = 4 kV, and $3V_{dc}/4$ = 6 kV. Once the flying capacitors are charged to their respective voltages, the FC voltage controller keeps constant voltage without significant variations and no voltage imbalances in any of the flying capacitors, regardless of whether there are voltage disturbances at the PCC during the simulation period. As the simulation results show, the dynamic performance of the repetitive control is not impaired by the FC voltage control system.

Table II summarizes the main information of the simulation results.

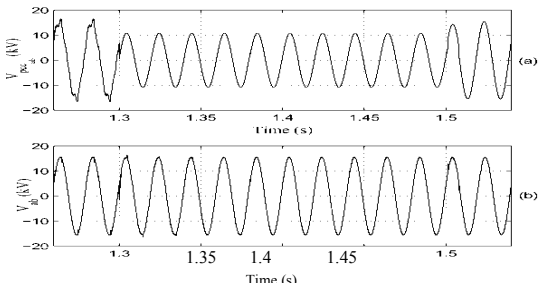

Fig. 16.Line-to-line voltage (1.26 s <t < 1.54 s) (a) at the PCC and (b) across the sensitive equipment.

V. CONCLUSION

Multilevel converters are becoming more popular in high-power MV applications. Among the various multilevel topologies, the flying capacitor offers advantages, such as the flexibility in the choice of switching combinations, which make this topology suitable for MV applications. one such application is in dynamic voltage restorers used to ameliorate voltage sags as well as other PQ phenomena, such as voltage imbalances and voltage harmonics. Nonetheless, such applications of a DVR demand more versatile control systems than the classical controller, such as the Pi regulator.

To this end, this paper has put forward a DVR based on a five-level flying-capacitor converter operated by a repetitive-control scheme. This control structure simultaneously cancels out voltage sags, voltage imbalances, and voltage harmonics other than high-frequency switching harmonics. The control system is split into three subsystems: the first one works to eliminate the resonance peak of the filter used in the converter output voltage; while the second one is the repetitive control, which ensures a fast transient response and zero-tracking error in steady-state for any sinusoidal reference and for any sinusoidal disturbance whose frequencies are an integer multiple of the fundamental frequency. Finally,

the third subsystem maintains constant, balanced voltages in the flying capacitors.

The control system, together with the DVR, has been implemented by using the graphical facilities available in PSCAD/ EMTDC. Comprehensive simulation results using an MV test system show the DVR's excellent performance and the control system in order to protect sensitive equipment from PQ disturbances.

REFERENCES

[1] M. H. J. Bollen, *Understanding Power Quality Problems: Voltage Sags and Interruptions.* Piscataway, NJ: IEEE Press, 2000.

[2] V. Immanuel and G. Yankanchi, "A waveform synthesis technique for voltage sag compensation using dynamic voltage restorer (dvr)," in *Proc. IEEE Power Eng. Soc. General Meeting*, Jun. 2006, pp. 1-7.

[3] N. G. Hingorani, "Introducing custom power," *IEEE Spectr.,* vol. 32, no. 6, pp. 41-48, Jun. 1995.

[4] Z. Changjiang, A. Arulampalam, and N. Jenkins, "Four-wire dynamic voltage restorer based on a three-dimensional voltage space vector pwm algorithm," *IEEE Trans. Power Electron.,* vol. 18, no. 4, pp. 1093-1102, Jul. 2003.

[5] L. Xu and V. G. Agelidis, "Flying capacitor multilevel pwm converter based upfc," *Proc. Inst. Elect. Eng., Electr. Power Appl.,* vol. 149, no. 4, pp. 304-310, Jul. 2002.

[6] E. Acha, V. G. Agelidis, O. Anaya, and T. J. E. Miller, *Power Electronic Control in Electrical Systems.* Oxford, U.K.: Newnes, 2001.

[7] C. Feng, J. Liang, and V. G. Agelidis, "Modified phase-shifted pwm control for flying capacitor multilevel converters," *IEEE Trans. Power Electron.,* vol. 22, no. 1, pp. 178-185, Jan. 2007.

[8] J. Arrillaga, Y. H. Liu, and N. R. Watson, *Flexible Power Transmission.The HVDC Options.*Chichester, U.K.: Wiley, 2007.

[9] A. Ghosh and G. Ledwich, *Power Quality Enhancement Using Custom Power Devices.* Norwell, MA: Kluwer, 2002. [10] J. Rodriguez, J.-S. Lai, and F. Z. Peng, "Multilevel inverters: A survey of topologies, controls, and applications," *IEEE Trans. Ind. Electron.,*vol. 49, no. 4, pp. 724-738, Aug. 2002.

[11] D. Soto and T. C. Green, "A comparison of high-power converter topologies for the implementation of facts controllers," *IEEE Trans. Ind. Electron.,* vol. 49, no. 5, pp. 1072-1080, Oct. 2002.

[12] L. Xu and V. G. Agelidis, "VSC transmission system using flying capacitor multilevel converters and hybrid pwm control," *IEEE Trans. PowerDel.,* vol. 22, no. 1, pp. 693-702, Jan. 2007.

[13] A. Shukla, A. Ghosh, and A. Joshi, "Static shunt and series compensations of an smib system using flying capacitor multilevel inverter," *IEEE Trans. Power Del.,* vol. 20, no. 4, pp. 2613-2622, Oct. 2005.

[14] A. Shukla, A. Ghosh, and A. Joshi, "Hysteresis current control operation of flying capacitor multilevel inverter and its application in shunt compensation of distribution systems," *IEEE Trans. Power Del.,* vol. 22, no. 1, pp. 396-405, Jan. 2007.

[15] P. C. Loh, D. M. Vilathgamuwa, S. K. Tang, and H. L. Long, "Multilevel dynamic voltage restorer," *IEEE Power Electron. Lett.,*vol. 2, no. 4, pp. 125-130, Dec. 2004.

[16] Z. Yin, M. Han, X. Zhou, and K. Yu, "Project study of dynamic voltage restorer," in *Proc. IEEE Power Eng. Soc. Transm.Distrib. Conf. Exhibit.: Asia and Pacific,* 2005, pp. 1-8.

[17] C. Meyer, C. Romaous, and R. W. DeDoncker, "Five level neutral-point clamped inverter for a dynamic voltage restorer," in *Proc. 11th Eur. Conf. Power Electronics and Applications,* Dresden, Germany, Sep. 2005, EPE, pp. 1-9.

[18] B. Wang, G. Venkataramanan, and M. Illindala, "Operation and control of a dynamic voltage restorer using transformer coupled h-bridge converters," *IEEE Trans. Power Electron.,* vol. 21, no. 4, pp. 1053-1060, Jul. 2006.

[19] T. Inoue and M. Nakano, "High accuracy control of a proton synchrotron magnet power supply," in *Proc. Int. Federation of Automatic Control, 8th Triennial World Congr.,* 1981, vol. XX, IFAC, pp. 216-221.

[20] S. Hara, Y. Yamamoto, T. Omata, and M. Nakano, "Repetitive control system: A new type servo system for periodic exogenous signals," *IEEE Trans. Autom. Control,* vol. 33, no. 7, pp. 659-668, Jul. 1988.

[21] K. Zhou and D. Wang, "Digital repetitive learning controller for three-phase CVCF PWM inverter," *IEEE Trans. Ind. Electron.,* vol. 48, no. 4, pp. 820-830, Aug. 2001.

[22] K. Zhou and D. Wang, "Digital repetitive controlled three-phase pwm rectifier," *IEEE Trans. Power Electron.,* vol. 18, no. 1, pp. 309-316, Jan. 2003.

[23] A. Garcia-Cerrada, O. Pinzon-Ardila, V. Feliu-Battle, P. Roncero-Sanchez, and P. Garcia-Gonzalez, "Application of a repetitive controller for a three-phase active power filter," *IEEE Trans. Power Electron.,* vol. 22, no. 1, pp. 237-246, Jan. 2007.

[24] H. Kim and S.-K. Sul, "Compensation voltage control in dynamic voltage restorers by use of feed forward and state feedback scheme," *IEEE Trans. Power Electron.,* vol. 20, no. 5, pp. 1169-1177, Sep.2005.

[25] T. J. Summers and R. E. Betz, "Dead-time issues in predictive current control," *IEEE Trans. Ind. Appl.,* vol. 40, no. 3, pp. 835-844, May/Jun.2004.

[26] P. Horowitz and W. Hill, *The Art of Electronics,* 2nd ed. Cambridge, U.K.: Cambridge Univ. Press, 1989.

[27] Y. Liang and C. O. Nwankpa, "A power-line conditioner based on flying-capacitor multilevel voltage-source converter with phase-shift pwm," *IEEE Trans. Ind. Appl.,* vol. 36, no. 4, pp. 965-971, Jul./Aug. 2000.

[28] L. Xu and V. G. Agelidis, "Active capacitor voltage control of flying capacitor multilevel converters," *Proc. Inst, Elect. Eng., Electr. Power Appl.,* vol. 151, no. 3, pp. 313-320, May 2004.

[29] C. Feng, "Switching frequency reduction in pulse-width modulated multilevel converters and systems," Ph.D. dissertation, Dept. Electroni. Elect.Eng., Faculty Eng., Univ. Glasgow, Glasgow, U.K., 2004.

◈◈◈

A SPEED CONTROL OF DIRECT FIELD ORIENTED INDUCTION MOTOR BY USING PID PLUS FUZZY CONTROLLER

GUNJI DONENDRA & K.S.R. ANJANEYULU

EEE Department, JNTUA College of Engineering, Anantapur.

Abstract: This paper presents the speed control of induction motor by the use of PID controller in series with one of the soft computing techniques, fuzzy logic. The PID controller is designed based on Ziegler-Nichols (Z-N) tuning technique. The Z-N PID is adopted because its parameter values can be chosen using a simple and useful rule of thumb. Fuzzy logic controller (FLC) is connected in series with the PID controller for the effective speed control of widely used direct field oriented induction motors (DFOIM). The FLC is developed based on the output of the PID controller, and the output of the FLC is the torque command of the DFOIM. Experimental results demonstrate that the proposed hybrid controller can lead to desirable robust speed tracking performance under load torque disturbances.

Keywords:*Induction motor, robust speed control, fuzzy logic controller, Ziegler-Nichols PID controller.*

I. INTRODUCTION

The field oriented induction machine (FOIM) [2] is one of the most widely used machines in industrial applications due to its reliability, relatively low cost and modest maintenance requirement. Usage of induction motors reminds us to develop a better control over it. These induction motors have the advantage of decoupling of the torque and flux control, which makes high servo quality achievable. However,the decoupling control feature can be adverselyaffected by load disturbances and parameter variations in the motor. This instinctly lowers the desired speed. Sothat the variable-speed trackingperformance of an Induction motor isdegraded. In order to attain the rated speedthere are many controllers likeconventional PI and PID controllers.But,these have the difficulty in making themotor closely followa reference speedtrajectory under torque disturbances. Inthis regard, an effective and robust speedcontroller design is needed.

Advanced control based on artificial intelligence techniqueis called intelligent control. Every system with artificialintelligence is called self-organizing system. The production of electronic circuits andmicroprocessors with high computation ability and operatingspeed has grown very fast. The high power, high speed andlow cost modern processors like DSP and IC'salong with power technique switches like IGBT made theintelligent control to be used widely in electrical drives.These Intelligent controls, act better than conventional adaptivecontrols. One of those intelligent techniques is fuzzy-logic. Fuzzy-logic-based intelligent controllers have been proposed for speed control of FOIM drives. Those intelligent controllers are associated with adaptive gains due to fuzzy inference and knowledge base. As a result, they can improve torque disturbance rejections in comparison with best trial-and-error PI or PID controllers. Nonetheless, no performance advantages of intelligent controllers in combination with a PI or PID controller are investigated.

Motivated by the successful development and application in[3]-[9]we propose a PID plus fuzzy controller consisting of a PID controller and a fuzzy logic controller (FLC) in a serial arrangement for speed control of FOIM drives, more specifically, direct field-oriented IM (DFOIM) drives. The Ziegler-Nichols (Z-N) method [8] is adopted for designing a PID controller (denoted as "the Z-N PID") because its design rule is simple and systematic. We next design a FLC carrying out fuzzy tuning of the output of the Z-N PID controller to issue adequate torque commands.

Based on a simulation model of the DFOIM drives incorporating the proposed controller, experiments are set up in a Matlab/Simulink environment. The results show that the incorporation of the proposed controller into the DFOIM drives can yield superior and robust variable-speed tracking performance.

II. INDUCTION MOTOR AND CONTROLSTRUCTURE

Field oriented control (FOC) technique is intended tocontrol the motor flux, and thereby be able to decompose theAC motor current into "flux producing" and "torqueproducing" components. These current components can betreated separately, and then recombined to create the actualmotor phase currents. This gives a solution to the boostadjustment problem, and also provides much better control ofthe motor torque, which allows higher dynamic performance. Field orientatedcontrolled machines need two constants asinput references: the torque component(aligned with the q co-ordinate) and theflux component (aligned with d coordinate).

As Field Orientated Control issimply based on projections the controlstructure handles instantaneous electricalquantities. This makes the control accuratein every working operation (steady stateand transient) and independent of the limited bandwidth mathematical model.We introduce the DFOIM drive

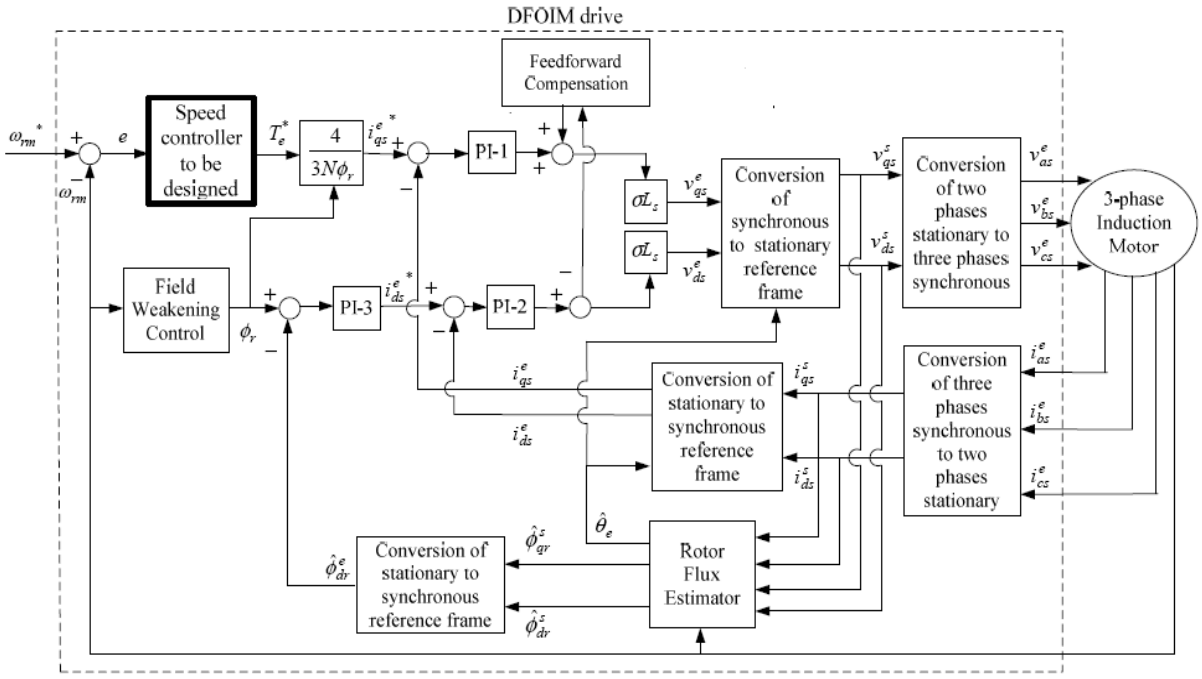

Figure 1. The block diagram of speed control of a DFOIM

shown inFig. 1. The dynamics of an inductionmotor can be described by synchronouslyrotating reference frame direct-quadrature(d-q) equations [2] as

$$\begin{bmatrix} V_{qs}^e \\ V_{ds}^e \\ 0 \\ 0 \end{bmatrix} = \begin{bmatrix} R_s + pL_s & \omega_e L_s & pL_m & \omega_e L_m \\ -\omega_e L_s & R_s + pL_s & -\omega_e L_m & pL_m \\ pL_m & (\omega_e - \omega_r)L_m & R_r + pL_r & (\omega_e - \omega_r)L_r \\ -(\omega_e - \omega_r)L_m & pL_m & (\omega_e - \omega_r)L_r & R_r + pL_r \end{bmatrix} \begin{bmatrix} i_{qs}^e \\ i_{ds}^e \\ i_{qr}^e \\ i_{dr}^e \end{bmatrix}$$

$$\omega_{rm} = \frac{2}{N}(\omega_e - \omega_r) \quad \ldots(4)$$

$$T_e = \frac{3}{4}N L_m (i_{qs}^e \cdot i_{dr}^e - i_{ds}^e \cdot i_{qr}^e) \quad \ldots(5)$$

$$T_e - T_L = J_m \frac{d\omega_{rm}}{dt} + B_m \omega_{rm} \quad \ldots(6)$$

where the notational superscript "e" stands for the synchronous reference frame; v_{ds}^e, v_{qs}^e ,i_{ds}^e ,i_{qs}^e ,and i_{qr}^e stand for the d-axis stator voltage, q-axis stator voltage, d-axis stator current, q-axis stator current and the q-axis rotor currents respectively; Rs , Rr , Ls and Lr denote the stator resistances, rotor resistances, stator self-inductances and rotor self-inductances. Lm denotes the mutual inductance; Te and T_L represent the electromagnetic torque and external force load torque respectively; J_m and B_m are the rotor inertia and the coefficient of viscous damping, respectively; ω_r and ω_{rm} denote the rotor and motor mechanical speeds; ω_e stands for electrical angular velocity; N is the number of poles of the motor mechanical speed; p stands for the differential operator (d/dt). The notational superscript "s" in Fig.1 stands for stationary reference frame.

For a DFOIM drive, the flux has to fall entirely on d-axis. Therefore, the q- axis rotor flux $\emptyset_{qr}^e$ is set to zero. The controllers PI-1, PI-2, and PI-3 are chosen to ensure that $i_{qs}^{e*} \cong i_{qs}^e$, $i_{ds}^{e*} \cong i_{ds}^e$and the flux command φ_r and the estimated d-axis rotor flux $\hat{\phi}_{dr}^e$ satisfies $\phi_r \equiv \hat{\phi}_{dr}^e$, respectively. The parameters τ and σ are given by $\tau = \frac{L_r}{R_r}$ and $\sigma = 1 - \frac{L_m^2}{L_s L_r}$To control the speed of the IM, the speed controller of the DFOIM drive transforms the speed error signal e into an appropriate electromagnetic torque command T_e^*.

III. THE PROPOSED PID PLUS FUZZYCONTROL

The structure of the proposed controller is shown in Fig. 2.This hybridcontroller comprises of PID controller inseries with the fuzzy logiccontroller. Fuzzy logic is developed basedon the output of the PID controller.

PID Controller:

The steps to acquire the Z-N PID [8] for speed control of the DFOIM in Fig. 1 are given as follows. First, we use a fixed step input ω_{rm} and a linear proportional speed controller. The proportional gain of the speed controller is increased until the DFOIM reaches its stability limit. As a result, we obtain the period Tu of the critical oscillation at the stability limit of the DFOIM with the critical proportional gain Ku. Next, the values of the parameters KP, TI , TD are given by

$$K_P = Ku/1.7 \quad \ldots. (5)$$

$$T_I = T_u/2 \quad \ldots. (6)$$

$$T_D = T_I/4 \quad \ldots. (7)$$

where KP is the proportional gain; TI is the integral time andTD is the derivative time.

Fuzzy Logic Controller:

The output of the PID controller [9] is given as the input to the fuzzy controller. This fuzzy logic involves computing using knowledge base and rule base. In fuzzy systems, input variables are assigned with a membership function. Each membership function is assigned with specified values. Fuzzy logic comprises of three stages.

In the fuzzification process, we only employ three input membership functions $\mu_N(x)$, $\mu_Z(x)$ and $\mu_P(x)$shown in Fig. 3 to map a crisp inputto a fuzzy set with a degree of certaintywhere $x = g(t)$ or $\Delta g(t)$ with $g(t) = K_1 f(t)$and $\Delta g(t) = K_2 \Delta f(t)$. Those threemembership functions are chosen becauseof their simplicity for computation since alarge number of membership functions andrules can cause high computational burdenfor a fuzzy controller. For any $x \in N$ where$N$ denotes the interval $(-\infty,0]$, itscorresponding linguistic value is 'N'.Moreover, for any $x \in P$ where P denotesthe interval $(0,\infty)$, its correspondinglinguistic value is 'P'. For any $x \in$ where$Z$ denotes the interval $[-b, b]$, itscorresponding linguistic value is 'Z'. Themembership functions $\mu_N(x)$, $\mu_Z(x)$ and $\mu_P(x)$are given by

$$\mu_N(x) = \begin{cases} 1, & x \le -b \\ \frac{-x}{b} & -b < x \le 0 \\ 0 & otherwise \end{cases} \quad \ldots(8)$$

$$\mu_N(x) = \begin{cases} \frac{x+b}{b}, & b < -x \le 0 \\ \frac{b-x}{b}, & 0 < x \le b \\ 0, & otherwise \end{cases} \quad \ldots(9)$$

$$\mu_N(x) = \begin{cases} 1 & b \le x \\ \frac{x}{b} & 0 < x \le b \\ 0 & otherwise \end{cases} \quad \ldots(10)$$

The fuzzy inference engine, based on the input fuzzy sets in combination with the expert's experience, uses adequate IF-THEN rules in theknowledge base to make decisions and produces an implied output fuzzy set u. For this particular application, the proposed IF-THEN fuzzy rule base is shown in Table 1 and is described as follows:

i. If $\Delta g(t) \in$ N, then $u(g(t), \Delta g(t)) = b$.
ii. If $\Delta g(t) \in$ P, then $u(g(t), \Delta g(t)) = -b$.
iii. If $\Delta g(t) \in$ Z and $g(t) \in$ N, then $u(g(t), \Delta g(t)) = -b$.
iv. If $\Delta g(t) \in$ Z and $g(t) \in$ P, then $u(g(t), \Delta g(t)) = b$.
v. If $\Delta g(t) \in$ Z and $g(t) \in$ Z, then $u(g(t), \Delta g(t)) = 0$.

Moreover, the Mamdani-type min operation for fuzzy inference is employed in this study. In this mamdani type fuzzy inference, membership functions like trapezoidal, triangular, are applied to the input variables.

	N	**Z**	**P**
N	b	b	B
Z	-b	0	B
P	-b	-b	-b

Table 1: Fuzzy rule base

In the defuzzification process, we employ the 'center of mass' defuzzification method for transforming the implied output fuzzy set into a crisp output, and obtain

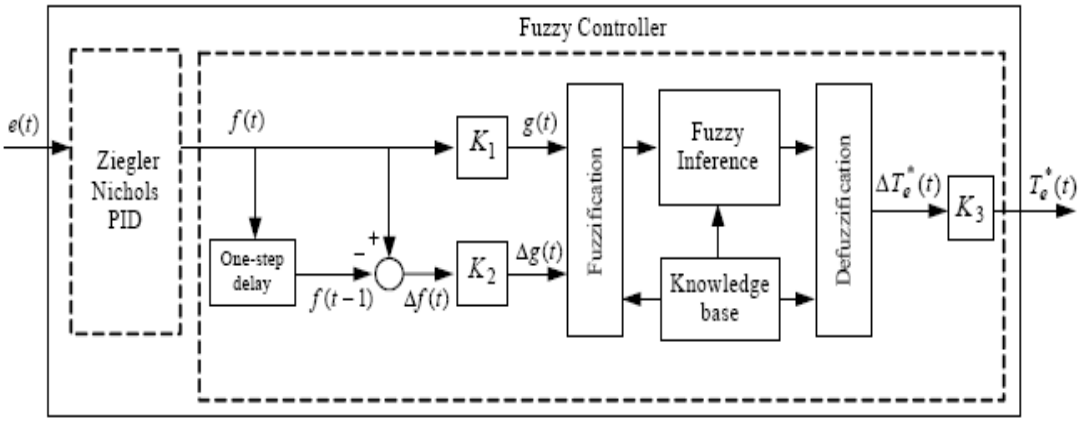

Figure 2 . The block diagram of the proposed controller

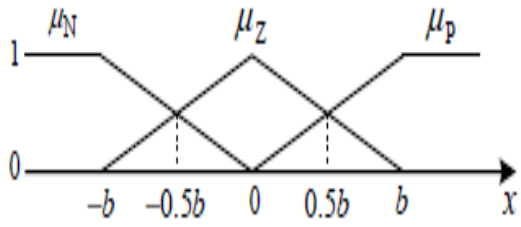

Figure 3.Membership functions with x =g(t) or Δg(t)

$$\Delta T_e^*(t) = \frac{\sum_{j\in FL(g(t))}\sum_{j\in FL(\Delta g(t))}\min\{\mu_i(g(t)),\mu_j(\Delta g(t))\}\times u(i,j)}{\sum_{j\in FL(g(t))}\sum_{j\in FL(\Delta g(t))}\min\{\mu_i(g(t)),\mu_j(\Delta g(t))\}} \quad \ldots.(12)$$

Where

$$FL(a) = \begin{cases}\{N,Z\} & \text{if } a\in N \text{ and } a\in Z\\ \{P,Z\} & \text{if } a\in P \text{ and } a\in Z\\ \{N\} & \text{if } a\in N \text{ and } a\notin Z\\ \{P\} & \text{if } a\in P \text{ and } a\notin Z\end{cases} \quad \ldots.(13)$$

The output of the fuzzy controller is given by $T^*_e(t) = K_3.\ \Delta T^*_e(t)$ .... (14)

IV. SIMULATION RESULTS

A computer simulation model of Fig. 1 is developed using the Matlab/Simulink software. The parameter values of the 0.14-hp squirrel-cage induction motor are given as follows:

Rs (Ω) =17 , Rr (Ω) = 11, Ls (H) = 0.196 , Lr (H) = 0.196 ,Lm (H) =1.88×10^{-3} , N = 4 , Jm (Kg-cm–s^2) = 2.4×10^{-4} , Bm (kg − cm) = 9.2×10^{-3} .

Based on the root-locus method and the control objectives of the PI controllers in Fig. 1, we obtain PI-1 as $220.4162(1+\frac{158.65}{s})$, PI-2 as $370.0613(1+\frac{175.64}{s})$ and PI-3 as $15.80574(1+\frac{13.019}{s})$. Given a fixed step input ω_{rm} rpm, weobtain the critical gain K_u = 2.2 and the critical oscillation period T_u = 0.049 of the DFOIM. From [10], we get the Z-N PID as $1.29(1+\frac{1}{0.0245S}+0.006125S)$. To design the fuzzy control part of the proposed controller in Fig. 2, we first set b = 9 and K_2 =1 .Then gains K_1 and K_3 are varied until the desired system response under no torque disturbance is achieved. Inthis regard, we get K_1 = 2 and K_3 = 3. The Simulink Fuzzy Logic Toolbox [5] is employed for fuzzy control simulations.

Fig. 4 shows that the proposed controller performs better than the Z-N PID under thecondition that the command speed is increased from 0 to 900 r.p.m and a load disturbance 1.1Nm is suddenly applied to the shaft at 4.2 sec. When we use only PID controller the speed of the induction motor decreased to 877 r.pm and when we use hybrid controller the speed was 898 r.p.m.

In Fig. 5, the command speed is increased from 0 r.p.m. and reaches 900 r.p.m at 4.25 sec, and then starts decreasing from 900r.p.m at 8.25 sec. In addition, no torque disturbance is applied to the shaft.

It shows that the proposed controlleroutperforms the conventional PID. The speed tracking response of the PID controller yields large fluctuations when thespeed command is 900 r.p.m. The tracking response of the PID controller cannot follow the command speed properly when the speed command is decreased from 900 to 0 r.p.m.

In Fig. 6, the command speed is the same as that in Fig. 5, and a load torque disturbance of 1.1N-m is

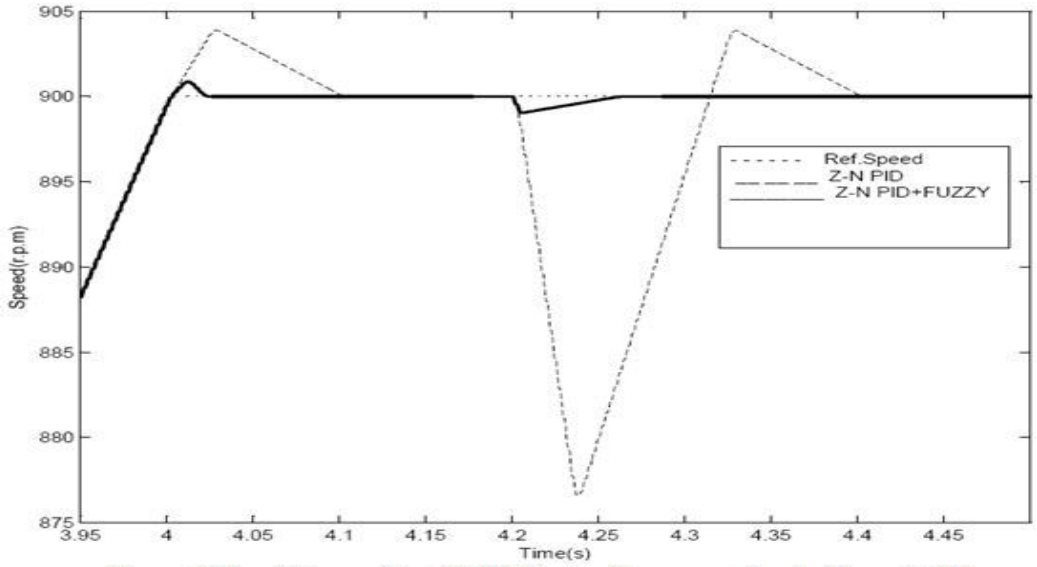

Figure 4: Simulation results of DFOIM using the proposed controller and Z-N PID under a load disturbance

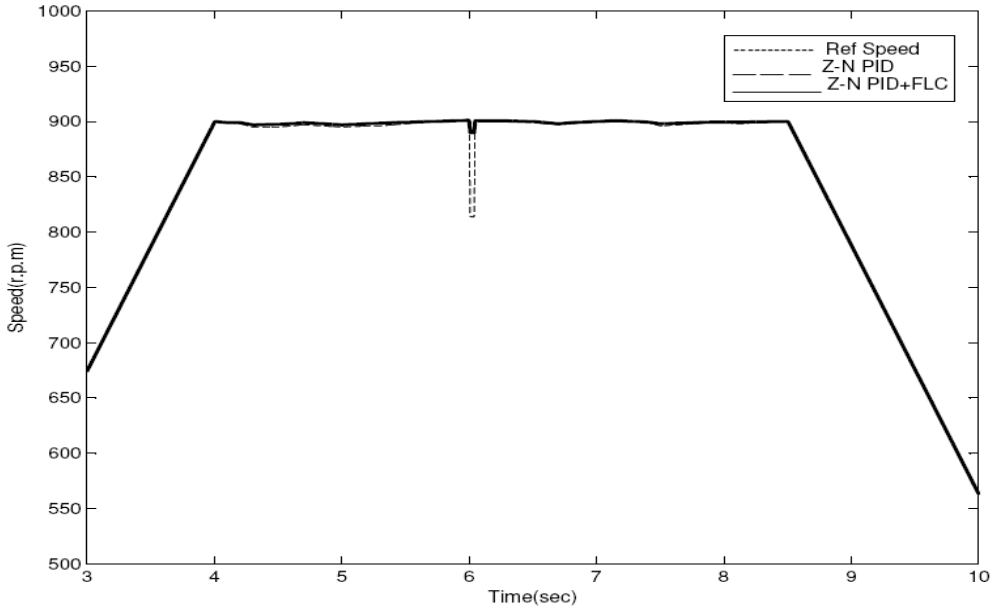

Figure.5 Response of DFOIM using Z-N PID and Z-N PID plus Fuzzy logic controllers under no load disturbance

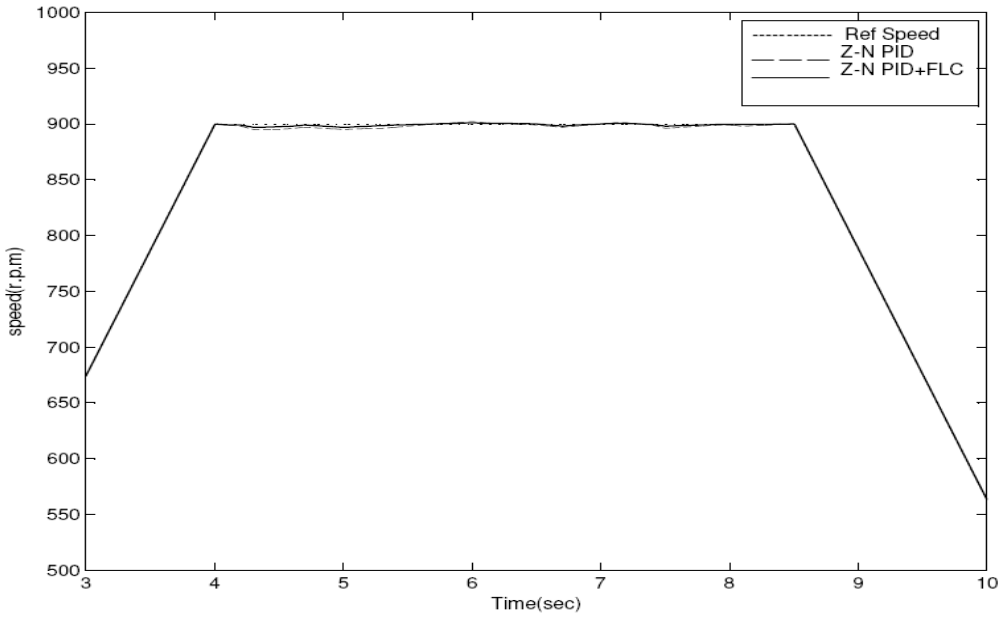

Figure.6 Response DFOIM using Z-N PID and Z-N PID plus Fuzzy logic controllers under a load disturbance of 1.1 N-m occurring at the 6th second

applied to the shaft at the 6th second. It is noted that the proposed controller yields much smaller tracking errors than the PID controller. In addition, the proposed controller takes shorter time to resume the command speed following than PID controller when the load disturbance takes place. Accordingly, it is suggested that the proposed controller has a robust performance.

V. CONCLUSION

In this paper, a novel hybrid Z-N PID plus FLC based speed control of a DFOIM has been presented. The proposed controller has exhibited the combined advantages of a PID controller and a FLC. Specifically, it can improve the stability, the transient response and load disturbance rejection of speed control of a DFOIM. The fuzzy logic and only with three membership functions are used for each input and output for low computational burden, which can

achieve satisfactory results. Simulation and experiment results have illustrated that the proposed controller scheme has a good and robust tracking performance. As suggested in [15] that a modified Z-N PID can perform better than a Z-N PID, our future effort will focus on how to further improve the performance of the proposed controller herein by incorporating a modified Z-N PID.

REFERENCES

[1] T.-J. Ho and L.-Y Yeh, "Design of a hybrid PID plus Fuzzy controller for Speed control of Induction motors," Department of Electrical Engineering, Chung Yuan Christian University, Chung- Li, Taiwan, 5th IEEE conference 2010.

[2] Paul C. Krause "Analysis of electrical machinery and drive systems", 2nd edition from Wiley Inter-science publications-2002.

[3] Leonid Reznik and Omar Ghanayem "PID plus fuzzy Controller structures as a design base for Industrial applications" in Industrial Research Institute, Victoria University of Technology.

[4] Bimal K. Bose, "Adjustable Speed AC Drives-A Technology Status Reviews", Proceedings of the IEEE, Vol. 70, No.2, February 1982.

[5] Naveed Ahmed, "Fuzzy logic Control Using Matlab", part-II FAST-NUCES, Khwarzimic Science Society.

[6] Texas Instruments, "Field Orientated Control of 3-Phase AC-Motors", Literature number: BPRA073, Texas Instruments Europe, February 1988.

[7] Soufien Gdaim, Abdellatif Mtibaa and Mohamed Faouzi Mimouni "Direct Torque control of Induction Machine based on Intelligent Techniques" International Journal of Computer Applications(0975-8887), Volume 10-No.8, November 2010.

[8] J. G. Ziegler and N. B. Nichols, "Optimal settings for automatic controllers", Trans. ASME, Vol. 64, pp. 759-768, 1942.

[9] V .Chitra, and R.S. Prabhakar, "Induction Motor Speed Control using Fuzzy Logic Controller" World Academy of Science, Engineering and Technology 23, 2006.

[10] Li Zhen and Longya Xu, "Fuzzy Learning Enhanced Speed Control of an Indirect Field-Oriented Induction Machine Drive" IEEE Transactions On Control Systems Technology, VOL. 8, NO. 2, MARCH 2000.

DESIGN OF DIFFERENT CONTROL STRATEGIES FOR A DIGITAL EXCITATION CONTROL SYSTEMS

T.HEMANTH KUMAR, P.BARAT KUMA & K.S.R. ANJANEYULU

EEE Department, JNTUA College of Engineering, Anantapur.

Abstract- This paper proposes the design of an indirect method for self tuning of the PID controller. The proportional-integral derivative (PID) controllers are the most popular controllers used in industry because of their remarkable effectiveness, simplicity of implementation and broad applicability. However, manual tuning of these controllers is time consuming, tedious and generally lead to poor performance. This tuning which is application specific also deteriorates with time as a result of plant parameter changes. This paper presents an artificial intelligence (AI) method of Recursive Least Square method (RLS) algorithm for tuning the optimal proportional-integral derivative (PID) controller parameters for industrial processes. This approach has superior features, including easy implementation, stable convergence characteristic and good computational efficiency over the conventional methods. Ziegler- Nichols, tuning method was applied in the PID tuning and results were compared with the RLS-Based PID for optimum control. Simulation results are presented to show that the RLS-Based optimized PID controller is capable of providing an improved closed-loop performance over the Ziegler-Nichols tuned PID controller Parameters. Compared to the heuristic PID tuning method of Ziegler-Nichols, the proposed method was more efficient in improving the step response characteristics such as, reducing the commissioning time and cost, with self-tuned PID gains, commissioning is accomplished very quickly with excellent performance results.

Index Terms—*Digital voltage regulator, Ziegler- Nichols method, Simulation, generator excitation, recursive least square, self-tuning of the PID controller.*

I. INTRODUCTION

An optimally-tuned excitation system offers benefits in overall operating performance during transient conditions caused by the following: 1) system faults; 2) disturbances; or 3) motor starting. During motor starting, a fast excitation system will minimize the generator voltage dip and reduce the I^2R heating losses of the motor. After a fault, a fast excitation system will improve transient stability by holding up the system and providing positive damping to system oscillations. Additional advantages include the following: 1) improved relay coordination; and 2) first swing transient stability. A well tuned excitation system will minimize voltage overshoot after a disturbance and avoid the nuisance tripping of the generator protection relays

Modern excitation control systems are constructed using either static or rotary excitation. The voltage source of an excitation control system is derived from the generator terminals (shunt configuration) or from a separate external power source. Illustrating generator gain. A linear model is applicable to the excitation control system with an external power input. For a shunt configuration, it is modeled as a bilinear system. A rotary excitation system with a shunt power input is considered here. The controller gains are determined using several excitation system parameters, such as the voltage loop gain, open-circuit time constants, etc. [1]. These parameters vary not only with the system loading conditions as illustrated by Fig. 1.

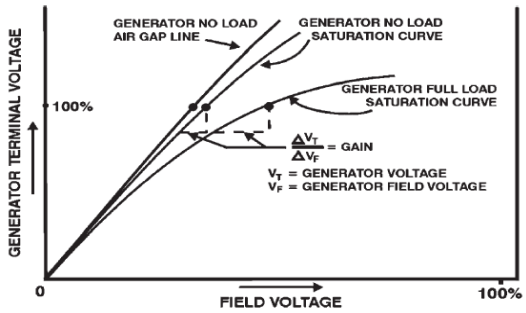

Fig.1 Generator saturation curve illustrating generator gain

but also with the system configuration-dependent gains such as the power input voltage. The calculation of loop gain requires several excitation system parameters that are generally not available during comissioning time [2].

Many times, there is no access to the actual equipment but only to a manufacturer's data sheet, or some typical data set. For this case, the only available Measurement to verify the excitation system performance as shown in fig.2 is the combined response of the exciter and generator.

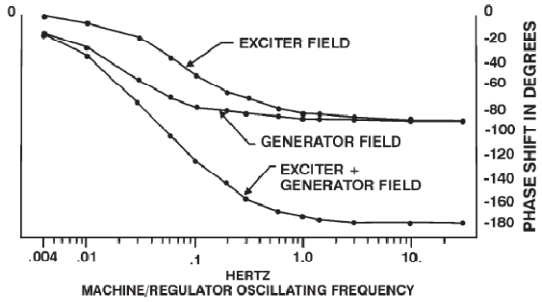

Fig.2 phase shift of exciter,generator and combined system

Under these conditions, commissioning of a new voltage regulator becomes a challenging task. One solution to reduce the commissioning time and cost is to automatically tune the PID controller. The simplified block diagram is illustrated in Fig.3 and the self-tuning controller was introduced in [6]. It continuously identifies time-varying system parameters and adjusts controller gains to minimize a properly selected performance index. Application to the automatic voltage regulators (AVRs) is reported.

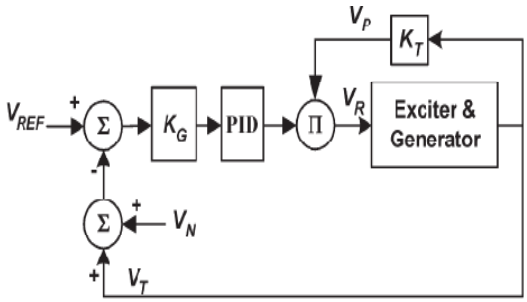

V_{REF} is the generator voltage reference
V_T is sensed generator voltage
V_N is noise in terminal voltage sensing
V_P is power input voltage
V_R is voltage regulator output

Fig.3 simplified block diagram of excitation control with AVR

Recently, several Particle Swarm Optimization (PSO)-based algorithms have been successfully implemented to determine the PID controller gains, [4] and [5]. These were developed for the linear system. Furthermore, these methods are not applicable if the time constants of the generator and exciter are not available.

II. TUNING OF PID CONTROLLER USING ZIEGLER NICHOLS METHOD

The first method of Z-N tuning is based on the open-loop step response of the system. The open loop system's S shaped response is characterized by the parameters, namely the process time constant T and L. These parameters are used to determine the controller's tuning parameters. The second method of Z-N tuning is closed-loop tuning method that requires the determination of the ultimate gain and ultimate period. The method can be interpreted as a technique of positioning one point on the Nyquist curve (Astrom and Hagglund, 1995). This can be achieved by adjusting the controller gain (Ku) till the system undergoes sustained oscillations (at the ultimate gain or critical gain), whilst maintaining the integral time constant (Ti) at infinity and the derivative time constant (Td) at zero. This paper uses the second method as shown in table 1.

Table.1 Ziegler-Nichols open-loop tuning rule

Controller	K_P	T_I	T_D
P	$\frac{T_P}{L_P K_P}$	∞	0
PI	$0.9\frac{T_P}{L_P K_P}$	$3.33\,L_P$	0
PID	$1.2\frac{T_P}{L_P K_P}$	$2\,L_P$	$0.5\,L_P$

III.SELF-EXCITED EXCITATION CONTROL SYSTEM

The basic block diagram of a self-exciting excitation control system with the PID block utilized in the AVR control loop is shown in Fig. 4. In addition to the PID block, the system loop gain (*KG*) provides an adjustable term to compensate for the variations in the system input voltage to the power-converting bridge. The transfer function $G_c(s)$ of the conventional PID controller may be expressed as

$$G_C(S)=K_G(K_p+\frac{K_I}{S}+\frac{K_D S}{1+T_D S}) \quad ..(1)$$

Where
K_G is the loop gain
K_P is the proportional gain
K_I is the integral gain
K_D is the derivative gain
T_D is the derivative filter time constant
s is the Laplace operator

As shown in Fig. 3, the PID controller output is multiplied by the power input voltage (V_P). For the external power input Fig. 3. simplified excitation control system with AVR. V_P becomes a constant. Thus, linear system theory can be applied for small-signal stability. If the power input is derived from the generator voltage for the self excitation application, i.e., $V_P = K_T V_T$ where K_T is a gain that represents a power transformer, the exciter field voltage is the PID control output multiplied by a factor of the generator terminal voltage and the excitation control system becomes a bilinear system.

1) Calculation of the RMS Value of generator voltage
Generator Voltage

The generator voltage (V_T) in the above figure is expressed as the rms value, which may be calculated based on the number of samples per period of the nominal generator frequency. If the system frequency varies, the sampling interval should be changed in order to calculate accurate rms and phasor information. A variable interval sampling scheme is utilized in some digital regulators.

(2). Consideration of Noise in Generator Voltage

Today's digital voltage regulators are designed to achieve about 0.25% regulation accuracy at rated voltage. Accuracy is mostly determined by the truncation error in the A/D converter and thermal noise in the interface circuits. In general, the calculation error is negligible since all calculations are achieved by a floating-point arithmetic. IEEE Std. 421.5 recommends a 2% step response for testing or analyzing performance of an excitation control loop. Thus, generator voltages due to small perturbation in excitation are measured with a very poor signal-to-noise ratio. For example, the relative accuracy of a 2% step response test may exhibit a 10% error in measurement, which makes it difficult to identify the exciter and generator time constants. This results in very slow convergence which is not compatible with today's fast excitation system requirements.

IV. SELF-TUNING STRATEGY

In order to make the self-exciting control system a linear system, a simple feedback linearization loop is implemented as shown in Fig. 4. The power input voltage is estimated every 50 ms based on the generator rms voltage scaled by the transformer ratio and rated exciter field voltage at no load. The controller output is scaled by the power input voltage to eliminate the bilinear effect.

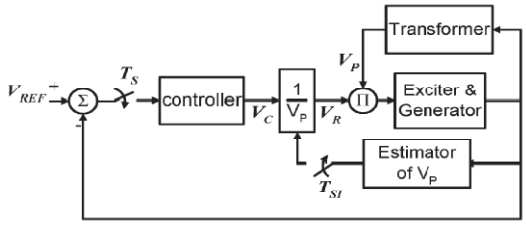

Fig. 4 Feedback linearization of self excited control system

As the sampling time (*TSI*) of the inner loop decreases, the bilinear characteristic disappears in the system response. The selection of 50 ms has been determined based on the simulation results with time constants of the industrial excitation control system under practical noise environment. With inner loop control implemented, a linear estimation algorithm can be utilized. Thus, the plant transfer function $G(s)$ is approximated as

$$G(s) = K_S\left(\frac{1}{1+ST_E}\right)\left(\frac{1}{1+ST'_{do}}\right) \quad ..(2)$$

Where Ks ,T_E and T'_{do} are the system gains, exciter and generator time constants respectively

A. Estimation of the System Gain

As shown in Fig. 1, the system gain varies with the operating conditions. Note that the system gain is the combination of the following: 1) the power amplifier; 2) exciter; and 3) generator gains. The gain K_G in Fig. 3 is used for compensating variations in the system configuration-dependent gains such as power input voltage (*VP*) and saturation effects, i.e., $K_G K_S$ =1. The gain K_G is estimated based on a steady-state condition near rated generator voltage. This is accomplished using a robust controller that includes a soft start feature. The soft start feature is designed to avoid a large voltage overshoot during voltage buildup. The PI controller is utilized to achieve a steady-state condition, at which the regulator output and terminal voltage are measured. The steady-state condition is determined when the generator voltage variation is less than 0.005 p.u. for more than 10 s. The regulator output and generator voltage are utilized to determine the system loop gain K_G. The steps for calculating the loop gain are as follows.

1) Check the residual voltage with zero regulator output.
2) Find the open-loop output corresponding to the residual voltage.
3) Find the regulator output corresponding to the nominal generator voltage using a PI controller.
4) Calculate the loop gain, *KG = VR/VT* where *VR* and *VT* are the PI controller output and generator voltage used in the PI controller, respectively.

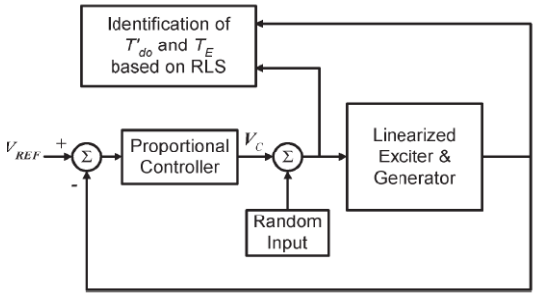

Fig. 5 Identification using RLS

B. Estimation of the Time Constants

RLS with linearization via feedback is depicted in Fig. 5. A closed-loop control system with proportional gain is used, which makes the system stable as well as it operates continuously in a linear region, i.e., not in the saturation region. The white noise disturbance is added to the P-controller output (*VC*). The variance of the white noise is automatically adjusted to maintain the terminal voltage within 0.6–1.0 p.u. The resultant regulator output and generator terminal voltage are sampled every 400 ms and are utilized for estimating the time constants. The closed-loop reference is selected to regulate at 80% of the rated voltage. The actual input to the exciter field is the controller output scaled with an estimate of the power input voltage. Thus, the bilinear characteristic caused by a shunt configuration is canceled and the exciter and generator can be modeled as a linear system.

Using the zero-order hold method to convert from continuous to discrete form, the generator output at the *k*th sample time ($k = 1, \ldots, N$) is expressed in terms of the regulator output, *uk* and the generator output y_k as

$$y_k = a_0 + a_1 y_{k-1} + a_2 y_{k-2} + b u_{k-1} + b_2 u_{k-2} \quad ..(3)$$

where a_0 is used to account for any bias error in the control system. In least square estimation, unknown parameters of a linear model are chosen in such a way that the sum of the squared errors between the actually observed and computed generator voltage is minimum

$$E(\alpha,N)=\sum_{k=1}^{N}(y_k - \emptyset_k^T \alpha)^2 \quad ..(4)$$

where $\alpha^T = [a1\ a2\ b1\ b2\ a0]$ and $\varphi Tk = [y_{k-1}\ y_{k-2}\ u_{k-1}\ u_{k-2}\ 1]$. Solving for the system parameter α, we develop the closed-form solution as follows:
It is possible to manipulate the above equation into a recursive form, which is more efficient for real-time estimation [3]. The recursive form is given by

$$\widehat{\alpha_k} = \left(\sum_{k=1}^{N}(\emptyset_k \emptyset_k^T)\right)^{-1}\left(\sum_{k=1}^{N}(y_k \emptyset_k)\right) \quad ..(5)$$

$$L_K = P_{K-1} - P_{K-1}\emptyset_k[\emptyset_k^T P_{K-1}\emptyset_k + \lambda]^{-1} \quad ..(6)$$

$$P_K = \frac{1}{\lambda}(I - L_K \emptyset_k^T) P_{K-1} \quad ..(7)$$

$$\widehat{\alpha_k} = \widehat{\alpha_{k-1}} + L_K[Y_K - \emptyset_k^T \widehat{\alpha_{k-1}}] \quad ..(8)$$

Where λ is a forgetting factor between zero and one. The forgetting factor of 0.9 is utilized based on experiments with various generators and the initial value of 30 is used for the diagonal element of the covariance matrix. With the estimated values α, the time constants of the generator and the exciter are calculated as follows

$$\widehat{T_{do}^{'}} = -T_S/\log\left(\frac{a1+\sqrt{a_1^2+4a_2}}{2}\right) \quad ..(9)$$

$$\widehat{T_{do}^{'}} = -T_S/\log\left(\frac{a1-\sqrt{a_1^2+4a_2}}{2}\right) \quad ..(10)$$

where Ts is the sampling time

C. Calculation of PID Gains

To simplify the design of the PID controller, we assume that $K_S = 1$, and $T_D = 0$. Thus, the plant transfer function $G(s)$ is given as

$$G(s) = \left(\frac{1}{1+ST_E}\right)\left(\frac{1}{1+ST_{do}^{'}}\right) \quad ..(11)$$

Two methods are suggested for designing PID controllers [1]. First, the pole-zero cancellation approach is considered. The PID controller design using pole-zero cancellation method forces the two zeros resulting from the PID controller to cancel the two poles of the plant. The placement of zeros is achieved via appropriate choice of controller gains. The open-loop transfer function of the system becomes

$$G(s).G_C(s) = \frac{k_d\left(s^2+\frac{k_p}{k_d}s+\frac{k_i}{k_d}\right)}{T_{do}^{'}T_E s\left(s+\frac{1}{T_{do}^{'}}\right)\left(s+\frac{1}{T_E}\right)} \quad ..(12)$$

For the pole-zero cancellation, we set

$$K_I = \frac{K_D}{T_{do}^{'}T_E} \qquad K_P = K_D\left(\frac{T_{do}^{'}+T_E}{T_{do}^{'}T_E}\right) \quad ..(13)$$

Thus, the transfer function gets reduced to

$$G(s).G_C(s) = \frac{K_D}{T_{do}^{'}T_E} \quad ..(14)$$

The closed-loop transfer function then becomes

$$\frac{c(s)}{r(s)} = \frac{G(s).G_C(s)}{1+G(s).G_C(s} = \frac{\frac{K_D}{T_{do}^{'}T_E}}{\frac{S+K_D}{T_{do}^{'}T_E}} \quad ..(15)$$

The time response of the closed-loop system to a unit step input is as follows:

$$C(t) = 1 - e^{-\frac{K_D t}{T_{do}^{'}T_E}} \quad ..(16)$$

If t_r is the specified rise time which is defined as the time required for the response to rise from 10%–90% of its final value, the value of K_D is obtained by

$$K_D = \frac{T_{do}^{'}T_E.ln9}{t_r K_G} \quad ..(17)$$

It can be seen that K_D depends on the plant parameters and the desired rise time. Once we establish K_D, we can calculate K_I and K_P from the equations discussed above.

At first, the idea of pole-zero cancellation might seem academic since the exact pole zero cancellation is virtually impossible. The root locus plots for cases where the actual and estimated time constants are off by ±20% appear significantly different. Experiment shows that in spite of these differences, the designed controller parameters result in performance that is acceptable for most generator sets with the exciter time constant about one-tenth of the generator time constant. Secondly, the PID controller is designed via a variation of pole

placement method. In this method, the desired closed loop pole locations are decided on the basis of meeting a transient response specification. In one possible approach, the design forces the overall closed-loop system to be a dominantly second-order system. Specifically, we force the two dominant closed-loop poles to be a complex conjugate pair, say $s = -a \pm jb$, resulting in an under damped response. The third pole is chosen to be a real pole, say $s = -c$, and is placed so that the natural mode of response from it is five times faster than the dominant poles. The open-loop transfer function $Gc(s)G(s)$ is given as

$$G(s).G_C(s) = \left(k_p + \frac{K_I}{s} + K_D s\right)\left(\frac{1}{1+ST_E}\right)\left(\frac{1}{1+ST'_{do}}\right) \quad ..(18)$$

The PID controller gains, K_I, and K_D are then analytically determined by solving the characteristic equation

$$\left(k_p + \frac{K_I}{s} + K_D s\right)\left(\frac{1}{1+ST_E}\right)\left(\frac{1}{1+ST'_{do}}\right) = -1 \quad ..(19)$$

For $s = -a + jb$, resulting in two equations, and $s = -c$ giving the third equation. We thus have three equations with three unknown controller gains which are solved to get these three gains. The controller also results in two zeros. The effect of the zeros on the transient response is compensated by the overdesign and involves a ziegler nichols method. The root locus of each method to see the effect of zeros is discussed in [1].

V. DESIGN OF SELF-TUNING DIGITAL VOLTAGE REGULATOR

The self-tuning method of a PID controller described in the previous section was derived for a rotary excitation system with the voltage source from the generator terminals (shunt configuration). This technique is also applicable to other types of excitation control systems with some modifications. In order to show its effectiveness and applicability to industrial environment, the proposed algorithm was implemented into an available commercial voltage regulator developed for a small size generator set (less than 10 MVA). In general, this type of regulator has been designed cost-effectively and the size of memory and computation power is limited. The rms calculation of the generator voltage is calculated every half cycle (8.3 ms for 60-Hz system). The self-tuning algorithm is updated every 400 ms. During calculation of the system gain KG, the amplitude of the regulator output is adjusted to maintain the voltage regulation in a linear region at about 80% of the rated generator voltage. A MATLAB program was developed for a simple user interface to the digital voltage regulator with the self-tuning function. The following features are implemented in the PC program:

1) Basic diagnostic functions
2) Estimation of the loop gain using closed loop with PI controller;
3) Estimation of the generator and exciter time constants using RLS;
4) Calculation of the PID controller gains using estimated time constants (T_E and T_{do});
5) Step response with real-time monitoring. The field engineer activates the self-tuning mode using this PC program. The system parameters (system gain and exciter/ generator time constants) are then estimated and the PID gains are calculated using either pole-zero cancellation or pole placement design methods.

VI. TEST RESULTS

The performance of the proposed self-tuning algorithm was verified using a implified first-order exciter and generator simulation models. Estimation results of the proposed method are shown in Table II & III

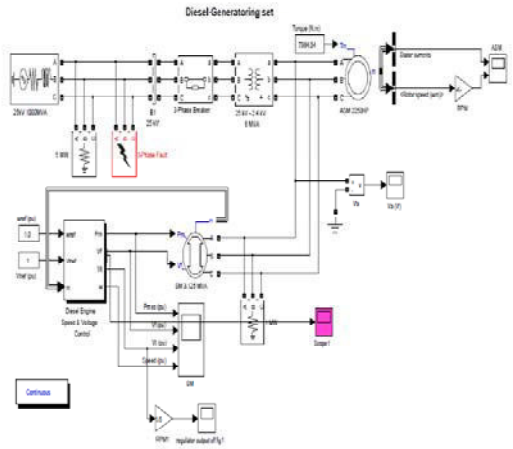

Fig. 6 Simulation diagram for generator output

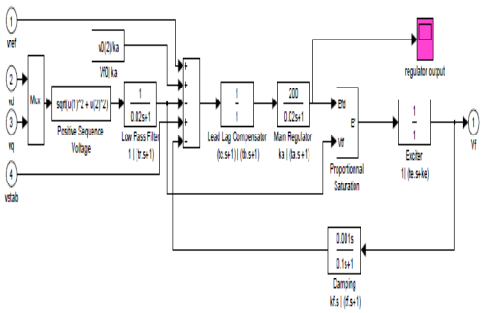

Fig. 7 Simulation diagram for regulator output

Table II: Optimized PID Parameters

Tuning Method	K_p	K_i	K_d
Z-N PID	190	540	30
RLS-PID	58	110	6.5

Table III: Estimation results of the proposed method for self excited external power input

Time constants $(T'_{do}T_{E},)$	RLS
(0.15,2.0)	(0.16,2.0)
(0.3,3.0)	(0.29,3.0)
(0.5,4.0)	(0.49,3.98)

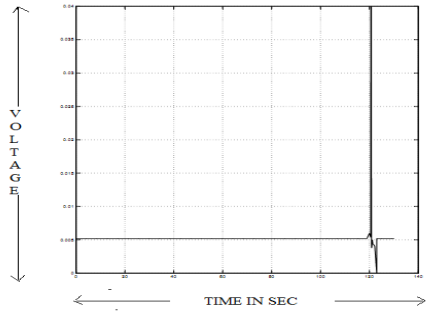

Fig. 7.1 the regulator output

In fig. 7.1 the regulator output by using Z-N values a peak over shoot occur due to the improper gains,

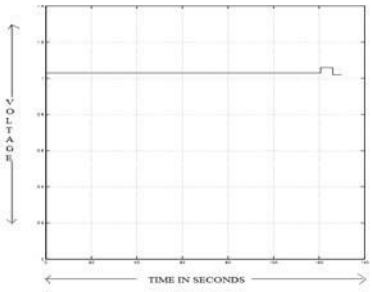

Fig.7.2 the generator output

In Fig 7. 2 the generator output is shown, the x-axis is the time in seconds and y axis is termed as voltage. the response due to the AVR response with Z-N values

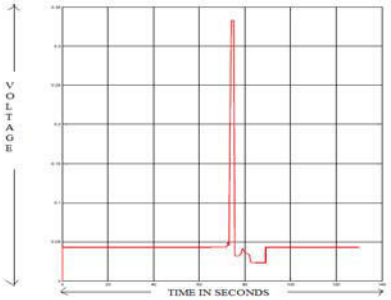

Fig. 7.3 the regulator output with self tuned values

In Fig 7.3 the regulator outputs AVR with self tuned values and the exciter ,generator time constants are existed. the peak over shoot reduced due to the self tuned gains.

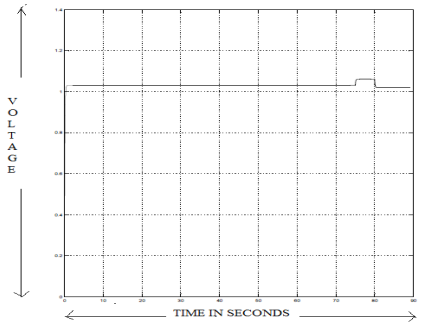

Fig. 7.4 the generator output with self tuned values

In Fig 7.4 the generator outputs AVR with self tuned values and the exciter, generator time constants are evaluated. The response of the generator values came in less commissioning time when compared to Fig 7.2.

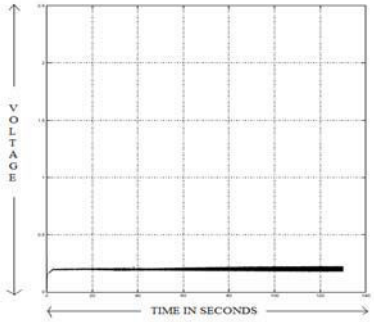

Fig. 7.5 the regulator output with self tuned values with proposed estimation

In Fig 7.5 the regulator outputs AVR with self tuned values and the exciter ,generator time constants with the proposed RLS method are commissioned .In Fig 7.1 the peak over shoot is maximum when compared to Fig 7.3 the peak over shoot reduced due to the self tuned gains and in Fig 7.5 the peak over shoot reduced much compared to Fig 7.3

In Fig 7.6 the generator outputs AVR with self tuned values and the exciter, generator time constants with the proposed RLS method are commissioned.

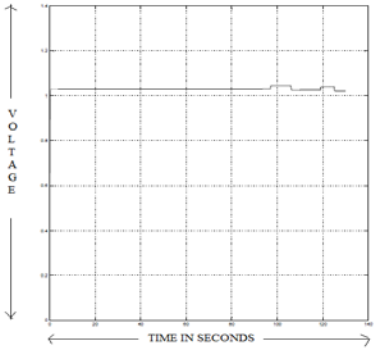

Fig.7.6 the generator output with self tuned values with proposed estimation

The performance of the proposed self-tuning algorithm was tested using a D-G Set, which consists of a 75-kW, 208-Vac, 1800-r/min, 3φ synchronous generator. The no-load excitation for this generator is provided by a self excited 0.3-A, 7-V dc, ac exciter., PID gains (KP = 190, KI = 540, KD = 30, and TD = 0.0) were selected that were obtained for another generator by a conventional method using Z-N method. Since the factory gain for KG = 50 caused a large overshoot, it was reduced to KG = 1.0 to achieve a reasonable response [see Fig. 7.1]. Voltage step response was carried out to compare the performance of these gains to the self-tuned gains. (KP = 58, KI = 110, and KD = 6.5). The time constant for the derivative term was selected as TD = 0.03 to reduce the noise effect. Significantly less commissioning time was required to establish the system PID constants using the self-tuning feature. The voltage step responses of the two methods are illustrated.Fig. 7.1 and 7.2 illustrates a large overshoot which is caused by improper gains. A fast step response with much less overshoot is obtained with the self-tuned gain [Fig. 7.3 and 7.4]. In Fig. 7.1 and 7.2, the voltage steps up and down responses are asymmetric. The large overshoot in the step up response is caused by an asymmetric high forcing limit. This is a typical response for a rotary excitation control system which has no negative field forcing. For this case, the selection of the proper controller gains is more important.

The proposed method was taken the values of gas turbine and a generator rated at 13.8 kV and 15 MVA. The step response using the self-tuned PID gains is illustrated in Fig. 7.5 and 7.6. With the proposed methods, a fast step response with much less overshoot was obtained within several minutes.

VII. CONCLUSION

When compare to the Ziegler Nichols method the self-tuning approach of a PID controller using RLS got the good performance results. The loop gain was estimated at a steady-state condition of the closed loop with a PI controller. Time constants of the exciter and generator were identified with RLS.. With self-tuning of the PID gains, commissioning of a generator excitation control system can be accomplished very quickly with excellent performance results.

REFERENCES

[1] K. Kim and R. C. Schaefer, "Tuning a PID controller for a digital excitation control system," IEEE Trans. Ind. Appl., vol. 41, no. 42, pp. 485–492, Mar./Apr. 2005.

[2] K. Kim, A. Godhwani, M. J. Basler, and T. W. Eberly, "Commissioning and operational experience with a modern digital excitation system," IEEE Trans. Energy Convers., vol. 13, no. 2, pp. 183–187, Jun. 1998.

[3] F. Fnaiech and L. Ljung, "Recursive identification of bilinear systems," Int. J. Control, vol. 45, no. 2, pp. 453–470, Feb. 1987.

[4] Z.-L. Gaing, "A particle swarm optimization approach for optimum design of PID controller in AVR system," IEEE Trans. Energy Convers., vol. 19, no. 2, pp. 384–391, Jun. 2004.

[5] M. Nasri, H. Nezanabadi-pour, and M. Maghfoori, "A PSO-based optimum design of PID controller for a linear brushless DC motor," in Proc. World Acad. Sci., Eng., Technol., Apr. 2007, vol. 20, pp. 211–215.

[6] K. J. Astrom and B. Wittenmark, "On self-tuning regulator," Automatica, vol. 9, no. 2, pp. 185–199, Mar. 1973.

[7] D. Xia and G. T. Heydt, "Self-tuning controller for generator excitation control," IEEE Trans. Power App. Syst., vol. PAS-102, no. 6, pp. 1877– 1885, Jun. 1983.

[8] J. Kanniah, O. P. Malik, and G. S. Hope, "Excitation control of synchronous generators using adaptive regulators. Part I—Theory and simulation results," IEEE Trans. Power App. Syst., vol. PAS-103, no. 5, pp. 897–903, May 1984.1

[9] J. Kanniah, O. P. Malik, and G. S. Hope, "Excitation control of synchronous generators using adaptive regulators. Part II—Implementation and test results," IEEE Trans. Power App. Syst., vol. PAS-103, no. 5, pp. 904–910, May 1984.

[10] J. Finch, K. J. Zachariah, and M. Farsi, "Turbogenerator self-tuning automatic voltage regulator," IEEE Trans. Energy Convers., vol. 14, no. 3, pp. 843–848, Apr. 1998.

OVERVIEW OF AN IMPLEMENTATION OF A NEW ZCS DC-DC FULL-BRIDGE BOOST CONVERTER

RASHMI TIWARI, ANTOSH KR SAHU, SMRITY, RAVI SHANKAR KUMAR, CHANDAN KUMAR & D.INDIRA

Dr.M.G.R University, India.

Abstract:-The paper presents the isolated full-bridge boost converter with active clamp and a new active-clamping algorithm to improve the efficiency . In the proposed method, the resonance between the clamp capacitor and the leakage inductor is utilized to reduce switching losses.The detailed analysis of a full bridge ZCS PWM converter that is suitable for high power dc applications. Based on the features of high voltage power supplies, the converter utilizes parasitic components, particularly for the high voltage transformer, and employs fixed frequency phase shift control to implement soft switching commutations. The current voltage fed bidirectional DC_DC converter can realize ZVS for the switches with the use of the phase shift technology. In order to solve the losses problems a novel phase shift plus PWM control ZVS bidirectional DC-DC converter is proposed, which adopts active clamping branch and PWM technology. Current-fed DC-DC converters like current fed full bridge converters or boost converters with autotransformer, which are appropriate solutions in medium power fuel cell systems, The need of clamping circuits is to protect the main semiconductors against overvoltage's. The energy of the clamping circuits is recovered. It is called active clamping and the energy is fed to the converter's secondary side. A new active snubber cell that overcomes most of the drawbacks of the normal "Zero voltage transition pulse width modulation" converter is proposed to contrive a new family of ZVT-PWM converters. Converter with snubber cell can operate at light load also .Also the auxiliary diodes are subjected to voltage and current values at allowable levels .Moreover the conductor has a simple structure ,low cost and ease of control. Additionally at full output power in the proposed converter, the main switch loss is about 27% and the total circuit loss is about 36% of that in its counterpart hard switching converter, and so the overall efficiency, which is about 91% in the hard switching case, increases to about 97%.

Keywords**:** *Active clamp, dc-dc power conversion,pulse width modulator, soft switching, full bridge converter, zero current switching, zero voltage switching, renewable energy system, Fuel cell system, Snubber.*

I INTRODUCTION

In the high power bidirectional DC-DC converter with an active clamp can be used to limit the overshoot of bridge switch's turn off voltage and enable the energy stored in the transformer leakage inductance to be used for ZVS. The turn off loss in the clamp switches contributes a significant portion to the total loss. We can minimize this loss by using a soft switching active clamp scheme utilizing the resonance between the clamp capacitor and the leakage inductor. Here in our proposed work high voltage version FB-ZCS PWM converter, including steady state analysis, small signal modeling, generalizing major features of the converter and simulation verification for a TWT(Traveling Wave Tube) application.[2] The proposed converter makes use of the parasitic components (capacitance and inductance) to implement ZCS operation. Main advantage is that, rectifier diodes at high voltage side operate with ZVS. A current-voltage-fed PSP ZVS BDC based on an isolated dual boost converter and a half bridge converter is proposed. The converter with an active clamping branch avoids the voltage spike, and also restrains the start-inrush current. By PWM control of the switches across the terminals are well matched, which reduces the circulating conduction losses, also realizes ZVS from no load to full load. The decoupling control of Phase-shift (PS) and PWM is realized by two independence close-loops control circuits.3] A 22-32V / 270V 1.5kW prototype is built to verify the operation principle of the proposed converter. Been widely used in industry due to their high power density, fast transient response and ease of control. Higher power density and faster transient response can be achieved by increasing switching frequency. However, the more switching frequency increases, the more switching losses and electromagnetic interference (EMI) noise occur. For this reason, the switching frequency can be increased by decreasing the switching losses through circuits called snubber cells. In literature, there are many types of proposed snubber cells, such as RC/RCD, polarized/nonpolarized, resonant/nonresonant, and active/passive snubbers. In resonant converters, switching losses are significantly reduced by means of the commutations which are realized with either zero voltage switching (ZVS) or zero current switching (ZCS). But, in these types of converters, excessive voltage and current stresses occur, and power density is lower and control is harder than normal PWM converters.

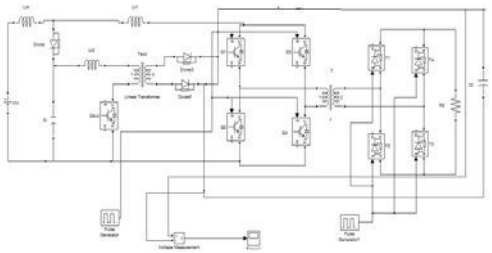

Fig 1 Basic dc to dc converter

II . OVERVIEW OF A SOFT-SWITCHING ACTIVE CLAMPING

The isolated full-bridge boost converter with active clamp is described and a new active-clamping algorithm to improve the efficiency is suggested. [2]The resonance between the clamp capacitor and the leakage inductor is utilized to reduce switching losses. The loss analysis is performed by simulation and the improved performance is confirmed by experimental results is obtained.

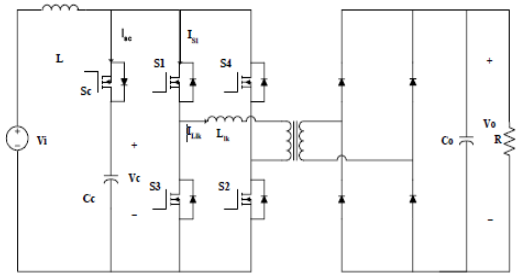

Fig :2.1 Full bridge isolated converter with active clamp

The efficiency of the converter can be improved by reducing the turn-off loss of the clamp switch. When the clamp branch conducts in the clamp capacitor and the leakage inductance resonate. By properly designing the resonant period, the clamp switch can be turned off at the nearly zero current switching condition. To achieve this, the design criterion of the clamp capacitor must be different from the previously proposed criterion.

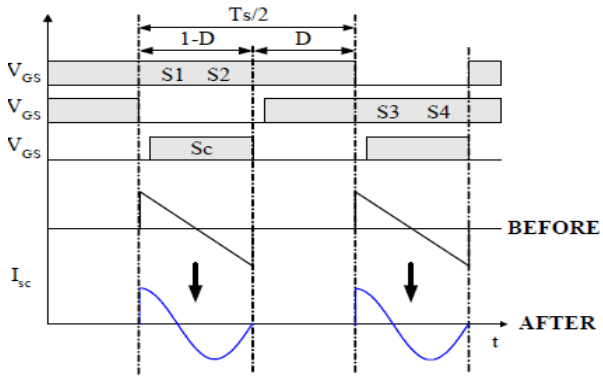

Once the effective duty ratio, D, is determined, the clamp switch on-time is made to be close to three-fourths of the resonance period by the following design criterion in Eq(2).Fig. 4 shows the ZCS turn-off condition meeting the proposed criterion. A soft-switching active clamp scheme for the high power isolated full-bridge converter is proposed. Using the resonance between the transformer leakage inductor and the clamp capacitor during the operation of the clamp branch, the switch turn-off loss is minimized, and the efficiency is improved. These results also lead to a significant simplification of the thermal design of the clamp switch.

II.2 Overview ZCS PWM converter for high voltage and high power application Here the detailed analysis of full bridge zero current switch PWM converter that is suitable for high voltage and high power DC applications. Based on the features of high voltage power supplies the converter utilizes parasitic components, particularly for the high voltage transformer and employs fixed frequency phase shift control to implement switching commutations.[3] Small signal model based on the averaging method is created and simulated results for typical travelling wave tube load are given

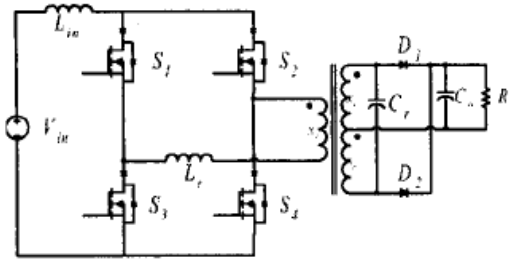

Fig: 2.2.1 A conventional FB-ZCS toplogy.

The simplified circuit is shown .in which capacitance is connected both primary and secondary side of transformer in order to reduce the harmonics

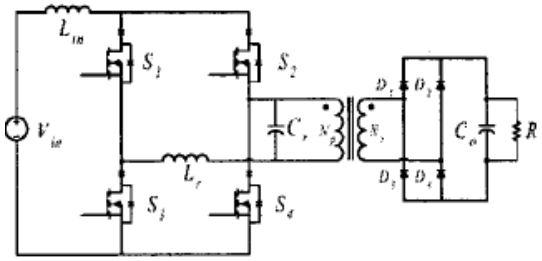

Fig:2.2.2 simplified high voltage FB-ZCS converter

The various steady state characteristics curves with the new simplified circuit is shown .

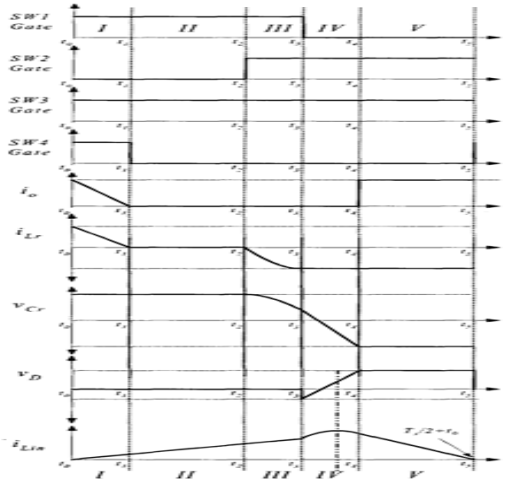

Fig: 2.2.3 half period waveforms of FB-ZCS converter

The waveforms obtained shows the feasibility of the simplified new circuit with capacitor connected in both primary and secondary winding of transformer .the converter has the ability to incorporate parasitic components and also to function with constant frequency operations.

II.3 OVERVIEW OF ZVS BIDIRECTIONAL CONVERTER WITH PHASE SHIFT PLUS PWM CONVERTER

The current voltage fed bidirectional DC-DC converter can realize ZVS for the switches with the use of phase shift technology .the current –fed switches suffers from high voltage spike and high circulating conduction losses.A current voltage fed PSP(phase shift plus) ZVS bidirectional converter based on an dual boost converter and a half bridge converter is proposed, in which the active clamping branch avoids the voltage spike, achieve ZVS of the switches and also restrains the start inrush current.[3]

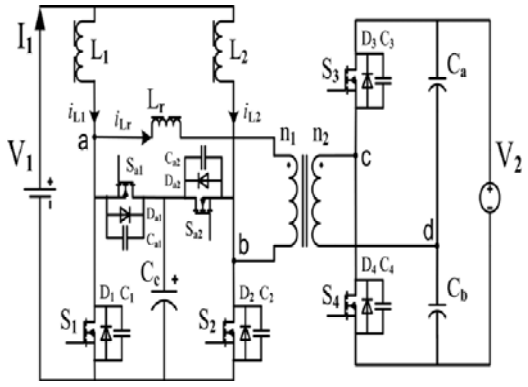

Fig:2.3.1 The novel PSP ZVS bidirectional converter

The BDC has two operation modes, the energy flowing from V1 side to V2 side is defined as Boost mode, and the counterpart is defined as Buck mode. Before the analysis, the following assumptions are given: 1) All the active power devices are ideal switches with parallel body diodes and parasitic capacitors, 2) The inductance $L1$ and $L2$ are large enough to be treated as two current sources with value of $0.5I1$,3) The transformer T is ideal one with series leakage inductor Lr. hows the key waveforms in the Boost mode. One complete switching cycle can be divided into ten periods .Because of the similarity, only a half switching cycle is described in detail. Stage 0 [Before $t0$]. S1, Sa2 and S4 are conducting. The current of the leakage inductor Lr isiLr=$-I(0)$. The power flows from V1 side to V2 side. Stage 1 [$t0$, $t1$]: At $t0$, Sa2 is turned off.Lr, $C2$ and Ca2 begin to resonant, $C2$ is discharged and Ca2 is charged. Stage 2 [$t1$, $t2$] At $t1$, the voltage across $C2$ attempts to overshoot the negative rail. D2 is therefore forward biased. During this period, S2 can be turned on at zero voltage. The voltage across Ca2 is clamped at VCc. The current of the leakage inductor Lr is stage [$t2$, $t3$]: At $t2$, S1 is turned off .Lr, $C1$ and Ca1 begin to resonant, $C1$ is charged, Ca1 is discharged. The current of Lr is Stage 4 [$t3$, $t4$] . At $t3$, the voltage across Ca1 attempts to overshoot the negative rail. Da1 is therefore forward biased. During this period, Sa1 can be turned on at zero voltage. The voltage across $C1$ is clamped at VCc. The current of Lr rises to a positive value.

[$t4$, $t5$] At $t4$, the current of Lris positive. D3 turns on. During this period, S3 can be turned on at zero voltage. The current of Lr is $iLr=I(0)$. The power flows from V1 side to V2 side. At $t5$, starting the second half cycle, which is similar to the first half cycle.

The waveform obtained from the proposed circuit is shown here in which it is in the boost mode

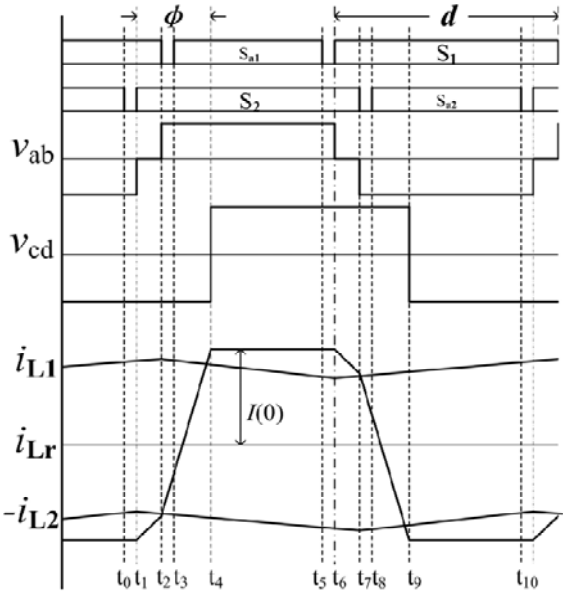

Fig :2.3.2 Key waveform in the boosting mode

An novel ZVS bidirectional dc-dc converter with PS plus PWM control, which has the following been used because, The converter avoids the voltage spike with the use of an active clamping branch Sa1, Sa2 and Cc. The PS plus PWM control reduces circulating current and expands the ZVS range. The decoupling control realizes the energy conversion freely, which has the high steady and dynamic performance.

II.4 OVERVIEW OF ACTIVE CLAMP CURRENT FED DC/DC CONVERTER IN FUEL CELL INVERTER

Current-fed dc/dc converters like current-fed full bridge converters or boost converters with autotransformer, which are appropriate solutions in medium power fuel cell systems, need clamping circuits to protect the main semiconductors against

overvoltages[4]. Depending on the stray inductances of the inductive components the power drawn by the clamping circuit can be up to 5-10 % of the converter's transferred power. The paper describes methods to recover the energy of the clamping circuit.

(sometimes called "active clamping") and to feed it directly into the converter's secondary side. Behaviour of the clamping circuits is shown and analysed. Also the semiconductor losses of the switches in the clamping circuit are derived for both converters

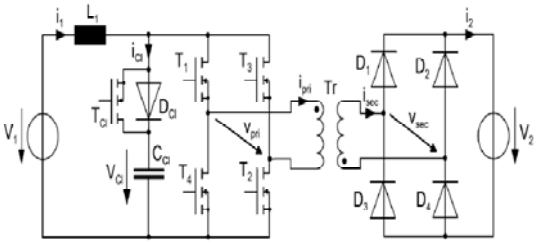

Fig :2.4.1 Current-fed dc/dc converter with galvanic isolation: current-fed full bridge converter.

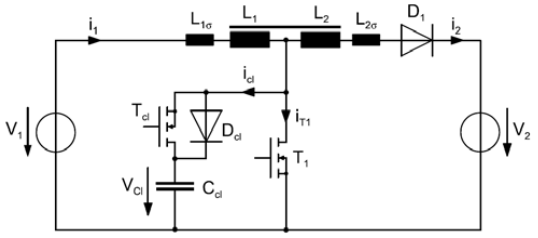

Fig :2.4.2 Current-fed dc/dc converter: boost converter with autotransformer.

For the analysis of the operating behaviour the same assumptions as for the full bridge converter have been made: no losses in semiconductors, capacitive and inductive components. The tapped inductor is modelled by the turns ratio n as defined in section 2.3, the primary leakage inductance L1□and the secondary leakage inductance L2□. Furthermore the short time of the switching-off commutation process of the secondary diode D1 is neglected. The simulated waveforms shown here are also conducive to illustrate the operating behaviour of the converters .shows waveforms for the current fed full bridge converter, fig. 6 shows waveforms for the boost converter with autotransformer both with internal energy feedback. In both simulation models the clamping transistor Tcl is driven using PWM. Figure 5 and show the waveforms for a clamping time interval shorter than its maximum permissible value (tcl < T/2 - td for the current fed full bridge converter; tcl < T - ton for the boost converter with autotransformer).

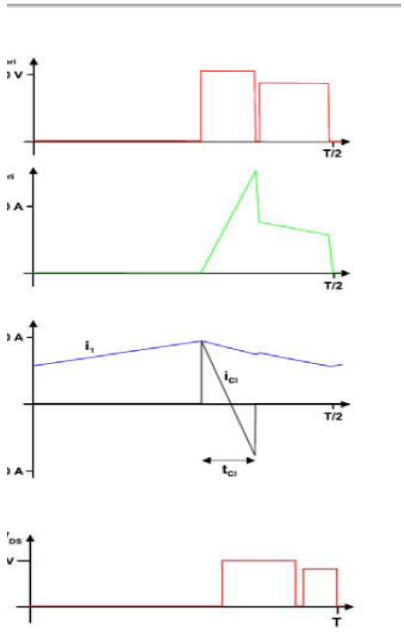

Fig :2.4.3 Waveforms of a current fed full bridge converter with internal clamping energy feedback (from simulation).

II.5 Overview of a new ZVT –PWM DC-DC converter

The paper describes a new active snubber cell that overcomes most of the drawbacks of the normal zero voltage transition –pulse width modulation (ZVT-PWM) converter is proposed to contrive a family of ZVT-PWM converters .most of the semiconductor devices in this converter are turned on or off under exact or near zero voltage switching or zero current switching [5].

Higher power density and faster transient response can be increased by increasing switching frequency. the more switching frequency ,the more switching loses and electromagnetic interference noise occur .the switching frequency can be increased by decreasing the switches loses through the circuits called the snubber cell.

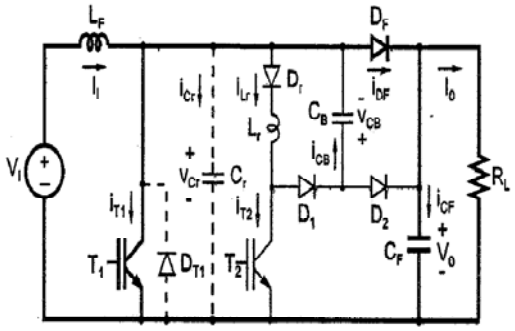

Fig 2.5.1:Circuit scheme of the proposed new ZVT-PWM converter.

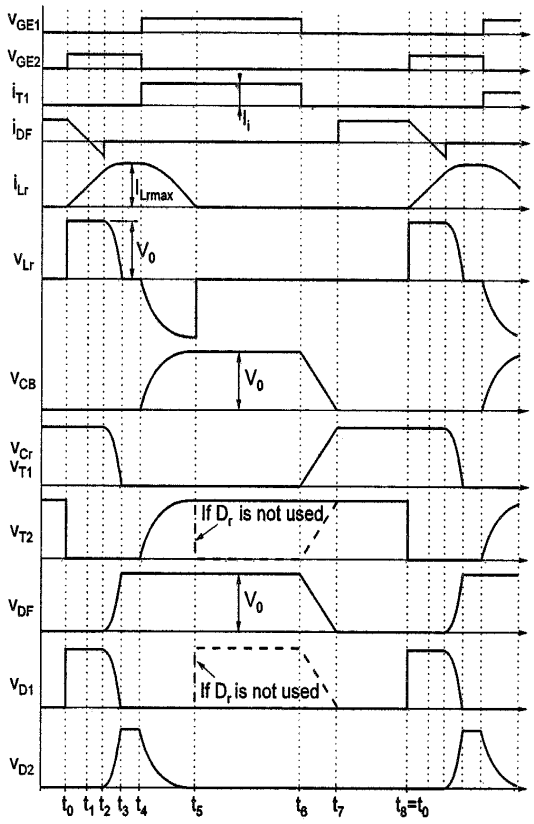

Fig 2.5.2 key waveforms concerning the operation stages in the proposed soft switching converter.

The proposed converter operates at light load condition without any problems .any additional voltage and current stresses on the main device d'nt take place and the auxiliary devices are subjected to allowable voltage and current values .additionally at full output power in the proposed soft switching converter ,the main switch loss is about 27% and the total circuit loss is about 36%.of that in its counter parts ,hard switching converter ,and so overall efficiency increases to about 97% from 91%.

III. PROPOSED WORK

Conventially the circuit used are generally consists of MOSFETS in the inverter circuit but in our proposed work we introduce a IGBT. Some the disadvantages in the exisisting circuits are When energy is transferred to load ,it is getting reduced and conduction loss also increases .Auxiliary circuit which is connected in parallel is active for short duration of time which produces circulating current which contributes to significant amount of losses .Soft switching is not possible in the existing system .Increased peak current stresses in the full bridge switches. An uncontrolled voltage spike and significant voltage ringing can appear across the main converter switches. To overcome this problem we introduced the proposed circuit

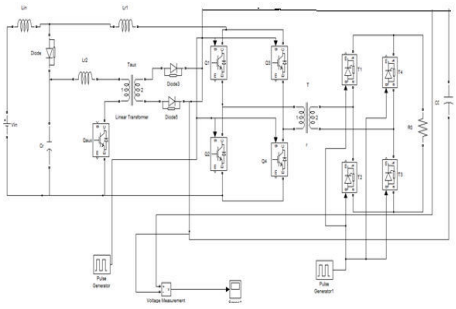

Fig : 3.1 proposed circuit

This circuit basically consists of the IGBT and have following advantages The presence of a transformer in the auxiliary circuit provides a path for energy that would be trapped in the auxiliary circuit[3.1]. Energy can be transferred to the output instead of contributing to conduction losses. The auxiliary circuit is adaptive as the greater the energy that would be trapped in the circuit, the greater the energy that is transferred to the output, since the trapped energy is the main cause of circulating current. Soft switching is possible in ZCS DC-DC PWM full bridge boost converter .Thus the proposed converter is more efficient than the existing converter. Power factor is also improved in the proposed system.

IV. CONCLUSION

We can conclude from the above case study base on the different converters is that a new ZCS PWM DC-DC full bridge boost converter is proposed for better output. The proposed converter is well suited to be used as a fuel cell converter where low input voltage to high output voltage conversion is required .The use of ZVS converters is preferred for applications where MOSFETs are used where the input voltage is high and the input current is low or medium, and where turn-on switching losses dominate. The use of ZCS converters is preferred in applications where insulated gate bipolar transistors (IGBTs) are used where the input current is high, and where conduction losses dominate.

V. REFERENCES:

[1] En-Sung Park Sung Jin Choi, J. Moon Lee and B.H. ChoV.; Fraidlin, S. A Soft-switching Active-Clamp Scheme for Isolated Full-Bridge Boost Converter

[2] Cchris Iannello ,Shiguo Lou ,Issa Battar "A full bridge converter for high voltage and current.

[3] Lizhi Zhu; Kunrong Wang; Lee, F.C.; Clamping for current-fed dc/dc converters with recovery of clampingenergy in fuel cell inverter systems," IEEE APEC 2000,Page(s): 309-313 vol.1

[4] K.Wang , F.C.Lee, and Jason Lai, "Operation Principles of Bidirectional full-bridge DC/DC converter with unified soft-switching scheme and soft-starting capability," IEEE PESC 2000, pp. 111-118

[5] A New ZVT-PWM DC–DC Converter

[6] K.Wang, Lizhi Zhu, Dayu Qu, Hardus Odendaal, Jason Lai, and Fred C.Lee, "Design, Implementation and Experimental Results of Bidirectional

[7] Lizhi Zhu, "A novel soft-commutating isolated boost full-bridge ZVS-PWM dc-dc converter for bidirectional high power applications," IEEE Trans. on PE, 2006,21(2):422-429
.

[8] Huafeng Xiao and Shaojun Xie, "A ZVS Bi-directional DC-DC Converter for High-low Voltage Conversion," IEEE IECON'05, 6-10 Nov., 2005:1154-1158.

[9] R. W. De Doncker, D. M. Divan, and M. H. Kheraluwala, "Power conversion apparatus for dc/dc conversion using dual active bridge," U.S. Patent 5,027,264, 2005
.

[10] M. H. Kheraluwala, R. W. Gascoigne, and D. M. Divan, "Performance characterization of a high-power dual active bridge dc-to-dc converter," IEEE Trans. on IA, 1992,28(6):1294-1031.

[6] Fang Z. Peng, Hui Li, and Gui-Jia Su, et al. "A new ZVS bidirectional dc-dc converter for fuel cell and battery application," IEEE Trans. on PE, 2004,19(1):54-65.

[7] Dehong Xu, Chuanhong Zhao, and Haifeng Fan, "A PWM plus phase-shift control bidirectional dc-dc converter," IEEE Trans. on PE, 2004,19(3):666-675.

[8] Sang-Kyoo Han, Hyun-Ki Yoon, and Gun-Woo Moon, et al. "A new active clamping zero-voltage switching pwm current-fed half-bridge converter," IEEE Trans. on PE, 2005,20(6):1271-1279.

◈◈◈

PLACEMENT OF SYNCHROPHASOR IN DEREGULATED POWER SYSTEM USING MODIFIED INTENSIVE WEED ALGORITHM.

VEENA.A, KRISHAN MOHAN, RIMA BARUA & ALOK KUMAR DAS

Dr.M.G.R University - EEE Department Research Paper Preparation Format as Per IET-UK

Abstract:- Various techniques stress on optimal placement of PMU in power system so as to increase the observability and redundancy. The PMU is a device that helps in fault detection prior to its occurrence. Before the advent of PMU State estimation was the method employed to detect faults. Since there were many disadvantages in it many methods of PMU came into existence. Following are the techniques discussed in the paper:**State Estimation, Intensive Weed Algorithm.**

INTRODUCTION:

The power system, in earlier days was dominated by Investors Owned Utilities. The generation, transmission, distribution was completely under the (IOU). This led to various complications in regards to protection and there was a remarkable increase in the faults. In the due course of time, various private owners came into existence. This gave birth to the concept of deregulated Power Systems. The private owners faced competitions among each other. This led to increased efficiency, reliable power distribution. The power quality increased many folds and the cost effectiveness played a vital role. But, still the problem of fault occurrence was persistent. Several blackouts were witnessed in various parts of the world. To prevent this various techniques came into existence, among which the newest is the placement of a Phasor Measurement Unit or a Synchrophasor. This is device which helps in detecting the fault prior to its occurrence, thus helping in rectifying the faults and protecting the power system. The main aim of this paper is to reduce the number of PMUs used in IEEE 9 bus system, so as to make most of the system observable under one single PMU.

STATE ESTIMATION:

One key element of modern energy management systems is a state estimator: a state estimator uses system inputs and a system model to obtain and depict the power system states (mainly bus voltage magnitudes and phase angles). Many utilities have state estimators in the package of energy management systems. Mr.Schweppe was one of the first to formulate static state estimation for a power network based on the power flow model. The basic idea is to estimate the states of the power network. There is no direct relation between the known states and the desired unknown quantities, which becomes a major drawback. Weighting is the practice of accounting for the confidence in a measurement. There are cases when we come across erroneous data. The data that are erroneous must be identified and eliminated.

One method for the detection of bad data is the examination of the measurements and if the measurements deviate from expected values by some preset threshold values or reference values.

DISADVANTAGES:

Due to the fact that state estimators tend to not accurately represent the system during times of use of incorrect measurements (a condition which is flagged by the estimator), the system operators might turn off this function, have low confidence in the displayed values, or ignore the displayed values.

Another problem that causes state estimators inaccuracies is the model itself. Generally the simple linear model

$$\mathbf{Hx=z}$$

is used where the

H = measurement model (processing matrix),

x = state vector, and **x** = measurements.

If the process matrix is incorrect, the model does not represent what is physically happening in the system. The detection of both erroneous data and improper formation of the process matrix may be done by examining the residual of the equation

Hx=z.

The common technique in correcting the issue of unobservable areas is to provide an estimate of what the readings are in the unobservable areas to create an entire system model.

PHASOR MEASUREMENT UNIT :

Phasor measurement unit is a device which records the phase angles between current and voltage and notes the rate of change of frequency w.r.t. time.

PMUs are equipped with Global Positioning Systems receivers. The GPS receivers allow for the synchronization of the several readings taken at distant points.

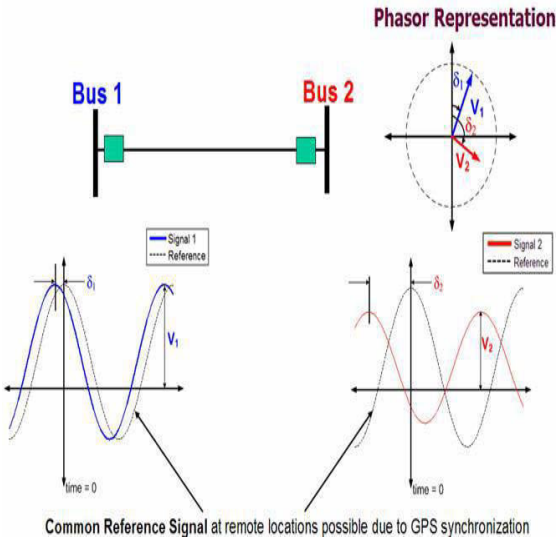

PMUs were developed from the invention of the symmetrical component distance relay **(SCDR).** The SCDR development outcome was a recursive algorithm for calculating symmetrical components of voltage and current. Synchronization is made possible with the advent of the GPS satellite system. The GPS system is a system of 36 satellites (of which 24 are used at one time) to produce time signals at the earth's surface. GPS receivers can resolve these signals into ***{x,y,z,t} coordinates***. The t coordinate is time.

This is accomplished by solving the

distance= (rate) (time)

Equation in three dimensions using satellite signals. The PMU records the sequence currents and voltage the reading with time obtained by the GPS receiver.

ADVANTAGES:

1. The PMU could measure, the once deemed as immeasurable, phase difference between voltage and current.
2. It is possible to achieve accuracy of synchronization of 1 microsecond or 0.021° for 60 hertz signal. This is well in the suitable range of measuring power frequency voltages and current. When completing a state estimation of a power system one of the states, which are being determined, is the voltage angle at each bus.

DISADVANTAGES:

The major drawbacks of PMU are as follows:

1. The device is very expensive.
2. It is very huge, making it immovable and difficult to use.

PROBLEM FORMULATION:

A PMU placed in a certain bus must make most of the system observable. Thus it is essential to make the system observable using the minimum number of PMU. Since PMU is an Expensive equipment reducing its numbers.

The problem formulation of PMU involves inclusion of two variables namely,

Cost variable: w_i

Decision variable: x_i

f(x): vector, whose value is non-zero.

$$\text{Min} \sum_{i}^{n} wi * xi$$

$$\text{s.t. } f(x) \geq 1$$

Where,

$$x_i = \begin{cases} 1 & if\ a\ \ PMU\ is\ \ placed\ at\ \ busi \\ 0 & otherswise \end{cases}$$

IEEE 9 Bus System:

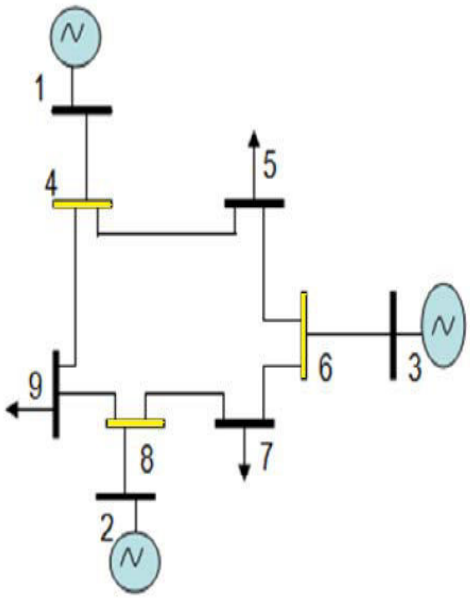

The bus connectivity matrix is denoted by 'A' therefore **let,**

A=

1	**0**	**0**	**1**	**0**	**0**	**0**	**0**	**0**
0	**1**	**0**	**0**	**0**	**0**	**0**	**1**	**0**
0	**0**	**1**	**0**	**0**	**1**	**0**	**0**	**0**
1	**0**	**0**	**1**	**1**	**0**	**0**	**0**	**1**
0	**0**	**0**	**1**	**1**	**1**	**0**	**0**	**0**
0	**0**	**0**	**0**	**1**	**1**	**1**	**0**	**0**
0	**0**	**0**	**0**	**0**	**1**	**1**	**1**	**0**
0	**1**	**0**	**0**	**0**	**0**	**1**	**1**	**1**
0	**0**	**0**	**1**	**0**	**0**	**0**	**1**	**1**

The matrix formed above is out of the case constraints denoted by *f(x)* which is > = 1.

$f_1 = x_1 + x_4$

$f_2 = x_2 + x_8$

$f_3 = x_3 + x_6$

$f_4 = f_1 + f_4 + f_5 + f_9$

$f_5 = f_4 + f_5 + f_6$

$f_6 = f_5 + f_6 + f_4$

$f_7 = f_5 + f_6 + f_7$

$f_8 = f_6 + f_7 + f_8$

$f_9 = f_2 + f_7 + f_8 + f_9$

$f(x) >= 1$

Various methods have come up trying to solve the issue of optimal PMU placement.

Among which few are as follows:

.Ant Colony Optimization

GPS timing

Binary Integer

Genetic Algorithm

Artificial Intelligence Technique

Modified Intensive Weed Algorithm.(MIWA)

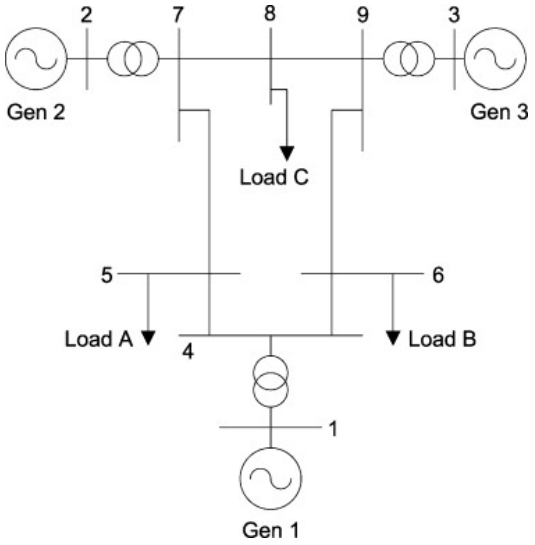

INTENSIVE WEED OPTIMIZATION ALGORITHM :

This technique uses the example of weeds to solve the PMU problem.

When seeds are spread across a stretch of land, the seeds bury themselves deep in the soil and start rooting. These seeds gradually develop into plants these plants inturn give seeds which again try to find space to grow… In this process the weeker plants tend to die and the stronger ones are alive. This goes by the famous principle of SURVIVAL OF THE FITTEST.

ALGORITHM:

1)A finite number of seeds is spread over the entire search area.

2) Each seed will develop and grow into a flowering plant and produce seeds depending on the fitness.

3) All the newly produced seeds are randomly dispersed to the whole search area to produce new plants.

4) This process gets repeated until maximum number of plants is reached; now only plants with best fitness can survive and produce seeds and others will get eliminated. The process will continue until maximum number of iterations is reached and hopefully the plant with the best fitness is closest to the optimal solution.

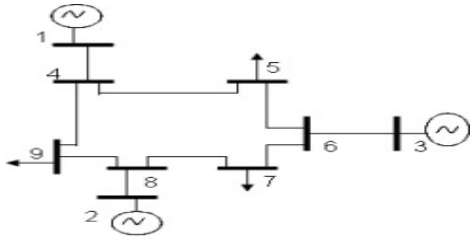

Flow Chart:

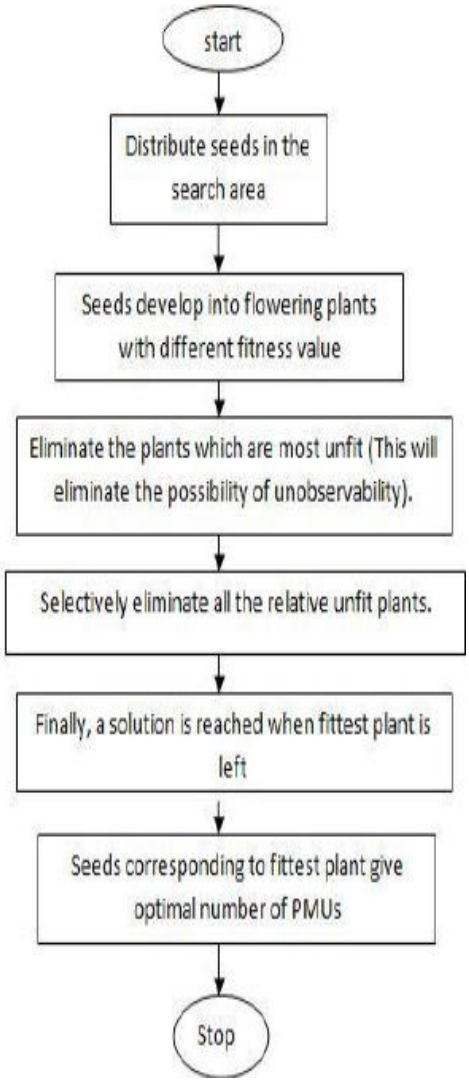

1. This is the first step in PMU placement problem. After connectivity matrix is formed the next step is initialization of seeds, i.e. a finite number of seeds is distributed in the whole search area.

2. A matrix of order 9x512 is formed. The number of entries is 512, which means 512 seeds are produced which will now develop in a flowering plant. The number is exactly 512 (2^ 9) as it is a 9-bus system and there is just two possible outcomes, 0 (PMU not placed at the respective bus) and 1 (PMU placed at the respective bus). Each seeds now develop into a plant, with each having different fitness values.

3. Each of 512 seeds develop into a plant, so in total, the number of plants is 512.

4. The two initial process of Modified Weed Growth algorithm has been already performed. The last step is elimination.

5. All plants which is most unfit, i.e. matrix with even one zero in any row is eliminated in the first step.

6. This step helps to eliminate all the possible chance of unobservability of any bus.

7. Similarly, all unfit plants are selectively removed and lastly a situation is reached in which optimal number of PMUs is found.

8. For a nine bus system the result is PMUs placed at 4,6,8 give us complete observability.

A=

1	**0**	**0**	**1**	**0**	**0**	**0**	**0**	**0**
0	**1**	**0**	**0**	**0**	**0**	**0**	**1**	**0**
0	**0**	**1**	**0**	**0**	**1**	**0**	**0**	**0**
1	**0**	**0**	**1**	**1**	**0**	**0**	**0**	**1**
0	**0**	**0**	**1**	**1**	**1**	**0**	**0**	**0**
0	**0**	**0**	**0**	**1**	**1**	**1**	**0**	**0**
0	**0**	**0**	**0**	**0**	**1**	**1**	**1**	**0**
0	**1**	**0**	**0**	**0**	**0**	**1**	**1**	**1**
0	**0**	**0**	**1**	**0**	**0**	**0**	**1**	**1**

7 Bus System:

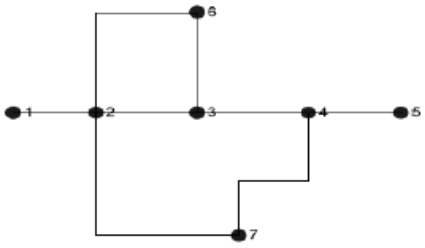

9 Bus System : (IEEE)

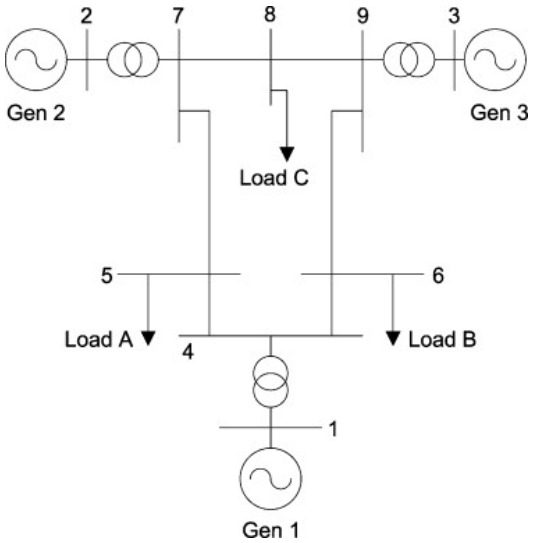

14 Bus System : (IEEE)

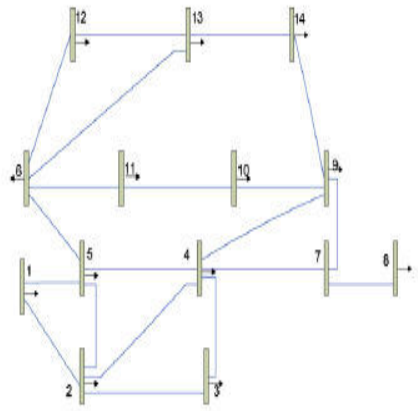

RESULT:

Bus System	System configuration	Optimal position of PMU	No. of PMUs
7 Bus System	Normal measurement condition without considering the effect of redundancy	2,5	2
	Normal measurement condition considering the effect of redundancy	2,4	
IEEE 9 Bus System	Normal measurement condition without considering the effect of redundancy	3,4,8	3
	Normal measurement condition considering the effect of redundancy	4,6,8	
IEEE 14 Bus System	Normal measurement condition without considering the effect of redundancy	2,8,10,13	4
	Normal measurement condition considering the effect of redundancy	2,6,7,9	

Effect after applying condition of redundancy

CONCLUSION:

Thus as we can see, various techniques of fault detection has proven to be useful in solving various faulty situations. But the most cost effective and reliable method is the intensive weed optimization method.

REFRENCES:

[1]. Dissertation based on Research of Mr. Qifeng Ding on optimal meter placement and transaction based loss on deregulated power system.

[2]. Report based on phasor measurement unit data in power system state estimation.

[3]. Paper based on Miwo.

[4]. Paper based on Ai technique.

◈◈◈

A RELIABLE AUTOMATIC METER READING SYSTEM USING POWER LINE DISTRIBUTION NETWORK

VIVEK BHASHKAR, SUSHIL KUMAR, CHANDAN PRASAD, GAUTAM KUMAR MODI, RAJKISHOR MAHTO

EEE department, Dr. M.G.R. Educational & Research Institute University, Chennai, Tamil Nadu

Abstract— The development of automatic meter reader (AMR) using zigbee is presented in this paper. This system consists of zigbee digital power meter installed in every consumer unit and electricity e-billing system at the energy provider side. The zigbee digital power meter is a single phase digital kWh power meter with embedded zigbee modem which sends the power usage reading using information back to the energy provider wirelessly. T the power provider side an e-billing system is used to manage all received meter reading, compute the billing cost, update the data base and to be published billing notification to its respective consumer through wireless. The working principle, hardware and software tools are also explained in detail.

Keywords— *AMR, zigbee, digital power meter, modem.*

I. INTRODUCTION

Meter reading and billing for consumption of electricity, water and gas is done by human operator from house to house and building to building since a long time back. It requires huge number of labour operators and long time working hour to achieve complete data reading and billing of a particular area. Reading error is a common cause of human operator billing. Sometimes the billing job is also slowed down due to bad weather condition. There are many such problems in the billing system which causes inconvenience to the power provider as well as the consumers. And this problem is increasing with the development of residential housing and commercial building in the developing countries. This has, in turn, resulted in increase of power provider billing cost. In order to reduce billing cost and overcome the above mentioned problems, AMR system is introduced.

Automatic meter reading system is a technology which is used to gather data from energy, water and gas metering devices and transfer it to central station in order to analyze it for billing purposes. It is an effective mean of data collection that allow substantial saving through meter re-read, greater data accuracy, allow frequent meter reading, improved billing and consumer service, more timely energy profiles and consumption trends update and better deployment of human resource. With the introduction of new technologies, analog electro-mechanical meters are being replaced by the digital meters which are more convenient to implement the automatic meter reading system.

To transfer the data from consumer's meter to the central station, various communication technologies have been proposed, including mobile technologies, based on radio frequency, transmission over the power line, or telephonic platforms.

II. HISTORY OF METERS

With the development of country's economy and the improvement of national power, the power requirement is still ever increasing due to use of improper power management systems and the conventional energy metering system. Over the past years, metering devices have gone through much improvement, and are expected to become even more sophisticated, offering more and more services.

Meters in the past, and today in a few countries, were electromechanical devices with poor accuracy and lack of configurability. Theft detection was also challenge. Such meters are limited to providing the amount of energy consumption on site. Therefore analog electro-mechanical meters are replaced by the digital meters.

Recent developments in this direction seem to provide opportunities in implementing energy efficient metering technologies that are more precise and accurate, error free, etc. The implementation of automatic meter reading system provides with many vital features as compared with the analog utility meter reading with man power. Some of these features are listed below,

- Higher speed.
- Improved load profile.
- Automatic billing invoice.
- Real time energy cost.
- Load management.
- Alarm warning.
- Remote power switches on/off.
- Tamper detection.
- Bundling with water and gas.

Automatic meter reading system provides a two way communication between the electricity company and the load by sending in a lot of power parameters and control signal to reach the goal of load management and power demand control. With rapid growth of mobile communication network, future application service will gradually concentrate on data transmission service.

The function of the meter can be depicted in the form of block diagram which is as follows.

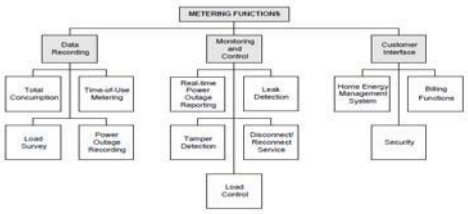

III. HISTORY OF AUTOMATIC METER READING SYSTEM

In 1972, Theodore George "Ted" Paraskevakos, while working with Boeing in Huntsville, Albama, developed a sensor monitoring system which used digital transmission for security, fire and medical alarm systems as well as meter reading capabilities for all utilities. This technology was spin off of the automatic telephone line identification system, now known Caller-ID.

In 1974, Mr. Paraskevakos was awarded a US patent for this technology.

In 1977, he launched Metretek which developed and produced the first fully automated, commercially available remote meter reading and load management system.

The primary driver for the automation of meter reading is not to reduce labour cost, but to obtain data that is difficult to obtain.

Early AMR system often consisted walk-by and drive–by AMR for residential customers and telephone based AMR for commercial or industrial customers. Consequently the sales of drive-by and telephone AMR has declined in the US, while sales of fixed network has increased .The US Energy Policy Act of 2005 asks that electric utility regulators consider the support "time-based rate schedule enable the electric consumer to manage the energy use and cost through advance metering and communication technology".

The trend now is to consider the use of advance meters as part of an Advance metering infrastructure.

The First Commercially Available Remote Meter Reading and Load Management System - Metretek, Inc. (1978)

AMR was first tested about 40 years ago when T&T conducted trials in cooperation with a group of utilities and Westinghouse. After those successful experiments, AT&T offered to provide phone-based AMR services at $2 per meter. The price was four times more than the monthly cost of a person to read the meter. Thus, the program was considered conomically unfeasible. However, in 1972, the General Electric Corporate Research Center, in conjunction with GE Meter Department in omersworth, New Hampshire, began an R&D effort for a remote meter reading system for centralized TOU (Time-Of-Use) metering called AMRAC. Meanwhile, at Rockwell International, a Utility Communication Division had been founded in 1977 to develop distribution carrier communication stems. In the fall of 1984, General Electric acquired from Rockwell International an exclusive license to commercialize their distribution line carrier product designs, related research and technology. The modern era of AMR began in 1985, when several major fullscale projects were implemented. Hackensack Water Co. and Equitable Gas Co. were the first to commit to full-scale implementation of AMR on water and gas meters respectively. In 1986, Minnegasco initiated a 450,000-point radio-based AMR system. In 1987, Philadelphia Electric Co, faced with a large number of inaccessible meters, installed thousands of distribution line carrier AMR units to solve this problem.[3] Advances in solid-state electronics, microprocessor components and low-cost surface-mount technology assembly techniques have naturally been the catalyst to produce reliable cost-effective products capable of m providing the economic and human benefits that justify the use of AMR systems on a large-scale basis.

Components of Automatic Meter Reading System

The general Automatic Meter Reading System onsists of the following four components.

1. Electrical meter:-
2. An electronic device that measures the amount of electrical energy supplied to a esidence or business. It is electrically fed and composed of electronic controllers. It incorporates an interface which allows data to be transmitted from the remote terminal to the collector.
3.
4. Collector:-
5. A collector is able to store and to process received information from many electrical meters according to the command from the upper concentrator. It can also forward the processing data to the concentrator. The number of electrical meters controlled by a collector can be determined by the specific applications.
6.
7. Concentrator:-

On the one hand, a concentrator sends commands to collector to receive meter readings periodically, such as on a monthly basis. On the other hand, it transmits

meter readings as well as load survey data to the database of central station for further analysis.

8. Central station (Control centre):-
Through the layered communication network, the large capacity computer manages every part of the AMR system, such as reading meters periodically or real-time, checking status of each concentrators, making fault diagnosis and alarming. Furthermore, tariff calculation and collection could be realized by interconnection with the power supply system.

A. Selection of communication technology

Apart from the four components of the AMR system , communication media is also present to establish the connection between collector and the concentrator. Various communication technologies in AMR have been proposed recently, including Supervisory Control and Data Acquisition (SCADA), telephone modem, internet, Ethernet, embedded RF module, WiFi, bluetooth, zigbee, mobile technologies, based on radio frequency, transmission over the power line, or telephonic platforms (wired or wireless),PLC, GSM etc. The inherent communication infrastructure presented by Power Line Carrier (PLC), which significantly reduces the cost of building a new communication network, makes PLC a favourable solution for AMR systems. However, since the low-voltage power supply networks are not designed for communications and bandwidth is limited, PLC alone can hardly scale to support a large network in addition to other shortcomings.

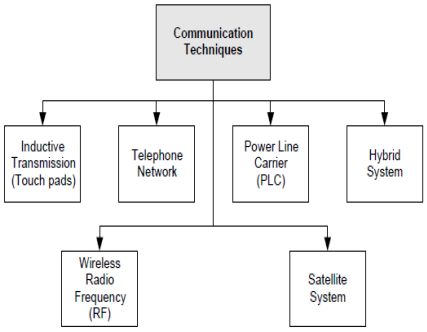

Figure 2 : Communication Techniques

With the rapid development of Global System Mobile (GSM) infrastructure and information communication technology (ICT) in the past few decades have made wireless automatic meter reading system more reliable and possible. But GSM signals are also effected by poor weather conditions. The availability of wireless communication method such as zigbee will play an important role in future for transmitting data at a favourable price from residential buildings to central billing centres and providing extra services for the user. With the advantages of high–speed, unlimited transmission range, zigbee is very suitable for the power applications. Therefore, in this paper we propose an effective solution for ARM combined with zigbee, which can provide the user and the utility with a real-time overview of consumption, thus promoting improvements in energy management and budget planning.

ZIGBEE

ZigBee-style networks began to be conceived around 1998, when many installers realized that both WiFi and Bluetooth were going to be unsuitable for many applications. In particular, many ngineers saw a need for self-organizing ad-hoc digital radio networks. The IEEE 802.15.4-2003 standard was completed in May 2003 and has been superseded by the publication of IEEE 802.15.4-2006. In the summer of 2003, Philips Semiconductors, a major mesh network supporter, ceased the investment. Philips Lighting has, however, continued Philips' participation, and Philips remains a promoter member on the ZigBee Alliance Board of Directors. The ZigBee Alliance announced in October 2004 that the membership had more than doubled in the preceding year and had grown to more than 100 member companies, in 22 countries. By April 2005 membership had grown to more than 150 companies, and by December 2005 membership had passed 200 companies. The ZigBee specifications were ratified on 14 December 2004. The ZigBee Alliance announced availability of Specification 1.0 on 13 June 2005, known as ZigBee 2004 Specification. In September 2006, ZigBee 2006 Specification is announced. In 2007, ZigBee PRO, the enhanced ZigBee specification was finalized. The first stack release is now called ZigBee 2004. The second stack release is called ZigBee 2006, and mainly replaces the MSG/KVP structure used in 2004 with a "cluster library". The 2004 stack is now more or less obsolete. ZigBee 2007, now the current stack release, contains two stack profiles, stack profile 1 (simply called ZigBee), for home and light commercial use, and stack profile 2 (called ZigBee PRO). ZigBee PRO offers more features, such as multi-casting, many-to-one routing and high security with Symmetric-Key Key Exchange (SKKE), while ZigBee (stack profile 1) offers a smaller footprint in RAM and flash. Both offer full mesh networking and work with all ZigBee application profiles. ZigBee 2007 is fully backward compatible with ZigBee 2006 devices: A ZigBee 2007 device may join and operate on a ZigBee 2006 network and vice versa. Due to differences in routing options, ZigBee PRO devices must become non-routing ZigBee End-Devices (ZEDs) on a ZigBee 2006 network, the same as for ZigBee 2006 devices on a ZigBee 2007 network must become ZEDs on a ZigBee PRO network. The applications running on those devices work the same, regardless of the stack profile beneath them.The ZigBee 1.0 specification was ratified on 14 December 2004 and is available to members of the ZigBee Alliance. Most recently, the ZigBee 2007

specification was posted on 30 October 2007. The first ZigBee Application Profile, Home Automation, was announced 2 November 2007.

ZigBee is a low-cost, low-power, wireless mesh network standard. The low cost allows the technology to be widely deployed in wireless control and monitoring applications. Low power-usage allows longer life with smaller batteries. Mesh networking provides high reliability and more extensive range. ZigBee chip vendors typically sell integrated radios and microcontrollers with between 60 KB and 256 KB flash memory. ZigBee operates in the industrial, scientific and medical (ISM) radio bands; 868 MHz in Europe, 915 MHz in the USA and Australia, and 2.4 GHz in most jurisdictions worldwide. Data transmission rates vary from 20 to 900 kilobits/second. The ZigBee network layer natively supports both star and tree typical networks, and generic mesh networks. Every network must have one coordinator device, tasked with its creation, the control of its parameters and basic maintenance. Within star networks, the coordinator must be the central node. Both trees and meshes allows the use of ZigBee routers to extend communication at the network level. ZigBee builds upon the physical layer and medium access control defined in IEEE standard 802.15.4 (2003 version) for low-rate WPANs. The specification goes on to complete the standard by adding four main components: network layer, application layer, ZigBee device objects (ZDOs) and manufacturer-defined application objects which allow for customization and favor total integration. Besides adding two high-level network layers to the underlying structure, the most significant improvement is the introduction of ZDOs. These are responsible for a number of tasks, which include keeping of device roles, management of requests to join a network, device discovery and security.

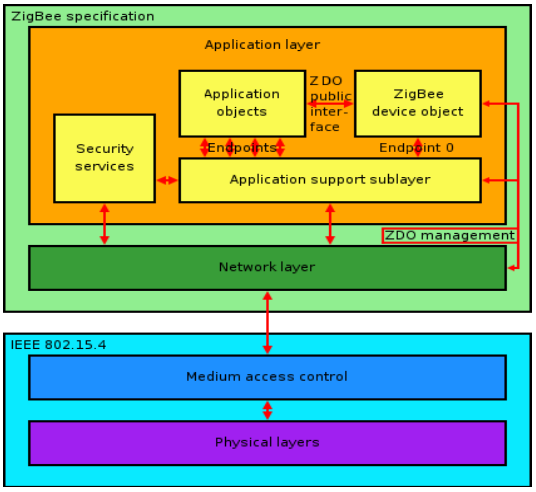

ZigBee protocol stack

ZigBee is not intended to support powerline networking but to interface with it at least for smart metering and smart appliance purposes. Because ZigBee nodes can go from sleep to active mode in 30 ms or less, the latency can be low and devices can be responsive, particularly compared to Bluetooth wake-up delays, which are typically around three seconds. [3] Because ZigBee nodes can sleep most of the time, average power consumption can be low, resulting in long battery life.

Market needs

The utilities and Electric Metering companies continually look for improved methods to support their day to operations, which include: Providing flexible billing dates for customers, Performing Monthly/Cycle billing reads, Implementing Time-of-Use billing, Capturing Peak Demand, Supporting Critical Peak Pricing events, Forecasting energy usage, Positive outage and restoration detection and notification., Theft detection, Remote connect and validation, Market advanced Electric Metering and billing programs

Market analysis

Within the typical ZigBee network there is a single "owner" or "stakeholder." This owner can determine which devices are allowed on the PAN by only sharing network keys with trusted devices. There may be two stakeholders for a single network: the utility and the end customer. Neither of these stakeholders necessarily trusts the other. The utility wants to be sure that the end customer cannot use ZigBee to inappropriately manipulate a load control or demand response system, or attack an energy service portal. The customers want to be sure that the energy service portal does not allow the utility to take liberties with their equipment or compromise their privacy. This results in four primary network ownership / deployment scenarios: utility-private, customer-private, shared, and bridged. Each of these scenarios has different implications. All of these scenarios are valid for EMI deployments, though their use may be specific to particular use cases or markets .

E.1. Utility private

Utility Private HAN might include an in-home display, or a load control device working in conjunction with energy service portal, but it would not include any customer controlled devices.

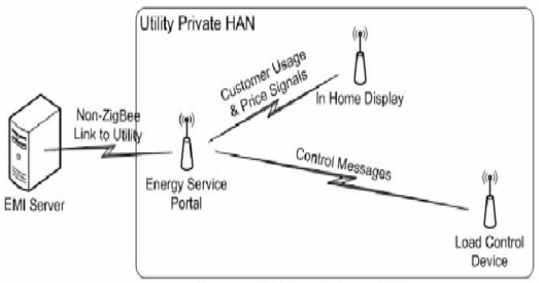

Figure 2 Utility Private HAN.

E.2. Customer-private

In the most extreme form, a customer private network might not even include an ESP on the ZigBee network, instead relying on some sort of customer provided device with non-ZigBee access to usage, consumption, and price data. Control messages in these examples would be one determined by the end customer, not the utility, and programmed into a home energy management console.

E.3. Customer and Utility Shared

The shared HAN represents the worst security scenario for an EMI deployment. Devices are on a network they cannot trust, with other devices they cannot trust. Application level authentication and authorization are required to support a shared network environment.

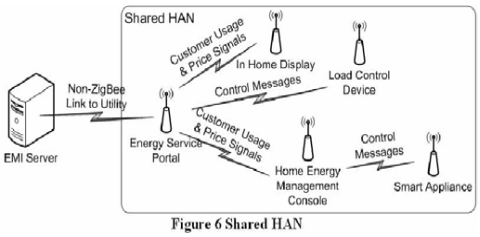

Figure 6 Shared HAN

E.4. Aplication- Llinked

As an example, in the scenario below, the Utility HAN is made available strictly to utility controlled devices. The Home Energy Management Console is a utility approved device that also lives on a customer provided HAN. It can respond to EMI commands, as well as sending out HA commands to devices within the home.

B. System architecture

Based upon the above proposed idea of the automatic meter reading system following block diagram is prepared.

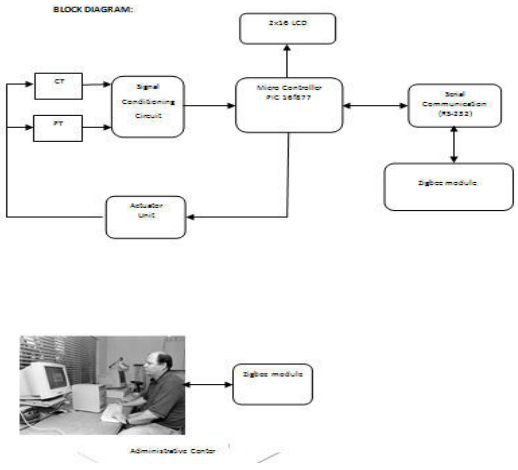

The power supply circuit required for this system is given below.

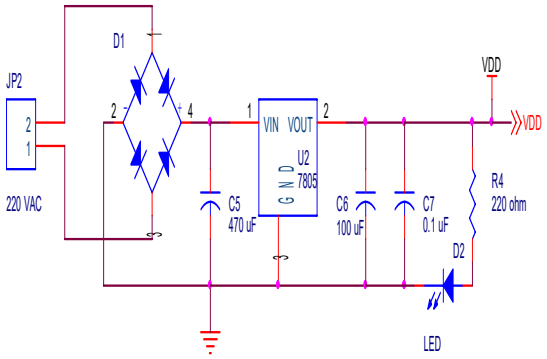

HARDWARE:- The hardware tools that are used in the system are as follows.

- Power supply[5v]
- PIC16F877A microcontroller
- Zigbee Module
- Current Transformer
- Voltage Transformer
- Display unit(LCD)
- Relay
- Max232 – serial communication

SOFTWARE:- Following software tools are recommended for the system proposed in this paper.

- MPLAB IDE
- Hitech c compiler
- Win pic programmer
- ORCAD design

IV. CONCLUSIONS

ZigBee technology is a new wireless protocol that widely used various areas for it excellent performance in reliability, capability, flexibility and cost. ZigBee corresponds to a large market. This paper provides an application in the field of automatic Electric Meter Reading System. With the developments of the ZigBee technology and the communication network technology of computer, wireless Electric Meter Reading System will grow up and practical mostly.

The automatic meter reading system presented in this paper absorbed many advanced study results in computer technology and communication technology. The meter-reading task can be finished at the management department of residence area by using this system. Meantime, the energy resources management departments can monitor the consumption of power in order to improve the utility of power. It's the basic to realize automatic deliver of energy resources. The system has many significant excellences, such as wireless, low-workload, great quantity of data transmission high-veracity and low-expenses.

ACKNOWLEDGMENT

This paper was supported by E.E.E. department of Dr. M.G.R. Educational and Research Institute University, Chennai. And the authors also gratefully acknowledge the efforts of Mrs. B.V. Harini for her effort, time and work on this project which made this publication possible.

REFERENCES

[1] ZigBee Alliance, ZigBee Specification Version 1.0, http:// www.ZigBee.org, December 14th, 2004

[2] Microchip Technology Inc. Microchip Stack for the ZigBee™

[3] Bharath, P.; Ananth, N.; Vijetha, S.; Prakash, K.V.J.; "Wireless Automated Digital Energy Meter" in Sustainable Energy Technologies, ICSET 2008.

[4] Chih-Hung Wu; Shun-Chien Chang; Yu-Wei Huang; "Design of a wireless ARM-based automatic meter reading and control system" in Power Engineering Society General Meeting, 2004. IEEE.

[5] Liting Cao, Jingwen Tian and Dahang Zhang, "Networked Remote Meter-Reading System Based on Wireless Communication Technology" in International Conference on Information Acquisition, 2006 IEEE.

DATAMINING USED IN SMALL BUSINESS THROUGH NEURAL NETWORK

MAZIDUL AHMED & JAYA CHOUDHARY

IT Department, CMJ University, Shillong, Meghalaya

Abstract:- The field of data mining through neural network has been developed past several years. Data mining technology provides a powerful tools set to generate various data- driven classification system. The applications of data mining through has been used to business. Several new algorithms has been commonly developed in terms of data mining through neural network. In terms of data mining through neural network used for business , there has always been comparison of methods in which very new methods are applied. This study mainly focuses on how data mining technique will be used for handling small business for finding out meaningful pattern from the database.

***Key terms*:-** *Data mining, Neural network, Time series analysis, Stopping rules, Decision trees, Rule induction and Data visualization.*

INTRODUCTION

In every business, each new step has been taken built upon the previous one . While taking each new step, data has to be collected , accessed and need decision support than can guide decisions in conditions of limited certainly. In this paper, I would be applying neural method to small business lending decisions. This study will drill through in data navigation from a small business to explore data in search of consistent patterns and or systematic relationships between variables and then to validate the findings by applying the detected patterns to new subsets of data. From data analysis, preparation of data , modeling, evaluation will be conducted and then neural network datamining concept is focused to use decision tree algorithm to segment customers as a point of reference to make prediction . Neural network as a device in small business can be a very useful tool for enhancing small business lending decisions and reducing loan processing time and cost.

OBJECTIVES OF THE STUDY

1. The main goal of the study is to identify customer who are likely to respond positively to a product and to target any advertising or solicitation towards these customers. For this neural networks is used to monitor customer behavior patterns over time and to learn to detect when a customer is about to switch to a competitor .
2. The study will check for forecasting sales. Here time series analysis will be used to take data from past and provide a look to the future even when there are seasonal increases or declines.
3. This study is to predict levels of risk for identifying credit ratings in business. It will analyse to detect anomalies in the business. Here market-based analysis will be used through data to let retailers know what products are being purchased together.
4. This study will also identify to integrated into complex modeling which would be checking for making decision process.
5. The study shall also check whether the organization can use it to solve combinatorial optimization problem to filter noise from measurement data to control ill-defined problems in summary to estimate sampled functions.

REVIEW OF LITERATURE

A review of literature of datamining technique had been used such as association rule, rule introduction technique , A priori algorithm and neural network .

Leonid churilov , A lyl lagirov, Daniel schwartg, kate smith and Michael dally had already studied about combined use of self organizing maps & non-smooth, non-convex optimization techniques in order to produce a working case of a data driven risk classification system. The optimization approach strengthens the validity of self organizing map results. This study will be applied to business data. Business data are partitioned into homogenous groups to support future business decisions.

METHODOLOGY USED

Here data have been collected the five selected samples of data from a water purifier N.E. based ISO certified company situated at beltola. Observation has been done through direct communication with the respondents and collection of data has been done through questionnaires and direct communication with the staff working in that organisation. From the statistical statement and reports of the company , An analysis has been done from monthly statement and reports and had been put to Back propagation algorithm, Network predictive model.

Backprogation algorithm:-This is a common methods of teaching artificial neural networks how to perform a given task.It is used in layered feed forward artificial neural networks.This means that the

artificial neurons are organized in layers and send their signals " forward" and then the errors are propagated backwards. This algorithm is to reduce this errors.

Feed forward neural network:-
It consists of three layers:- an input layer, hidden layer (H)and output layer. In each layer there are one or more processing elements(P.Es). PEs is meant to simulate the neurons is the brain and this is why they are often referred to as neurons or nodes. A PE receives inputs from either the outside world or information on associations, classifications, clusters and forecasting .

Network Predictive Model:-
Classification and prediction is a predictive model. The most common action in datamining is classification. It recognizes patterns that describe the group to which an item belongs. It does this by examining existing items that already have been classified and inferring a set of rules. Prediction is the construction and use of a model to assess the class of an unlabeled object or to assess the value or value ranges of a given object is likely to have. The next application is forecasting . This is different from predictions because it estimates the future value of continous variable based on patterns within the data.

Here training data's are taken as input to artificial neural network and then determines how the neural interconnection weights are corrected due to differences in the actual and desired output for a member of the training set. Datas taken from the company are used for network training and verification which is composed of monthy figures for individual equities listed from Apr 2011 to Mar 2012. We used the rate of turn over as our output by training network with 1,2,3,4, and 5 hidden layers by using back propagation algorithm. Normalisation is the key part of neural network and would enable us to predict more accurate rate of turn over. Normalised data is used for training neural network with backpropagation algorithm. We normalize inputs so that input value lies between 0 and 1. We have developed three modules:-First module is used for calculating weights by using backpropagation algorithm. Secondly module is used for predicting rates of turn over in every months by denormalizing by using weights. We got from first module.Third module is used for getting sale of products and then we get predicted turn over every month from trained network with different hidden layers. We generate signals to know whether that ordered products should be sold and then compare it with the actual turn over of monthly target. By this comparision we got correction of our prediction.

Data Analysis and Findings
MONTHLY SALES REPORT:-

SNO.	SAMPLE PERIOD	ACTUAL SALE(%)	PREDICTED SALE(%)
1.	30/04/2011	42	68
2	1/06/2011	45	68
3	31/06/2011	67	79
4	30/07/2011	56	78
5	1/08/2011	48	57
6	31/08/2011	89	86
7	30/09/2011	53	59
8	30/10/2011	69	70
9	30/11/2011	47	59
10	31/12/2011	34	47
11	31/01/2013	36	49
12	28/02/2013	47	50
13	31/03/2013	57	59

PREDICTIVE MODEL OF SALES REPORT

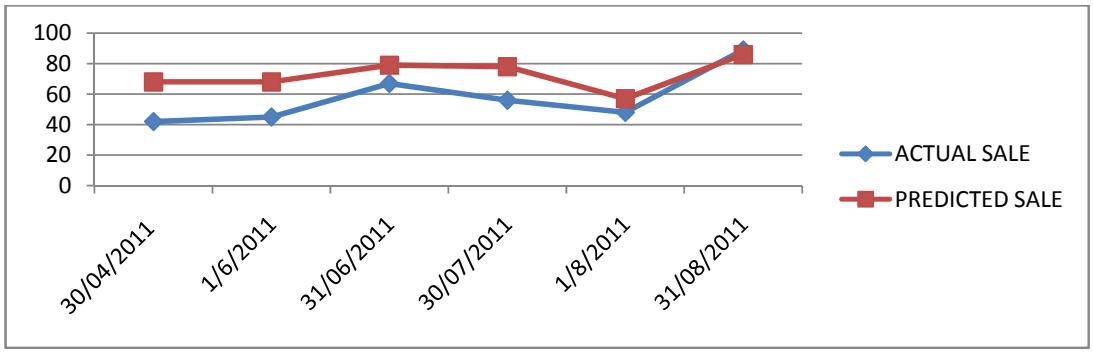

The simplified process for training a FFNN is a as follows:-

1. Input data is presented to the network and propagated to the network until it reaches the output layer . This forward process produces a predicted output.
2. The predicted output is substracted from the actual output and an error value for the networks is calculated.
3. The neural network then uses supervised learning, which in most case is back propagation to train the network. Back propagation is a learning algorithm for adjusting the weights. It starts with the weights between the output layer PE's and the last hidden layer PE's and works backwards through the network.
4. Once back propagation has finished, the forward process starts again and this cycle is continued until the error between predicted and actual output is minimized. The back propagation algorithm performs learnings on a feed – forward neural network.

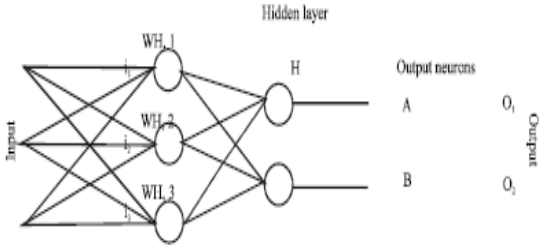

There are connections between the PE's in each layer that have a weight(parameter) associated with them. This neuron has three weights feeding into it, $w_{H,1}$ $w_{H,2}$ and $w_{H,3}$. This weight is adjusted during training. Information only travels in the forward direction through network:- There are no feedback loops.

In the back propagation, the artificial neurons are organized in layers and send their signals "forward" and then the errors are propagated backwards. The back propagation algorithm uses supervised learning, which means that we provide the algorithm with examples of the inputs and outputs .we want the network to compute, and then the error(difference between actual and expected results) is calculated. The idea of back propagation algorithm is to reduce the error until ANN learns the training data.

The technique used in back propagation algorithm is:-

a) Present a training sample to the neural network.
b) Compare the networks output to the desired output from that sample. Calculate the error in each output neurons.
c) For each neuron, calculate what the output should have been and a scaling factor, how much lower or higher the output must be adjusted to match the desired output. This is the local error.
d) Adjust the weights of each neuron to lower the logical error.

Algorithm used

1. Initialize the weights in the network.
2. Repeat:-
   For each example e in the training set do
   a) O=neural-net-output(network,e); Forward pass
   b) T=Teacher output for e
   c) Calculate error(T-O) at the output units.

The below graph of figure shows the turn-over of sales report of different periods

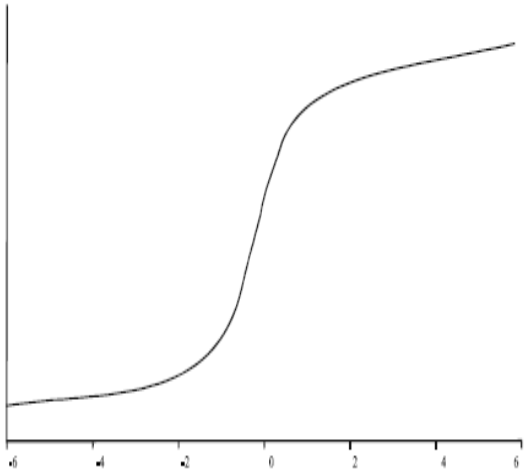

CONCLUSION

This paper presents technical analysis and fundamental analysis to create a feed forward multilayer perceptron neural network predictive model trained with backprogation algorithm for improved accuracy of sales prediction. To determine the performance of our model, an empirical study was carried out with the companys sales data obtained from different companys, where the turn over of different period was compared with the use of only technical analysis. The empirical results obtained showed high level of accuracy for monthly sales prediction with different approach performing better .Therefore, these approaches has the potential to enhance the quality of decision making of company in the sales market by offering more accurate sales prediction compared to existing technical analysis based approach. In future work, we intend to determine the critical impact of specific fundamental analysis on quality of sales and turn-over prediction.

REFERENCES

[1]. Data Mining With Neural Networks: Solving Business Problems ... :- Xianjun Ni

[2]. Itelligent Engineering Systems Through Artificial Neural Networks, Volume 7

[3]. M. Craven & J. Shavlik (1997). Using Neural Networks for Data Mining.

[4]. Wong BK, Bodnovich TA, Selvi Y. A bibliography of neural network business application research: 1988}September 1994. Expert Systems 1995;12(3):253}61.

[5]. Stock Rate Prediction Using Backpropagation Algorithm: Results with Different Number of Hidden Layers :-Asif Ullah Khan, Mahesh Motwani , Sanjeev Sharma , Abdul Saboor Khan and Mukesh Pandey

[6]. Stock Price Prediction using Neural Network with Hybridized Market Indicators:-1Adebiyi Ayodele A., 1Ayo Charles K., 1Adebiyi Marion O., and 2Otokiti Sunday O.

[7]. M.T. Philip, K. Paul, S.O. Choy, K. Reggie, S.C. Ng, J. Mak, T. Jonathan, K. Kai, and W. Tak-Lam,

[8]. "Design and Implementation of NN5 for Hong Stock Price Forecasting", Journal of Engineering

[9]. Applications of Artificial Intelligence, vol. 20, 2007, pp. 453-461.

A SYSTEMATIC APPROACH ON SCRAP REDUCTION USING OPTIMIZATION TOOL

B.GOPINATH, RAMKUMAR.K, SUDHARSHAN & SAI RANJITH.K

Dept. of Mechanical Engg, Easwari Engg,College, Chennai-600089,India

Abstract:-In today's scenario the scrap materials or the wastage in every industry, across the globe have resulted in major depreciation in the total company costs and revenue, so industries emphasize on the concept of optimization to reduce the unwanted scrap that is being produced during various manufacturing processes. In order to reduce these side effects, the fundamental requirement is to reduce the scrap discharge before the manufacturing process is completely done and bring an optimized method which has been case studied in this paper in a a tubular components manufacturing industry near Chennai which is collaboration with a UK based industry.

I. INTRODUCTION:

In this journal paper we have found a new technique to reduce the scrap, which is the algorithm being used as a input to the software LINGO 9.0, gives the accurate amount of scrap that is being reduced. Based on observation made in the industry, we have identified a problem in the slitter section by using cause & effect diagram. The main objective of the case study is to minimize trim losses and to increase the yield .Also necessary tabulations and graphs are made which represents the scrap details and the customer requirements.

The following section contains (ii) Methodology being used for optimization (iii) Software used to solve the analysis (iv) Results that emerges from the given input from the software (v) conclusions and future descriptions.

Causes in a cause & effect diagram are frequently arranged into four major categories. While these categories can be anything, you will often see:

- manpower, methods, materials, and machinery (recommended for manufacturing)
- Equipment, policies, procedures, and people (recommended for administration and service).

CAUSES

MATERIAL:

- Indefinite shapes at coil ends.
- Coil bending.
- Uneven coil width.
- Rust.

II METHODOLOGY USED

CAUSE & EFFECT RELATIONSHIP:

The cause & effect diagram is the brainchild of Kaoru Ishikawa, who pioneered quality management processes in the Kawasaki shipyards and in the process, became one of the founding fathers of modern management. The cause and effect diagram is used to explore all the potential or real causes (or inputs) that result in a single effect (or output). Causes are arranged according to their level of importance or detail, resulting in a depiction of relationships and hierarchy of events. This can help you search for root causes, identify areas where there may be problems, and compare the relative importance of different causes.

MAN POWER:

- Excess shear cutting in slit.
- Cutting to maintain equal slit length.

MACHINE:

- Coil bits
- Maintenance

Uneven length of strips.

- Excess raw material supply from vendor.

MEASUREMENT:

- Sample cuts in strips and coils.

EFFECT MODELLING PROCEDURE:

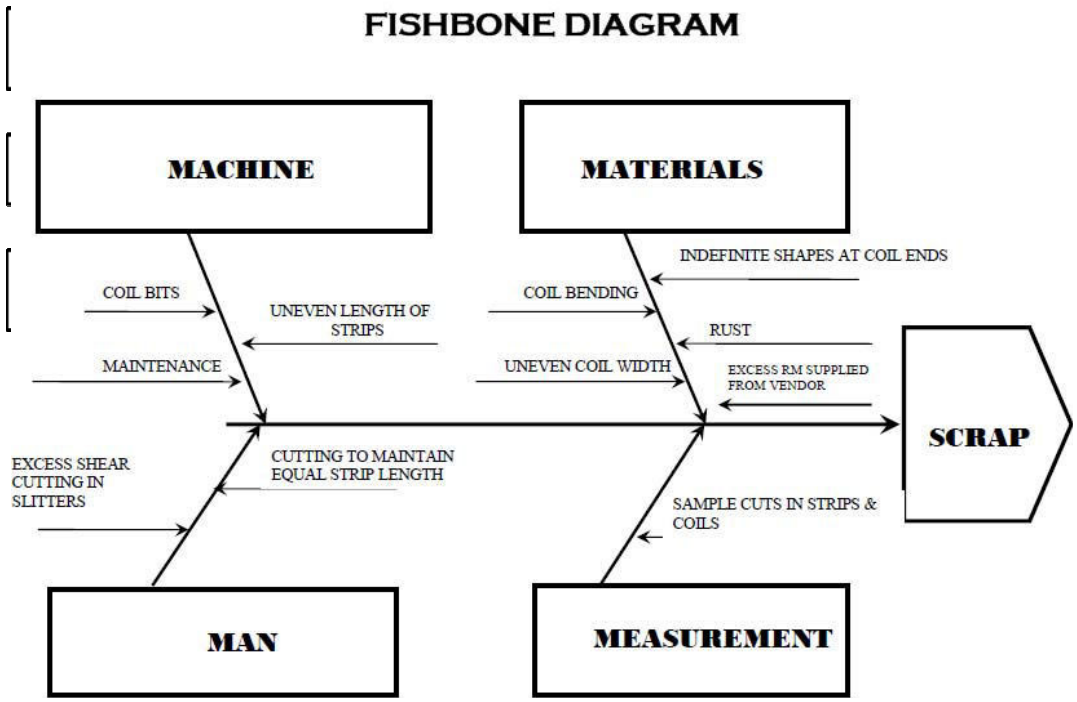

PROBLEM IDENTIFICATION:

Based on observation made in the industry, we have identified a problem in the slitter section by using cause & effect diagram.

PROBLEM DEFINITION:

Object is to minimize trim losses and to increase the yield.

DATA COLLECTION:

SLITTERS

TYPE OF SLITTERS

- 1500mm
- 1800mm

1500mm

THICKNESS	CUSTOMER	SLIT WIDTH
1.6	CUSTOMER 1	49 68 78 84 89 99 110 120 140 140 141 223
	CUSTOMER 2	58.5 84

3.9	CUSTOMER 1	114 194 234	
	CUSTOMER 2	114 134 154 194 233.5	
	CUSTOMER 3	114 154 194	
	CUSTOMER 4	54	

	CUSTOMER 3	70.5 90.5 100.5
	CUSTOMER 4	184

III SOFTWARE

The software that is being used here for the optimization is LINGO 9.0 version where it requires some basic initial boundary conditions and modal assumptions. They are defined as follows:

MODEL ASSUMPTIONS:

- Coil thickness is constant.
- Various customer requirement (slit or Roll) with same thickness, and Coil width constant.

Decision Variable:

x_i – Required no of setups , i = 1,2,3 ……..5.

k_j - Slit or Roll width required by the customer , j = 1,2,3……45Inputs given to the software as per the requirements:

Objective function:

To minimize trim losses;

MIN = 6250 -((622 * K1) + (194 * K2) + (68 * K3) + (90.5 * K4) + (99 * K5) + (290 * K6) + (140 * K7) + (483 * K8) + (58.5 * K9) + (622 * K10) + (194 * K11) + (68 * K12) + (90.5 * K13) + (99 * K14) + (290 * K15) + (140 * K16) + (483 * K17) + (58.5 * K18)+ (622 * K19) + (194 * K20) + (68 * K21) + (90.5 * K22) + (99 * K23) + (290 * K24) + (140 * K25) + (483 * K26) + (58.5 * K27) + (622 * K28) + (194 * K29) + (68 * K30) + (90.5 * K31) + (99 * K32) + (290 * K33) + (140 * K34) + (483 * K35) + (58.5 * K36)+ (622 * K37) + (194 * K38) + (68 * K39) + (90.5 * K40) + (99 * K41) + (290 * K42) + (140 * K43) + (483 * K44) + (58.5 * K45));

IV . RESULT

LINGO OUTPUT:

Feasible solution found.

Objective value:	39.00000
Extended solver steps:	398
Total solver iterations:	17699

Variable	Value	Reduced Cost
	K1	0.000000 -622.0000
	K2	0.000000 -194.0000
	K3	2.000000 -68.00000
	K4	5.000000 -90.50000
	K5	0.000000 -99.00000
	K6	0.000000 -290.0000
	K7	0.000000 -140.0000
	K8	0.000000 -483.0000
	K9	11.00000 -58.50000
	K10	0.000000 -622.0000
	K11	0.000000 -194.0000
	K12	3.000000 -68.00000
	K13	1.000000 -90.50000
	K14	0.000000 -99.00000
	K15	1.000000 -290.0000
	K16	0.000000 -140.0000
	K17	1.000000 -483.0000
	K18	3.000000 -58.50000
	K19	2.000000 -622.0000
	K20	0.000000 -194.0000
	K21	0.000000 -68.00000
	K22	0.000000 -90.50000
	K23	0.000000 -99.00000
	K24	0.000000 -290.0000
	K25	0.000000 -140.0000

Thus the above model has been solved using LINGO package. The minimum amount of trim losses is 39mm.

V. CONCLUSION AND FUTURE WORKS

Thus, getting a precise solution from the LINGO 9.0 software a minimum trim losses of about 39mm has been reduced considerably , also we have optimized the scrap losses or the trim losses for a width of 1250mm coil and slitter type of 1500mm and 1800mm with respect to the customer requirements.

Our future works includes:

- Width of the coil can be changed from 1250mm to 1500mm and also use of different slitter type.
- Instead of using LINGO 9.0 software other software packages like LINDO, etc., can be used.

REFERENCE

[1]. Scrap reduction in the extrusion process: the case of an aluminium production system Original Research Article Applied Mathematical Modelling, Volume 11, Issue 2, April 1987, Pages 141-145M.T. Tabucanon, T. Treewannakul

[2]. Scrap tires to crumb rubber: feasibility analysis for processing facilities Resources, Conservation and Recycling, Volume 40, Issue 4, March 2004, Pages 281-299Nongnard Sunthonpagasit, Michael R. Duffey

[3]. State-of-the-art review of optimization methods for short-term scheduling of batch processes Review ArticleComputers & Chemical Engineering, Volume 30, Issues 6–7, 15 May 2006, Pages 913-946Carlos A. Méndez, Jaime Cerdá, Ignacio E. Grossmann, Iiro Harjunkoski, Marco Fahl

[4]. A review of optimization techniques in metal cutting processes Original Research ArticleComputers & Industrial Engineering, Volume 50, Issues 1–2, May 2006, Pages 15-34Indrajit Mukherjee, Pradip Kumar Ray

[5]. Appendix ii: Lingo softwareProcess Systems Engineering, Volume 7, 2006, Pages 389-394

HYBRID POWERED THREE-PORT THREE PHASE BIDIRECTIONAL CONVERTERS

MELCOM MARSHAL, PRAVEEN KUMAR SHUKLA, PRAVEEN KUMAR RAHUL SHARMA & M. VENAMATHI

Dr M.G.R University, India.

Abstract— Renewable energy sources such as Fuel-Cells, Photo-Voltaic (PV) arrays are increasingly being used in automobiles, residential and commercial buildings. For stand-alone systems energy storage devices are required for backup power and fast dynamic response. A power electronic converter interfaces the sources with the load along with energy storage. Existing converters for such applications use a common dc-link. High frequency ac-link based systems have recently been explored due to its advantages of reduced part count, reduced size and centralized control. Such a high frequency ac-link based converter is termed as a multi-port converter in literature, to whose ports are connected the energy sources, energy storage devices and the load. The proposed converter consists of three high-frequency inverter stages operating in a six-step mode, and a high-frequency three-port three-phase symmetrical transformer. The converter provides galvanic isolation and supports bidirectional power flow

Keywords— bidirectional, galvanic isolation, multiport structure, triple active bridge, photovoltaic arrays, dual –PI-loop.

I. INTRODUCTION

In the past decades, traditional power converter topologies have been evolving in various directions, for example, from single-phase to multiphase interleaving, and from two-level to multilevel. Nowadays, most dc-dc power converters deal with single-input and single-output. Recently, attention has been paid to multiport converters. Multi-port converter has several ports to which the sources or loads can be connected shown in Fig. 1.

Fuel-cell automobiles are considered to be an option for future clean energy automobiles. The primary source will be fuel-cells with the power during acceleration and deceleration supplied from batteries. Fuel-cells have slow dynamic response and hence energy storage is essential in such an application. Batteries can be charged from fuel-cells and during regenerative braking operation. Three-port converter fits well into this fuel-cell vehicle application. A three-port energy management system accommodates a primary source and a storage and combines their advantages automatically, while utilizing a single power conversion stage to interface the three power ports. Having the two energy inputs, the instantaneous power can be redistributed in the system in a controlled manner.

A second advantage of using such a system is that the primary source only needs to be sized according to the average power consumed by the load for a specific application, not necessarily to the peak power. Such operation would avoid oversizing of the primary source and is economically beneficial. Moreover, with the auxiliary storage, not only can the system dynamics be improved, but also the storage acts as a backup energy source in the event of a main source failure.

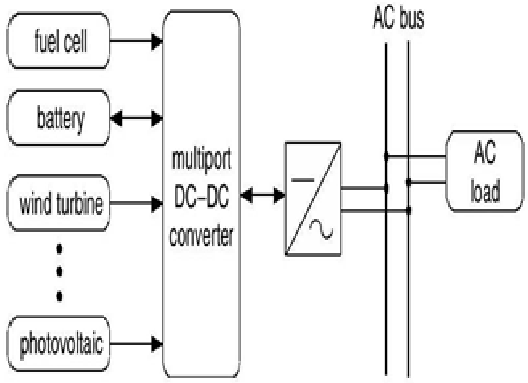

Fig. 1 Multiport Structure

Rooftop solar panels are being widely used to power residential and commercial buildings. Energy storage will be used to store excess power and also as a backup unit to supply vital equipment. Due to cost reasons energy storage is applicable more in off-grid applications. A three-port converter with one of the ports connected to the solar panel or the front-end converter of the solar panel, another port connected to the battery and the third port to the load can be used for such an application. It is also possible for the utility to use energy storage in these buildings to meet peak power demands. The converter is a direct extension of the single-phase version of the three port converter. The three-phase configuration enhances the current rating of the system and thus the power rating. The converter is promising for electrical vehicles (e.g., fuel cell/battery cars) and electricity generation system. The transformer design, system modelling, operation principle, principle, control strategy, and simulation results are presented in the following sections

.

II. THREE PORT CONVERTER CIRCUIT

Earlier the three-port triple-active-bridge (TAB) topology has been proposed for small power applications .To extend the topology towards high-power applications, the standard way is to replace the single-phase bridge with a three phase bridge, which enables higher current handling ability. The resulting converter topology is shown in Fig. 2.

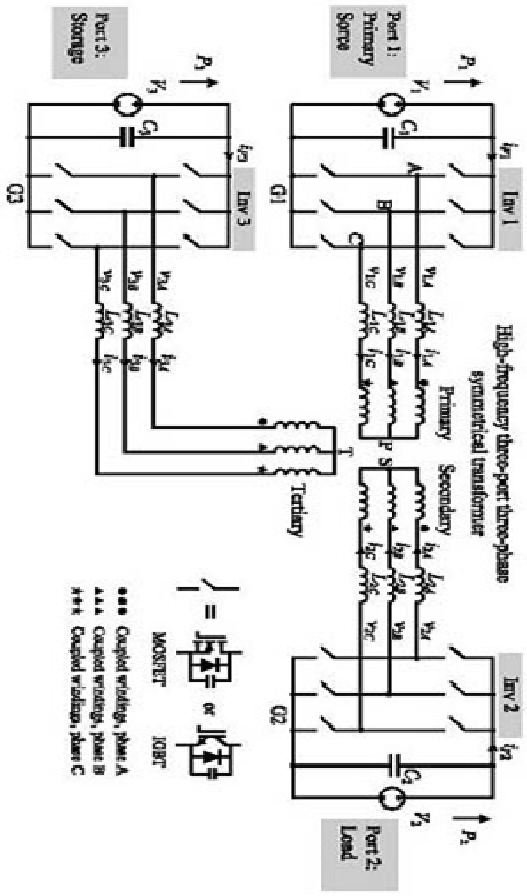

Fig. 2 Topology of the proposed high-power three-port three-phase triple-active-bridge (TAB) bidirectional dc-dc converter

The concept of dual-active-bridge (DAB) converter for three phase is applied to the TAB converter in this paper. As shown, the circuit consists of three inverter stages operating in a six step mode with phase shifts being controlled. The three bridges are interconnected by a three-port three-phase symmetrical transformer, and the inductors in the circuit represent the inductance of the transformer. The transformer can be either in Y-Y or in Δ-Δ connection. Note that coupling of the windings is between the ports and there is no interphase coupling. As indicated in the figure, windings marked with the same symbol are coupled. The major advantage of the three-phase version is the much lower VA rating of the filter capacitors. Thanks to the nature of the symmetry, the current stress of the switching device is significantly reduced compared to the single-phase version. As the current through the transformer windings is much more sinusoidal than in the single-phase situation (this is shown in the simulation section), there are less high frequency losses in the transformer. The proposed converter has the potential for high-power applications (say, tens of kilowatts). The operating principle is very similar to the single-phase version. In addition to galvanic isolation, a major advantage of this converter is the ease of matching the different voltage levels in the overall system. The leakage inductances of the transformer are an integral part of the circuit. With reference to the primary side, each bridge generates a high-frequency six-step mode voltage with a controlled phase angle. The control scheme aims to regulate the output voltage and power of the primary source simultaneously, using two phase shifts as control variables. The storage supplies/absorbs the transient power difference between the load and the primary source. This is an automatic system, matching the variations of the power drawn by the load while the power of the primary source is kept at constant.

III. MODELING OF TRANSFORMER

In this section, the effect of the non-idealities of the three-winding transformer is discussed. Specifically, the effect of the magnetizing inductance and the three leakage inductances Llk1, Llk2 and Llk3, as shown in Fig. 2. The main challenge of the proposed high-power three phase three-port converter is the design of the three-phase symmetrical transformer. It is important to keep the symmetry of the leakage inductances. Otherwise, the current (transferred power) will not be equal for the three phases. The transformer construction may be necessary to be physically symmetrical in order to have an identical leakage inductance in each phase. Otherwise, the external inductances should be adjusted to achieve an equal per-phase leakage inductance.

Basically, there are two ways to wind a transformer: conventionally and coaxially. The spatial three-phase symmetrical transformer can easily be extended to the three-port version as illustrated in Fig. 3.

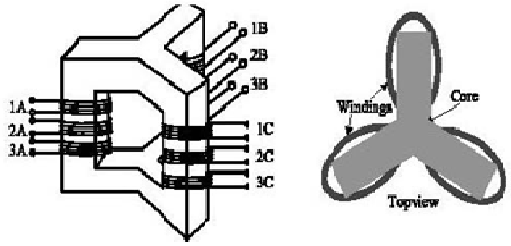

Fig. 3. Conventionally wound three-port three-phase spatially symmetrical transformer

However high-frequency core shapes are unavailable. For a simple solution it would be possible to design the transformer as three separated sub-transformers since there is no interphase coupling; however this results in a higher transformer core loss, because the flux canceling effect does not apply (the sum of the three phase fluxes equals zero). Coaxial winding techniques are commonly used in radiofrequency transformers. Fig. 4 shows the structure of a coaxially wound transformer.

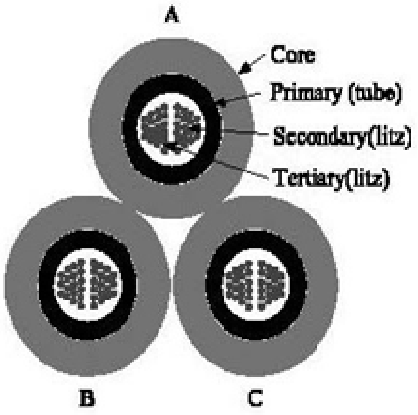

Fig. 4. Coaxially wound three-port three-phase symmetrical transformer.

This technique offers a feasible solution to contain the leakage flux within the inter-winding space and thus prevents the core from being saturated locally. As a result, the core and copper losses are lower, and localized heating is avoided. Coaxial windings can lead to low loss, low leakage inductance power transformers in high-frequency soft-switched dc-dc and resonant converters.

The primary of each phase consists of a straight tube of circular cross section. The star point is realized by shorting the tubes at one end. Toroidal cores are slipped over each tube to form the magnetic medium. The secondary and tertiary wires can now be wound inside the primary tube. For the proposed converter, the windings can be arranged as: the primary using a tube and the secondary and tertiary using twisted litz wires. With the coaxial winding techniques, the leakage inductance can be minimized. Hence external inductors should then be designed according to the desired amount of power flow.

IV. THREE PORT SYSTEM MODELING

The power flow in the three-port system has been extensively investigated. Since no interphase coupling exists in the system, one can analyse the circuit based on the per-phase model. For phase A, the circuit model shown in Fig. 5(a) can be viewed as a network of inductors driven by controlled voltage sources that are phase-shifted with respect to each other. The controlled phase displacements impose the power flow between the ports. Fig. 5(b) illustrates the modeling approach based on a Δ-model equivalent transformer representation. The Δ-model facilitates the system's analysis, and simple formulas allow converting the parameters from a T-model to the Δ-model description.

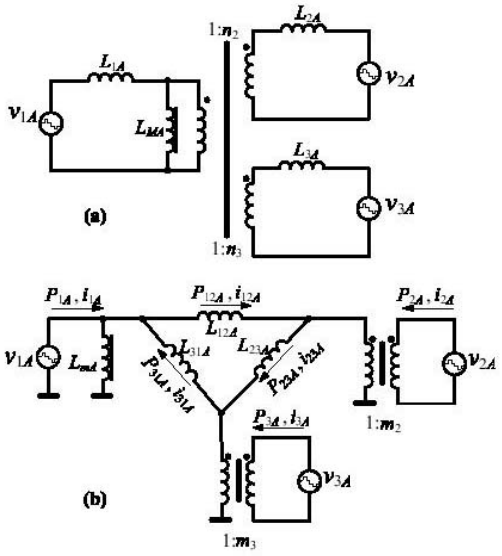

Fig. 5 T-model (a) and Δ-model (b) representation of the three-port transformer and inductors network (per-phase model: phase A).

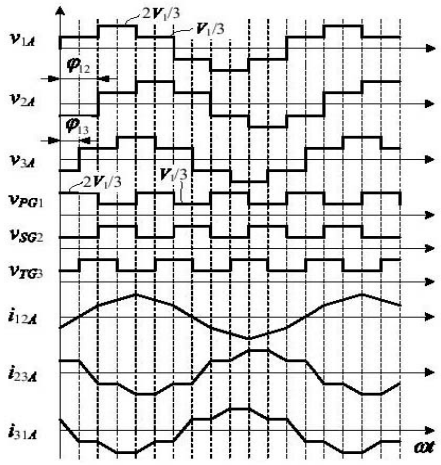

Fig. 6 Idealized operating waveforms (phase A) of the proposed three-port three-phase TAB converter at □12 = π/3 and □13 = π/6.

According to the definitions in Fig. 5(b), for a lossless system the power flow in the system can be described as

$P1_A = P12_A - P31_A$

$P2_A = P23_A - P12_A$

$P3_A = P31_A - P23_A$

$P1_A + P2_A + P3_A = 0$

where $P1_A$, $P2_A$, $P3_A$ are the powers delivered by the primary source, load and storage through phase A, respectively. A positive value means supplying the power and a negative value suggests consuming the power. Note that for a lossless system, we have $P3_A = -P1_A - P2_A$; therefore $P3_A$ is redundant. The same model can be applied to phase B and C. Obviously, the total power of the port is the sum of the power through each phase:

$P1 = P1_A + P1_B + P1_C$
$P2 = P2_A + P2_B + P2_C$
$P3 = P3_A + P3_B + P3_C$.

Again, P3 is redundant because $P3 = -P1 - P2$. The average power consumed by the load over a typical operating cycle shall be equal to the power delivered by the primary source. The storage port thereby functions as an external leveling device, smoothing out the fluctuation in the instantaneous power drawn by the load port.

V. CONTROL STRATEGY

The control scheme aims to regulate the output voltage and the power of the primary source simultaneously by using the two phase shifts as control variables. An arbitrary power flow profile in the system can be achieved by phase shifting the three inverter stages as in the single-phase version . The storage supplies/absorbs the transient power difference between the load and the primary source. Since the three-port converter can be viewed as a two-input two-output first-order system, the control system can be implemented with PI regulators based on the dual-PI-loop control strategy .

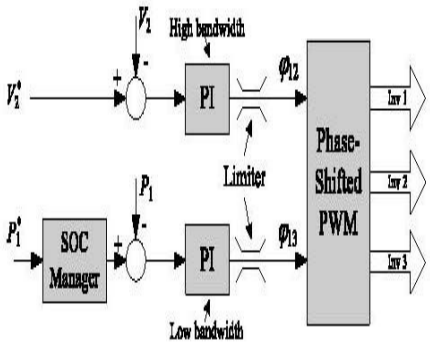

Fig. 7 Control scheme employing two PI compensators.

Fig. 7. Control scheme employing two PI compensators being employed to regulate the output voltage and the other controlling the power of the primary source, as illustrated in Fig. 7. Also incorporated in the control scheme is a state-of charge (SOC) manager for the storage .

The three-port converter can be modeled, using an averaging method, as three controlled dc current sources whose amplitudes are determined by the two phase shifts [9]. The current at each port (iP1, iP2 and iP3, see Fig. 2) can be averaged over one switching cycle, being a function of the two phase shifts. We can assume that the voltages at the ports are kept constant. Then the average current is the power divided by the port voltage. Thereby, the current source functions can be obtained. They are nonlinear functions of the two phase shifts and should be linearized at the operating point for a control oriented model .

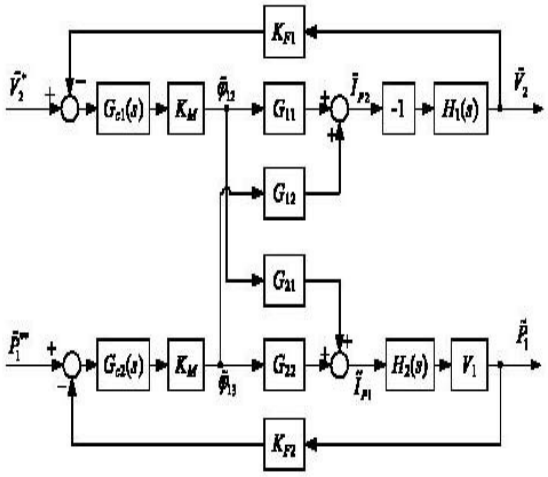

Fig. 8 Small signal control loop block diagram of the three-port TAB converter

The control variables are □12 and □13. Fig. 8 shows the small signal control loop block diagram of the TAB converter, where Gc1(s) and Gc2(s) are the transfer functions of the PI controllers. G11, G12, G21 and G22 are the small signal linearized gain of the converter, which can be derived from the power flow equations . The block with gain "-1" is due to the definition of the direction of iP2 . The block with gain "V1" is needed because the power is equal to the average current times the port voltage. KM is the gain of the phase shift modulator. H1(s) is transfer function of the load port formed by the filter capacitor C2 and the equivalent load resistance RL. The two PI control loops are coupled and influence each other . The bandwidth of the voltage control loop (□12) is tuned higher (5 to 10 times higher) than that of the power control loop (□13) so that the interaction is reduced.

VI. RESULTS AND DISCUSSION

To investigate the performance of the proposed topology, the converter and control scheme were simulated with MATLAB under a variety of operating conditions. Table I gives a list of parameters used for simulation including the controller parameters. A standard voltage set, 48 V primary sources, 48 V storage and 800 V dc output, is

assumed. Because of the high switching frequency (100 kHz), high power (10 kW) and the low voltage (48 V), the required inductances are very small for the source and storage sides in this simulated case. Suppose that the system is symmetrical; that is, all the inductances are equal when referred to the primary. Then the power rating of each port is identical. For the situation that the average power of the storage port over one switching cycle is zero, the phase shifts should obey □13 = 0.5□12. Simulation results in Fig.9 illustrate the operating waveforms of the converter, i.e., the voltages applied to the transformer and inductors network and the corresponding currents through the windings at □12 = π/6 and □13 = π/3. In this operating point the average power of the storage port equals zero.

TABLE I
SIMULATION PARAMETERS FOR THREE PORT SYSTEM

Description	Symbol & Value
Primary source voltage	$V_1 = 48$ V dc
Load side voltage	$V_2 = 800$ V dc
Storage voltage	$V_3 = 48$ V dc
Switching frequency	$f_s = 100$ kHz
Transformer turns ratio	$n_2 = 16.7$, $n_3 = 1$
Inductance	$L_{1A} = L_{1B} = L_{1C} = 0.05$ μH
Inductance	$L_{2A} = L_{2B} = L_{2C} = 0.05$ μH
Inductance	$L_{3A} = L_{3B} = L_{3C} = 14$ μH
PI controller $G_{c1}(s)$	$K_1 = 1000$, $\tau_1 = 10$ ms
PI controller $G_{c2}(s)$	$K_2 = 0.2$, $\tau_2 = 10$ ms
LPF time constant $H_2(s)$	$\tau_I = 1$ ms
Phase shift modulator gain	$K_M = \pi/500$
Feedback gain	$K_{F1} = 1$
Feedback gain	$K_{F1} = 1$
Nominal load resistance	$R_L = 64\ \Omega$ (for 10 kW)
Output filter capacitor	$C_L = 5000$ μF

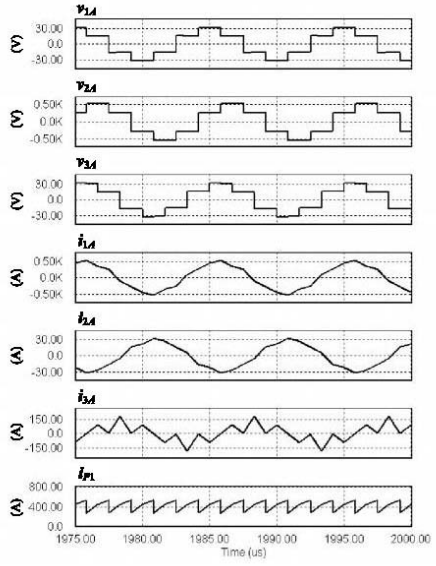

Fig. 9 Simulation results showing the voltages generated by the three-phase bridges

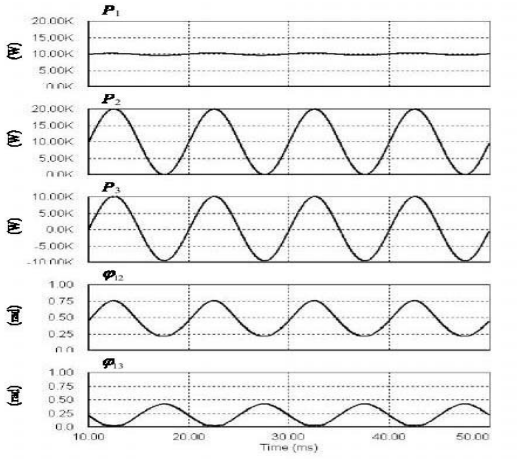

Fig. 15 Simulation results of power flow control with an inverter-type load.

Suppose that the power flow of the primary source is unidirectional, i.e., P1 > 0 under all situations. The maximum power flow to the load port occurs when □12 = π/2 and □13 = 0. For this particular operating point, results from simulation are shown in Fig. 9. As can be seen, the currents are close to sinusoidal waves. Due to the fact that the converter is symmetrical in three phase, the only possible control variable is the phase shift between the bridges. Therefore, other control methods such as duty ratio control to extend soft-switching region cannot be implemented in this topology straightforwardly. This converter will be soft-switched under the condition that all the dc voltages at the ports remain near constant. The converter suffers from a limited soft-switched operating region if one or more ports have a wide operating voltage.

V. CONCLUSION

In this paper, a high-power three-port three-phase bidirectional dc-dc converter has been proposed. The converter comprises a high-frequency three-port transformer and three inverter stages operating in a high-frequency six-step mode. The circuit interfaces a primary source and storage to load and manages the power flow in the system. With the external leveling system the operation of the primary source can be optimized, for instance, operating it at a constant power. The converter provides galvanic isolation and supports bidirectional power flow for all the power ports. The advantage of the three-phase version compared to the single-phase one is the higher current handling capability and much lower current ripple at the dc side, thereby lower VA rating of filter capacitors owing to the interleaving effect of the three phase. Promising for power generation systems utilising multiple sustainable energy sources, a family of multiport bidirectional DC–DC converters has been presented in this paper, based on a general

topology that uses a combination of a DC-link with magnetic coupling. In this way, multiple sources can be interconnected without the penalty of extra conversion stages or additional switches. The resulting converter features a simple topology, minimum conversion steps, low cost and compact packaging.

REFERENCES

[1] H. Tao, A. Kotsopoulos, J. L. Duarte, and M. A. M. Hendrix, "Family of multiport bidirectional DC-DC converters," IEE Proceeding Electric Power Applications, vol. 153, no. 3, pp. 451–458, May 2006.

[2] J. L. Duarte, M. Hendrix, and M. G. Simoes, "Three-port bidirectional converter for hybrid fuel cell systems," IEEE Trans. Power Electron., vol. 22, no. 2, pp. 480–487, Mar. 2007.

[3] H. Tao, A. Kotsopoulos, J. L. Duarte, and M. A. M. Hendrix, "Multi input bidirectional DC-DC converter combining DC-link and magnetic coupling for fuel cell systems," in Proc. IEEE Industry Application Society Conference and Annual Meeting (IAS'05), Hong Kong, China, Oct. 2005, pp. 2021–2028.

[4] A. D. Napoli, F. Crescimbini, L. Solero, F. Caricchi, and F. G. Capponi, "Multiple-input DC-DC power converter for power-flow management in hybrid vehicles," in Proc. IEEE Industry Application Society Conference and Annual Meeting (IAS'02), Oct. 2002, pp. 1578–1585.

[5] D. Liu and H. Li, "A three-port three-phase DC-DC converter for hybrid low voltage fuel cell and ultra capacitor," in Proc. IEEE The 32nd Annual Conference of the IEEE Industrial Electronics Society (IECON'06), Paris, France, Nov. 2006, pp. 2558–2563.

[6] M. Michon, J. L. Duarte, M. Hendrix, and M. G. Simoes, "A threeport bi-directional converter for hybrid fuel cell systems," in Proc. IEEE Power Electronics Specialists Conference (PESC'04), Aachen, Germany, Jun. 2004, pp. 4736–4742.

[7] H. Tao, A. Kotsopoulos, J. L. Duarte, and M. A. M. Hendrix, "A soft-switched three-port bidirectional converter for fuel cell and super capacitor applications," in Proc. IEEE Power Electronics Specialists Conference (PESC'05), Recife, Brazil, Jun. 2005, pp. 2487–2493.

[8] C. Zhao and J. W. Kolar, "A novel three-phase three-port UPS employing a single high-frequency isolation transformer," in Proc. IEEE Power Electronics Specialists Conference (PESC'04), Aachen, Germany, Jun.2004.

AUTOMATIC AMBULANCE RESCUE SYSTEM

Reena kumari[1],Nithya.R[2],Nitesh kumar[3], G.Gugapriya[*]
[1,2,3]EEE UG Students, Dr.M.G.R University, India.
*Senior Lecturer, Dr.M.G.R University, India.

Abstract—**In this paper,we describe a system offering a solution to the problem of ambulancemanagement and emergency incident handling in the prefecture of Attica in Greece. It is based on a Geographic Information System (GIS) coupled with Global Positioning System (GPS) and Global System for Mobile Communication (GSM) technologies.EMS ambulance is designed to provide medical care or treatments to patient at the emergency site. If intensive care is needed, the patient will be send to the nearest hospital. Quick response and comprehensive care is vital in this case. Paper describes the application of A* Algorithm and road network as parts of the development for the ambulance routing system. we developed the vehicle collision warning system that detects car crash and warns the danger to drivers in advance. This vehicle collision warning system is implemented by using sensors and GPS system. The proposed system contacts the ambulance emergency system, locates the correct and nearest available ambulance, accesses a Smart Online Electronic Health Record (SOEHR) that can critically assist in pre-hospital treatments; and identifies availability of the nearest available specialized hospital all through communication with the Hospital Emergency Department System (HEDS) which provides early and continuous information about the incoming patient to the hospital.**

Keywords--**GPS, GSM,GIS,AARS,collision warning, vehicle collision**

I. INTRODUCTION

The efficient management of ambulances in order to achieve fast transportation of patients to the appropriate hospital is a vital aspect of the quality of health services offered to citizens. Accomplishing an effective routing and districting of ambulances will minimize their response time. Therefore, the introduction of computer-based systems can drastically improve the way emergency incidents are being handled. In this paper, we describe a system offering a solution to the problem of ambulance management and emergency incident. It is based on a Geographic Information System (GIS) coupled with Global Positioning System (GPS) and Global System for Mobile Communication (GSM) technologies. The design of the system was the result of a project funded by the Greek Secretariat of Research and Technology. The system will operate in the National Centre of Immediate Assistance which deals with emergency medical incidents by coordinating and routing ambulances to appropriate hospitals as well as offering medical care to patients during their transport to hospitals.There are various means of transportation including car, motorcycle and bicycle. The number of tourists who are notaccustomed to theroads using the transportation is increasing and the rate of traffic accidents is also growing. Therefore, the ways to prevent traffic accidents and reduce the accident rate are required. This project describes the vehicle collision warning system that detects the car crash in advance and warns the danger to drivers. The system uses GPS to locate one's car and others. In addition, the types of transportation are recognized by identification device in GPS. This data helps to predict vehicle collision and warns drivers to prepare for the accident. The Emergency Medical Services (EMS) ambulance is designed to give medical care or treatments to patient at theemergency sites and/or directly send the patients to hospitalwhere intensive care by doctors can be given. The EMSambulance provided is equipped with basic life supportequipment to help whenever an emergency occurs. The main problem in this is the hectic situation during peak hour, where most vehicles are trapped and gradually move. The peak hours identified is from 7 a.m. to 10 a.m., from 12 p.m. to 2 p.m., and from 4 p.m. and above. This is the time where people busy to go to school or work, lunch and go back home, respectively. There are also traffic light, toll and roundabout. The objective of this system is to respond to the needs of an efficient and error free emergency system which, in cases of emergency (e.g. car accidents) can quickly and accurately find the right ambulance and send it to the place of accident without or minimal human intervention in order to reduce human errors and to accelerate the response process. All of the current ambulance systems rely on calls from people who give information about the accident and the accidents approximate location. Most human operators use a traditional or computer aided dispatching system to find an ambulance. These types of systems might record mistaken information from the caller, or transfer and enter wrong data into the dispatch system. As a consequence, patients might risk substantial harms to their health or may even lose their lives because of human errors or late arrival of an ambulance or wrong information or treatment.

II. LITERATURE REVIEW

A. An information system for effective management of ambulance.

1. General function of GIS

GIS technology integrates common database operations such as query and statistical analysis with the unique visualization

and geographic analysis benefits offered by maps. A GIS facilitates the modelling of spatial networks offering algorithms to query and analyse them. It usually provides tools to find the shortest or minimum impedance route through a network and heuristic procedures to find the most efficient route to a series of locations commonly called the traveling salesman problem. Allocation functions assign portions of the network to a resource supply location and tracing tools provide a means to determine whether one location in a network is connected to another. Distance matrix calculation can be used to calculate distances between sets of origins and destinations whereas location-allocation functions determine site locations and assign demand to sites. Finally, street addresses can be converted to map coordinates (address geocoding). These capabilities of GISs to analyse spatial networks enable them to be used as Decision Support Systems for the districting and routing of vehicles.

2. Basic concept of GPS technology

The Global Positioning System (GPS) is a world radio navigation system funded andcontrolled by the U.S. Department of Defence. **It is used for the determination of the exactpositions of various objects located anywhere on the Earth's surface**. The GPS consists of twenty-four satellites that orbit the Earth in twelve hours, the groundstations and the receivers. The satellites function as reference points that determine anobject's position with great accuracy. The GPS receiver, installed on the object, calculates itsdistance from three different satellites by using the travel time of the signals transmitted fromeach satellite. Due to atmospheric distortions, errors are introduced into the satellite signals affecting the determination of the objects' positions. **However, with various techniques theseerrors can be effectively dealt with.Due to the advances in integrated circuits technology, the GPS receivers are small andinexpensive**. Therefore, almost every organization can afford to pay for the use of the GPStechnology. Nowadays, the GPS is used in vehicles, ships, airplanes, and even laptopcomputers.

3. Basic concepts of GSM Technology

During the early 1980s, analog cellular telephone systems were experiencing rapid growthin Europe. Each country developed its own system, which was incompatible with everyoneelse's in equipment and operation. To deal with this undesirable situation, the GSM, apan-European public mobile system, was developed and standardized by the European Telecommunication Standards Institute in the late 1980s. During the 1990s the GSMstandard was expanded in every continent.The primary service supported by the GSM is telephony. Speech is transmitted through theGSM network as a digital stream. An emergency service is also available, wherethe nearest emergency service provider is notified by dialling three digits (similar to 911).GSM users can send and receive data, at rates up to 9600 bps, to users on theplaintelephone service, ISDN, Packet Switched Public Data Networks, and Circuit Switched Public Data Networks .In addition, the GSM offers a Short Message Service (SMS), a bi-directional service forshort alphanumeric messages. For point-to-point SMS, a message can be sent to anothersubscriber to the service, and an acknowledgement of receipt is provided to the sender. SMS can also be used in a cell-broadcastmode, for sending messages such as traffic updates.

B. The Vehicle Collision Warning System based on GPS

The vehicle collision warning system proceeds with two steps. First step is the AIS which obtains the location data of vehicle. The second step is the collision warning using the vehicle warning algorithm. The figure 1 explains the scenario. In this scenario, the driver receives the collision warning from GPS data collected in AIS when the system detects vehicle collision.

Every vehicle sends its location data to the AIS andcollects the other vehicle's location data from the AIS. By using the collected location data, the collision warning system in each vehicle warns the vehicle collision to the driver based on speed, direction, and distance. This will help drivers predict the vehicle collision and prevent them from traffic accidents.

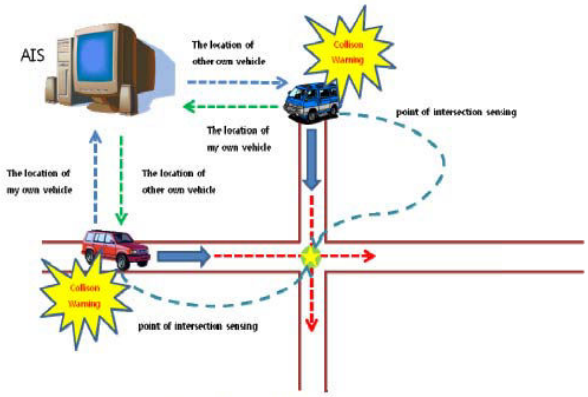

Figure 1. The vehicle collision warning scenario

This vehicle collision warning system consists:

1. *The sensor and GPS data collection module*

The sensor and GPS module collect the sensor and location data in a device of the vehicle and send the data to the management system.

2. *The algorithm for sensing the collision*

The distance that the sensor detects is measured based on the vehicle's course. This distance increases in proportion to speed. The direction of the vehicle is used for measuring the point of intersection in order to prevent any accidents. In addition, if person or a bicycle is within the vehicle's direction, the driver receives the warning sign.

3. Warning module

When the collision is detected through the collision algorithm, the warning module gives warning sign to the driver.

4. *The transportation distinguish module*

Every vehicle has its own identification ID to transmit it to the management system.

5. *The management for collision warning system*

The GPS reception module, the sensor reception module and the vehicle identification module are retrieved in this process. Based on the retrieved data the collision algorithm is executed. If it detects collision, the warning module sends the warning sign.

C. An Application of the A*Algorithm on the Ambulance Routing

This only focuses on the application of A*algorithm in finding the shortest distance of the ambulances. In this paper, the shortest distance for ambulances for the area serviced by ambulance located at the KKSA is projected by using A* Algorithm and road network for ambulance routing system. The objectives of this project are to develop an ambulance road network in 5 kilometres for the area under study and to apply a suitable mathematical model to minimize ambulance travelling distance.

1. Data Collection

The data on ambulance services are collected from the KKSA. Data includes information about the location and information related to the routing of ambulances. Road network developed involved all major roads which connected to the designated hospital. The road network consists of nodes and edges, which will be the directional links that connects the two nodes between them. The route with the shortest total distance is determined by applying the A*algorithm.

2. A* Algorithm Model

Here, the A* algorithm will be applied to determine the shortest path of ambulance distance from KKSA to other locations.

The models are:

$f(n) = g(n) + h(n)$

where,

n : A node on the network

$f(n)$: The estimated cost of the least-cost path to a goal node through n

$g(n)$: The cost of reaching node n from the start node

$h(n)$: An estimated cost of getting from node n to a goal node.

This process repeats until the goal node reached. The algorithm choose their node based on the cost from the start node plus an estimated of the goal node.

3. Computing the data

The A* algorithm is applied to determine the shortest path from KKSA to incident site. The shortest paths are based on incident site and current ambulance station. A preliminary study was done manually to calculate the shortest path for the ambulances. The distances are given in kilometres (km).

D. Mobile emergency system and integration

The new system is also intelligent when it comes to finding the right ambulance, hospital and doctor that are suitable for the conditions and location of the accident.

1. System component and architecture

The system consists of 5 components:

i. The Emergency requester device (Emergency application for mobile devices): This is a mobile phone equipped with a Geographical Positioning System (GPS).
ii. The Main Central System (MCS): This is the main server for the whole system.
iii. The Ambulance system: Each ambulance system is equipped with a GPS and navigation system. The system has a touch screen (specifying availability and reaction).
iv. The Online Electronic Health Record (OEHR): This is the patient's Smart Online Health Record.
v. The Hospital Emergency Department System (HEDS).

2. System processes

a) Reporting an accident

The start of the system will be triggered by the Emergency requester device reporting an accident. With a simple mobile application installed on the device, the caller can quickly and easily enter information about the accident such as the number of injured people and number of cars involved in the accident. The application will automatically send the coordinates of the mobile phone to MCS.

b) Finding an ambulance

MCS receives the emergency request from the requester and without human intervention; sends a request to all available ambulances to report their GPS coordinates (other algorithms are also available where the ambulance continually reports coordinates to the MCS. The selection of specific algorithms depends on how busy the environment is).MCS will then compare accident and ambulance coordinates and send a job request to the nearest ambulance based on the navigation system map rather than direct

distance. The Ambulance officer has 10sec to accept or reject. In the event of accepting the job, MCS will send the accident's coordinates to the ambulance and automatically the ambulance system outlines the road map to the accident location. If the ambulance officer rejects the job or does not reply within 10 seconds, the MCS will pick up the second nearest ambulance to the accident, assuming that in 10seconds positions of ambulances don't change much. In case of a longer delay the MCS will start the process from the beginning.

c) *Ambulance system processes*

i. Setting up availability and communicating with MCS

The ambulance officer can setup the status of the ambulance to available or not available. They can also accept or reject jobs. In case of rejection, the details with reasons for rejection should be entered into the system. When the ambulance accepts the job, their status will show as "in mission".

ii. Accessing SOEHR

After picking up the patient or the injured, the ambulancesystem can access the SOEHR using the patient's fingerprint.The ambulance officer can then quickly and easily enter thepatient's current medical conditions such as injuries, broken bones, and unconsciousness. The SOEHR, based on the patient's medical history and their current conditions will recommend urgent and pre-hospital treatment.

iii. Finding a Hospital

The ambulance needs to find the right hospital for the patient on-board. The proposed ambulance system, based on the patient's conditions, distance, availability and specialty of hospitals, will select the right hospital and the navigation system will automatically show the route to the hospital. The identity of the patient will be communicated to HEDS. All hospitals GPS coordinates will already be in the database of the ambulance system.

d) Preparing for incoming patient and monitoring incoming ambulances

Once the ambulance selects a hospital, the Hospital Emergency Department System (HEDS) books a bed or place for the incoming patient and accesses the patient's health record. The ambulance system starts to communicate continuously the ambulance coordinates to HEDS so the department's medical staff can monitor the incoming ambulance on the HEDS. HEDS will show in real-time all the incoming ambulances on a map with a list of information about distances and time. Department staff will prepare what they plan to do for the incoming patient including operation theatre, medications, and consultants if required. By the HEDS, staff can update the availability of beds or operation theatres based on the discharge or transfer of patients.

I. RESULTS AND DISCUSSION

In this paper, we describe a system offering a solution to the problem of ambulancemanagement and emergency incident handling in the prefecture of Attica in Greece. It is based on the integration of GIS, GPS and GSM technologies. The design of the system was the result of a project funded by the Greek Secretariat of Research and Technology. The system will operate in the National Centre of Immediate Assistance. The described system will improve the services provided to citizens.

This system will help to reduce traffic accidents of tourists and will enable drivers to predict possible accidents as well as to prepare for them.

The propose algorithm is hoped to increase the efficiency and to enhance the quality of the EMS ambulance management.

II. PROPOSED WORK

Our system consists of four main units, whichcoordinates with each other and makes sure thatambulance reaches the hospital without any timelag. Thus our system is divided into following fourunits,

- THE VEHICLE UNIT
- THE MAIN SERVER UNIT
- THE AMBULANCE UNIT
- THE NODE UNIT(TRAFFIC JUNCTION UNIT)

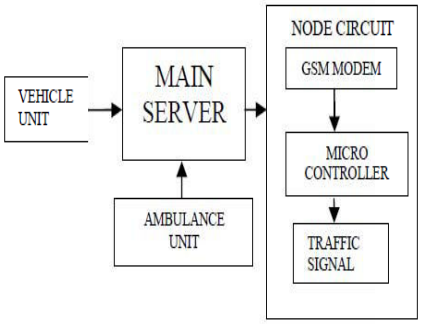

Fig.2.AARS system

1. Vehicle unit

According to our system, every vehicle should have a vehicle unit. The vehicle unit consists of a vibration sensor, controller, siren, a user interface, GPS system and a GSM module. The vibration sensor used in the vehicle will continuously sense for any large scale vibration in the vehicle. The sensed data is given to the controller.

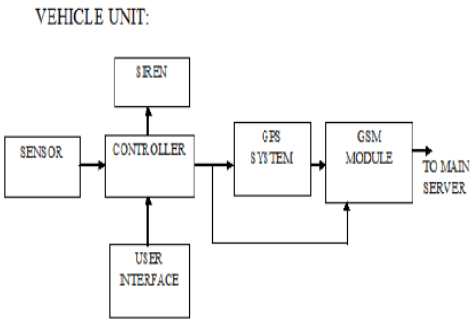

Fig.3.vehicle unit

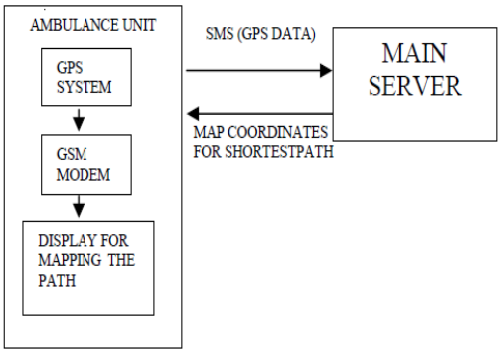

Fig.4.ambulance unit

The controller compares it with a threshold value which is an empirical value and ifit equals or exceeds that, then the controller automatically switches on a siren inside the vehicle. A programmed timer is also triggered. In case of a minor accident, the passenger probably would not need the service of the ambulance, and can therefore switch off the siren before the timer counts to zero, by resetting the entire vehicle unit through the user interface, which is connected to the controller. Or else, if he is unconscious or fatally wounded and needs an ambulance, then the siren is left ON and when the timer counts to zero, it would trigger both the GSM MODULE and the GPS SYSTEM inside the vehicle. The GPS SYSTEM finds out the current position of the vehicle (latitude and the longitude) which is the location of the accident spot and gives that data to the GSM MODULE. The GSM MODULE sends this data to the MAIN SERVER whose GSM number is already there in the module as an emergency number.

1. Main server unit

The main server is the central brain of our ITS. It communicates as well as controls every part of the system. The server objectives can be mainly classified into:

- FINDING THE NEAREST AMBULANCE TO THE ACCIDENT SPOT
- SENDING CO-ORDINATES TO THE AMBULANCE
- CONTROLLING THE NODES IN THE SHORTEST PATH

2. Ambulance unit

The ambulance unit has a GPS SYSTEM and a GSM MODEM for transmitting GPS data to the Main Server. The server receives the GPS data sent by the ambulance at regular intervals of time. The server sends the co-ordinates of all the nodes' in the path to the ambulance. The ambulance unit on receiving the co-ordinates plots them on to a map with the last two coordinates as the accident spot and the hospital location to get the shortest path to the hospital.

3.Node unit

A node can possibly operate in two modes namely,the normal mode and the ambulance mode. Normal mode is usual traffic control by a micro controller in a junction. In normal mode, traffic flow in each direction of the mode will be given equal importance. In the ambulance mode, the direction in which the ambulance heads is given importance and is kept in the ON state, till the ambulance leaves the junction (node).

- The node will receive a START SIGNAL from the main server as an control message which contains the direction that must be kept in ON state so that the ambulance can pass through the junction without waiting.
- The direction retrieved from the control message is given to the micro controller.
- That particular direction is kept in the ON state as long as another message (STOP SIGNAL) is received from the main server.
- GPS co-ordinates of the ambulance and the node matches i.e. when the ambulance crosses then node. The node then will return to its normal mode of operation.

a) INTERRUPT SERVICE ROUTINE ALGORITHM

- Wait for the reception START message along with data.
- Retrieve the data of the signal to be made green.
- Make the corresponding signal to be green.
- Wait for the reception of next message or stop signal.
- If the message is received return to normal mode.

b) NODE ACCESS AND CONTROL

The nodes in the shortest path are accessed and **controlled only when the ambulance reaches a distance of around say 1km from the node**. These locations are stored as the 1km markings. Since the signal should not be kept in ON state for a long time, the node access control is done in the following steps:

- The server first plots a map with the nodesneeded for the shortest path and makes 1kmmarkings for each node.
- The locations of 1km markings' (latitude and longitude) are taken from the map and stored in the NODES database.
- When the ambulance's GPS location and location of any one of the 1km markings matches, the corresponding GSM ID with the signal direction from the map is taken by the server and is compared with the shortest path nodes' GSM IDs.
- If that node is present in the path, the START SIGNAL is sent to that GSM ID.
- Now, the node is kept in ON state till the ambulance crosses the node. Once it crosses the node, the server sends a STOP SIGNAL to the node which brings the node to normal mode of operation.
- **The resolution of the GPS coordinates is that 1 second represents a 101.2ft in latitude and 61.6ft in longitude**. Thus in every comparison with respect to ambulance unit, it is enough to note the GPS co-ordinate till the accuracy of second's.

III. CONCLUSION

In this paper, a novel idea is proposed for controlling the traffic signals in favour of ambulances during the accidents. The AARS can be proved to be effectual to control not only ambulance but also authoritative vehicles. Thus AARS if implemented in countries with large population like INDIA can produce better results. The AARS is more accurate with no loss of time. But there may be a delay caused because of GSM messages since it is a queue based technique, which can be reduced by giving more priority to the messages communicated through the server.

IV. REFERENCES

[1]. Wang Wei, Fan Hanbo, Traffic Accident Automatic Detection and Remote Alarm Device.

[2]. Zhaosheng Yang. Study on the schemes traffic signal timing for Priority Vehicles Based on Navigation System, 2000.

[3]. Xiaolin Lu, Develop Web GIS Based Intelligent Transportation Application Systems with Web Service Technology, Proceedings of International Conference on ITS Telecommunications, 2006.

[4]. M. Feldmann and J. P. Rissen. "GSM network systems and overall system integration", Electrical Communication, 2nd Quarter 1993.

[5] C. Franklin, "An introduction to geographic information systems: linking maps to databases", Database, 1992, 15 (2), pp. 12-21.

[6] FitzGerald G, Tippett V, Elcock M, et al. "Queensland Emergency Medical System: A structural and organizational model for the emergency medical system in Australia". *Emergency MedicineAustralasia*[serial online]. December 2009;21(6):510-514

[7] Atkin C, Freedman I, Rosenfeld J, Fitzgerald M, Kossmann T. "The evolution of an integrated State Trauma System in Victoria, Australia". *Injury* [serial online]. November 2005;36(11):1277-1287

[8] R. Cocks and E. Glucksman, "What Does London Need From its Ambulance Service?" BMJ, vol. 306, 1993, pp. 950.

[9] J. A. Lawrence and B. A. Pasternack, Applied Management Science, John Wiley & Sons, Inc. 1998.

[10] Kijima, K. and Furukawa, Y., 2003 "Automatic collision avoidance system using concept of blocking area", Proceeding of MCMC 2003.